DSPACE

https://dspace.org/

Simulation of a Wet Flue Gas Desulphurization (WFGD) plant in support of continuous grid supply of electricity and compliance to SO2 emission limits

Lekhuleni , Tsholofelo Bernice

2024
University of the Witwatersrand, Johannesburg
https://hdl.handle.net/10539/45409

Lekhuleni , Tsholofelo Bernice. (2024). Simulation of a Wet Flue Gas Desulphurization (WFGD) plant in support of continuous grid supply of electricity and compliance to SO2 emission limits [Masters dissertation, University of the Witwatersrand, Johannesburg]. WIReDSpace.

Downloaded from a DSpace repository. https://dspace.org/



Simulation of a Wet Flue Gas Desulphurization (WFGD) plant in support of continuous grid supply of electricity and compliance to SO_2 emission limits

MSc. Dissertation

Prepared by

Tsholofelo Lekhuleni (2106723)

Submitted to

School of Chemical Engineering and Metallurgical Engineering, Faculty of Engineering and Built Environment, University of Witwatersrand, Johannesburg, South Africa

Supervisor: Professor Jean Mulopo

May 2024

Abstract

The wet flue gas desulphurization plant is susceptible to attrition and corrosion due to the corrosive nature of its operation. It is crucial to prevent plant downtime at any cost, as a plant failure in the WFGD could disrupt electricity supplies to the national grid. Plant failures can be avoided by using models to optimize plant operations and assure higher system performance.

In this work, the Aspen simulation was used to forecast the following parameters for a wet flue gas desulphurization process:

- Lowest limestone concentration or quality as absorber feed,
- Highest volume of gas that can be treated,
- Maximum sulphur content that could be treated in the absorber tower.

Various reactions such as limestone dissolution, SO_2 absorption and crystallization were simulated in Aspen. An equilibrium relation was established where the SO_2/SO_3 relationship in the absorber reaction could be used to predict the lowest concentration of limestone slurry and the highest volumetric flowrate that could be treated in the absorber. The pH drops in the absorber and the formation of gypsum (CaSO4) also supported the findings of the equilibrium relationship. The lowest limestone concentration limit is 16% compared to a design base of 31%. The maximum volumetric flowrate is in the range of 4,0-4.5 x 10^6 m^3/h. The maximum sulphur content that could be treated is 1.6% S on a mass basis compared to a design base of 0.9%. However, the maximum sulphur was reduced to 1.41 % due to the limestone control dosing valve which can only supply 90000 kg/h instead of the maximum requirement of 94315 kg/h. The equilibrium relations, pH, and gypsum production can all be used to establish safe operating regimes for the WFGD plant.

Keywords

Wet flue gas desulphurisation
Liquid-gas ratio
Limestone reactivity
Coal quality

Declaration

I declare that this thesis is my own, which is unaided work except where acknowledged in the text. It is being submitted and carried out in fulfilment of the requirements for the degree Master of Engineering in Chemical Engineering at the Johannesburg Campus of the University of the Witwatersrand. It has not been submitted before for any submission at any other university.

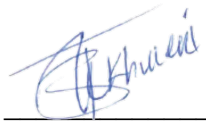

_____

Tsholofelo Lekhuleni
27 May 2024

Dedication,

To my two boys, Kgoši & Kefentše.
GOD SURELY has a plan for us!
Jeremiah 29:11

Acknowledgements

Thank you to,

- GOD, for your promise kept! You are faithful. Covenant keeping God! Amen!
- My mother, and father for always encouraging me to reach out for more.
- My family for their continual encouragement and support while I was working on the thesis.
- My supervisor, Professor Jean Mulopo for guidance, support, and availability. Thank you for continuously encouraging me. Thank you for the opportunity to be led by you. May God richly bless you!
- My manager, Pearl Mazibuko for giving me an opportunity and supporting my career growth in a time when site required more hands-on support, but you still encouraged further studies. It's an honour to work with you.
- Finally, ESKOM, for allowing me to continue with further studies, funding my studies and managing talent in the workplace in trying times.

Abbreviations

AR	Aspen Reactions
ESP	Electrostatic precipitator
GWh	Gigawatt hour
ID	Induced draught
LSFO	Limestone forced oxidation
MW	Megawatt
PSD	Particle size distribution
TWh	Terawatt hour
STP	Standard temperature and pressure
WFGD	Wet Flue gas Desulphurisation

Symbols

C’	total dissolved concentration of a specie	mol/L
C_{ai}	concentration of the solute gas A in the liquid phase	mol/cm^3
C_{gi}	concentration of component in gas phase at the interphase	mol/cm^3
C_{li}	concentration of component in liquid phase at the interphase	mol/cm^3
C_g	concentration of the component in the bulk fluid	mol/cm^3
C_l	concentration of component in the bulk fluid	mol/cm^3
H	Henry law constant.	L·atm/mol.
k_1	equilibrium constant of component 1	mol/L atm
k_2	equilibrium constant of component 2	mol/L atm
P_{ai}	partial pressure of the solute gas A at the interphase	kPa
P_1	Pressure of stream 1	kPa
P_2	Pressure of stream 2	kPa
T_1	Temperature of stream 1	K
T_2	Temperature of stream 2	K
V_1	Volume of stream 1	m^3/h
V_2	Volumes of stream 2	m^3/h
y*	vapour pressure of the component	N/ m^2
δ_g	thickness of the stagnant film in the gas phase	cm
δ_l	thickness of the stagnant film in the liquid phase	cm

Subscripts

l	component is a liquid
g	component is a gas
aq	component is in an aqueous state

Table of Contents

Abstract ..... - 2 -
Declaration ..... - 3 -
Dedication, ... - 4 -
Acknowledgements ..... - 5 -
Abbreviations ..... - 6 -
Symbols ..... - 6 -
Subscripts ..... - 6 -
List of Figures ..... - 10 -
List of Tables ..... - 11 -
1. CHAPTER 1: INTRODUCTION ..... - 12 -
1.1 PROBLEM STATEMENT ..... - 15 -
1.2 RESEARCH OBJECTIVE(S) ..... - 15 -
1.3 BENEFITS OF THE STUDY ..... - 16 -
1.4 METHODOLOGY ..... - 16 -
1.5 DISSERTATION STRUCTURE ..... - 17 -
CHAPTER 2: CASE STUDY BACKGROUND ..... - 18 -
2.1 Process Overview ..... - 18 -
2.2 Process Challenges ..... - 2 -
2.2.1 Liquid-to-gas ratio imbalance ..... - 2 -
2.2.2 High Ash Ingress ..... - 3 -
2.2.4 Ultimate Challenge ..... - 4 -
CHAPTER 3: LITERATURE REVIEW ..... - 5 -
3.1 Coal-fired power station ..... - 5 -
3.1.1 Coal handling and milling ..... - 6 -
3.1.2 Ash system ..... - 6 -
3.1.3 Water & Steam system ..... - 6 -
3.1.4 Air & Flue gas system ..... - 6 -
3.2 SO_2 Emissions ..... - 6 -
3.3 Flue Gas Desulphurisation Technology ..... - 8 -
3.3.1 Wet Flue Gas Desulphurisation System Chemistry ..... - 10 -
3.3.1.1 Limestone handling and preparation ..... - 11 -
3.3.1.2 Limestone slurry distribution ..... - 12 -

3.3.1.3 Flue Gas path ..... - 12 -
3.3.1.4 Air supply ..... - 12 -
3.3.1.5 Absorber/Scrubber ..... - 12 -
3.3.1.6 Demister/Humidity eliminator/Mist eliminator ..... - 13 -
3.3.1.7 Absorber slurry discharge stream ..... - 13 -
3.3.1.8 Gypsum dewatering and handling ..... - 13 -
3.4 Operational conditions that impact WFGD performance ..... - 14 -
3.4.1 Efficiency of the particulate control device ..... - 14 -
3.4.2 SO_2 Concentration ..... - 15 -
3.4.3 Limestone Reactivity ..... - 15 -
3.4.4 pH ..... - 16 -
3.4.5 Liquid to gas ration (L/G) ..... - 17 -
3.4.6 Oxidation ..... - 18 -
3.5 Models to Describe Gas Absorption ..... - 18 -
3.5.1 Mass Transfer ..... - 18 -
3.5.2 Reaction Kinetics ..... - 21 -
3.5.3 Data Driven Models ..... - 21 -
3.5.4 Limitations of the models ..... - 22 -
4 CHAPTER 4: PROCESS MODEL DESCRIPTION AND METHODS ..... - 23 -
4.1 Process model/simulation review ..... - 23 -
4.1.1 Simulation Tool: Aspen Plus ..... - 23 -
4.1.2 Property Method ..... - 24 -
4.1.3 Absorber Unit operation ..... - 24 -
4.1.4 Stream Class ..... - 25 -
4.2 Methodology ..... - 26 -
4.2.1 Data Selection for Model (Operational conditions) ..... - 26 -
4.2.1.1 Flue Gas flowrate ..... - 26 -
4.2.1.2 Absorber Inlet Outlet temperature ..... - 26 -
4.2.1.3 Absorber pH and density ..... - 28 -
4.2.1.4 Oxidation air ..... - 29 -
4.2.1.5 Limestone consumption ..... - 29 -
4.2.1.6 SO_2 emissions ..... - 30 -
4.2.1.7 Absorber Carbonate and sulphite analysis ..... - 31 -
4.2.1.8 Coal specifications and Emissions for Case study 3 ..... - 31 -

4.2.2 Model ..... - 32 -
4.2.3 Model Assumptions ..... - 33 -
4.2.4 Property Method ..... - 33 -
4.2.5 Chemical Reactions ..... - 33 -
4.2.6 Unit Operations Selection ..... - 34 -
4.2.7 Convergence ..... - 35 -
4.2.8 Base Model: Normal Operation ..... - 35 -
4.2.8.1 Process Flow ..... - 35 -
4.2.8.2 Simulation Inputs ..... - 37 -
4.2.8.2.1 Flue Gas ..... - 37 -
4.2.8.2.2 Limestone ..... - 37 -
4.2.8.2.3 Oxygen into CSTR ..... - 37 -
4.2.8.2.4 CSTR conditions ..... - 38 -
4.2.8.2.5 Flash separator and Recycle split ..... - 38 -
4.2.8.2.6 Hydrocyclone ..... - 38 -
4.2.8.3 Mass balance ..... - 38 -
4.2.8.4 Model Sensitivity ..... - 40 -
5 CHAPTER 5: RESULTS AND DISCUSSIONS ..... - 62 -
5.1 Case study 1: Low Limestone reactivity ..... - 62 -
5.2 Case study 2: Liquid to gas ratio imbalance ..... - 66 -
5.3 Case study 3: Variable Sulphur content ..... - 72 -
6 CHAPTER 6: CONCLUSIONS AND RECOMMENDATIONS ..... - 78 -
6.1 Recommendations and current model use ..... - 79 -
6.2 Further improvements and studies ..... - 79 -
REFERENCES ..... - 80 -
8. APPENDIX ..... - 85 -
8.1 Appendix A: ..... - 85 -
8.1.1 Flue Gas Volume Calculation ..... - 85 -
8.1.2 CSTR Volume Calculation ..... - 85 -
8.2 Appendix B: Case Study 1 Results ..... - 86 -
8.3 Appendix C: Case study 2 Results ..... - 87 -
8.4 Appendix D: Case Study 3 Results ..... - 88 -
8.5 Appendix E: Aspen Simulation Base Case ..... - 106 -

List of Figures

Figure 1-1: Electricity generated by source in 2021 with total 215 377 GWh (StatsSA, 2021) - 12 -
Figure 1-2: World Electricity generation in 2018, with a total of 26618.9 TWh (IEA, 2018).- 13 -
Figure 1.4-1 Research methodology.....- 16 -
Figure 2.1-1: WFGD Plant Process Flow .....- 1 -
Figure 2.2.1-1: Deposits on spray headers.....- 3 -
Figure 2.2.2-1: Limestone slurry buildup .....- 3 -
Figure 3.1-1: Typical coal-fired power station (Eskom Holdings SOC Ltd, 2021) .....- 5 -
Figure 3.2-1: SO_2 emissions (kt/year) across the world.....- 7 -
Figure 3.3-1 Classification of FGD technologies (Srivastava & Jozewicz, 2001).....- 9 -
Figure 3.3-2 Typical FGD plant process flow diagram (Córdoba, 2015).....- 10 -
Figure 3.3.1-1: Mass transfer and Chemical reactions for WFGD system.....- 11 -
Figure 3.4.4-1: Form of SO_2 present in reaction tank solution (Steinmuller Engineering, 2013)...- 17 -
Figure 3.5.1-1Mass transfer across phase boundary (Alstom Thermal Systems, 2014).....- 18 -
Figure 3.5.1-2 Absorption of a solute gas A in a liquid solvent from a gas mixture.....- 19 -
Figure 3.5.1-3: Two film theory (Liu, 2023) .....- 20 -
Figure 4.2.1.1-1: Actual Volumetric Flue Gas Flowrates.....- 26 -
Figure 4.2.1.2-1: Actual Inlet absorber temperature.....- 27 -
Figure 4.2.1.2-2: Actual Inlet and Outlet absorber temperature .....- 27 -
Figure 4.2.1.3-1: Actual absorber pH .....- 28 -
Figure 4.2.1.3-2: Actual absorber density.....- 28 -
Figure 4.2.1.4-1: Actual oxidation air.....- 29 -
Figure 4.2.1.5-1: Actual Limestone feed to absorber .....- 30 -
Figure 4.2.1.6-1: Actual SO_2 emissions.....- 30 -
Figure 4.2.1.7-1: Actual absorber carbonate and sulphite concentrations in the reaction .....- 31 -
Figure 4.2.8.1-1: WFGD Absorber Base Model.....- 36 -
Figure 4.2.8.4-1 RADFRAC Outlet Sulphur vs Flue Gas inlet temperature .....- 40 -
Figure 4.2.8.4-2 RADFRAC Absorber slurry SO_2 concentration (left) vs flue gas pressure & RADFRAC Outlet SO_2 (right) vs Flue Gas Pressure .....- 41 -
Figure 5.1-1: WFGD Absorber with variable slurry feed.....- 63 -
Figure 5.1-2: Absorber slurry SO_2/SO_3 vs $CaCO_3$ feed.....- 64 -
Figure 5.1-3: Sulphite-carbonate equilibrium (TNO,EnBW, CSIRO, 2011) .....- 65 -
Figure 5.1-4: Absorber SO_2 and SO_3 performance against pH.....- 65 -
Figure 5.1-5: Absorber slurry pH vs $CaCO_3$ % in feed slurry .....- 66 -
Figure 5.2-1: L/G ratio against Boiler load.....- 67 -
Figure 5.2-2: WFGD Absorber with variable flue gas flow volume .....- 68 -
Figure 5.2-3: Absorber SO_2/SO_3 vs flue gas volumetric flowrate .....- 69 -
Figure 5.2-4: Absorber and reclaim water pH .....- 70 -
Figure 5.2-5: Absorber outlet SO_2 emissions .....- 70 -
Figure 5.2-6: Gypsum production with increasing flue gas flow .....- 71 -
Figure 5.3-1: Actual absorber carbonate and sulphite concentrations in the reaction.....- 77 -

List of Tables

Table 2.2.2-1Consequence of equipment failure ..... - 4 -
Table 3.2-1: Subcategory 1.1: Solid fuel installations (Minimum Emission Standards) ..... - 7 -
Table 3.5.2-1 Acid-Base Equilibrium constants (Neveaux & Moullec, 2011)..... - 21 -
Table 4.1.4-1: Stream Classes (WR Training Pro, 2023) ..... - 25 -
Table 4.1.4-2: Substream Class in Aspen (WR Training Pro, 2023)..... - 25 -
Table 4.2.1.8-4.2.1.8-1: Fuel specifications (Coal) & Projected Emissions..... - 32 -
Table 4.2.8.2.1-1:Flue Gas Conditions ..... - 37 -
Table 4.2.8.3-1 Base model mass balance ..... - 39 -
Table 5.1-1: Low $CaCO_3$ feed to absorber..... - 62 -
Table 5.2-1: High flue gas flow ..... - 67 -
Table 5.3-1:Inlet absorber sulphur content ..... - 72 -
Table 5.3-2: Normal operating coal (Base Case 1.1 % S content) analysis Aspen simulation output. ..... - 74 -
Table 5.3-3: Test Coal (1.6 % Sulphur content) analysis Aspen simulation output. ..... - 75 -
Table 5.3-4: Maximum sulphur 1.41% for limestone supply limit..... - 76 -
Table 8.2-1Case study 1 Results ..... - 86 -
Table 8.3-1 Case Study 2 Results ..... - 87 -
Table 8.4-1 Case Study 3 Results ..... - 88 -
Table 8.4-2: Limestone Limit Results ..... - 97 -

CHAPTER 1: INTRODUCTION

Coal is currently the largest source of energy available for many industries. The combustion of coal involves the reaction of carbon, sulphur, and nitrogen with oxygen and the production of oxides associated with the base component (Munawer, 2018). The power generation sector in South Africa is significantly reliant on substantial quantities of coal to produce electricity. Subsequently, hazardous flue gas is discharged into the atmosphere, thereby causing a significant contribution to air pollution. Sulphur dioxide (SO_2) in particular, is a prominent gas responsible for acid rain and its enduring ecological consequences, including air, water, and land pollution.

Eskom generates approximately 95% of the electricity used in South Africa according to research conducted in 2017; and approximately 95% of its generating capacity is from the coal-fired fleet (Girmay & Chikobvu, 2017). The reliance on coal has decreased to 86.1 % in 2021 (StatsSA, 2021). The electricity generated by sources in South Africa is given in Figure 1-1, where the contribution of nuclear, diesel and renewables is given. The reliance on coal for electricity in South Africa is substantially high in relative percentage when compared to the world electricity generation statistics recorded in 2018 as given in Figure 1-2 (IEA, 2018).

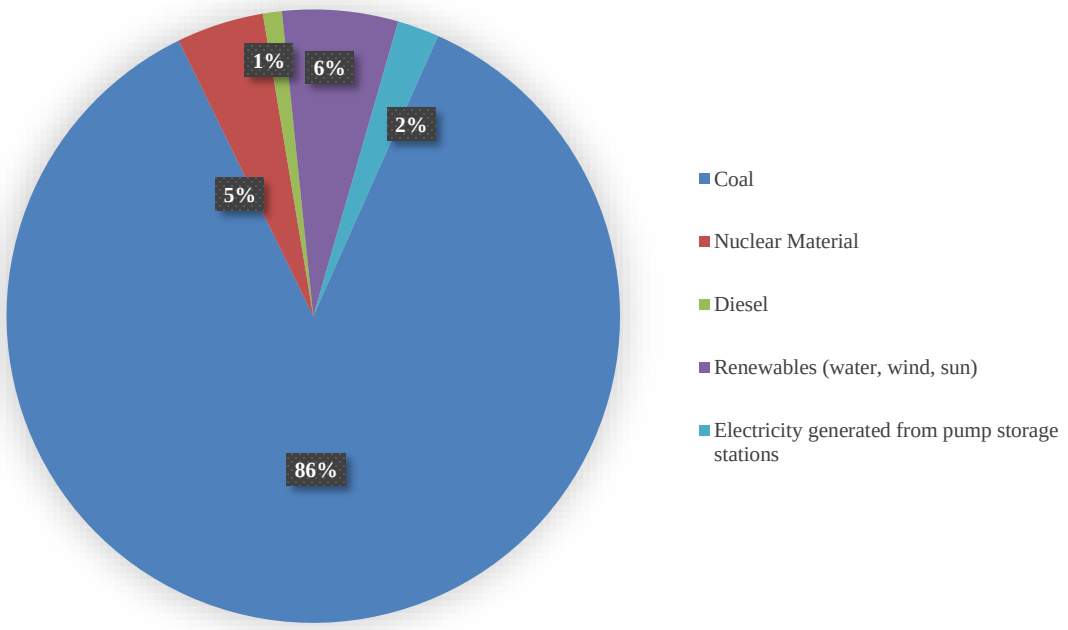

Figure 1-1: Electricity generated by source in 2021 with total 215 377 GWh (StatsSA, 2021)

Power generation is responsible for 82% of generated SO_2 emissions in South Africa (Moganelwa, Schafer, & Godana, 2018). In light of global concerns about public health and environment degradation, in 2010, new emission limits were set by the Department of Environmental Affairs, entailing that all new coal-fired power stations (solid fuel installations) in South Africa are required to install technologies that reduce the emissions of priority gases by 2015 (South African Government Gazette, 2010).

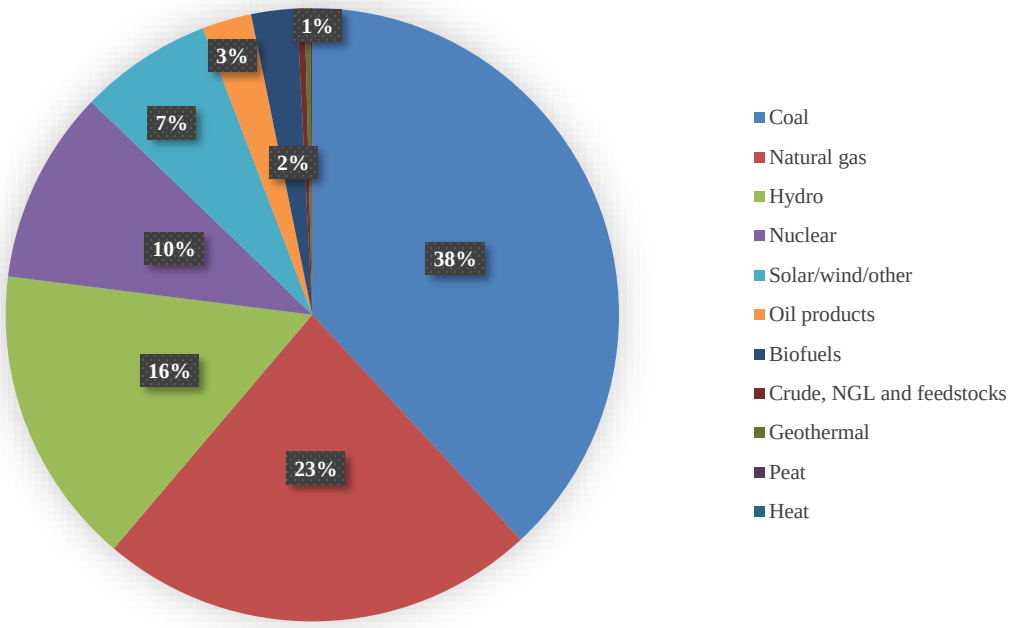

Figure 1-2: World Electricity generation in 2018, with a total of 26618.9 TWh (IEA, 2018)

As the largest power producer in South Africa, Eskom has committed to progressively reduce its environmental footprint and carbon emissions as detailed in "Roadmap for Eskom in a reformed electricity supply industry" (RSA DPE, 2019). Eskom has invested in technology to reduce emissions of sulphates, nitrates, and particulate matter in some of the coal-fired power stations. Eskom power station A has already been retrofitted with a Wet Flue Gas Desulphurisation (WFGD) system. A similar project is being implemented at another newly built Power Station (RSA DPE, 2019).

The wet FGD system instead of the dry FGD system is industrially preferred particularly because of the higher desulphurisation rates that it can achieve, which are between 95-98% SO_2 removal. (Arif Arif, 2015). The dry system efficiency is between 50 and 90% depending on the reagent used (Gingerich, Grol, & Mauter, 2018).The WFGD system is attractive considering the stricter emission limits set in 2010. However, the wet type of FGD is more prone to erosion and corrosion damage, due to the corrosive nature of flue gas requiring treatment and the base reagent used for desulphurisation. Common failures of the WFGD system are erosion of rubber lining, piping, and corrosion on absorption equipment. (Gong & Yang, 2018). Scaling, mist eliminator blockage, and poor reagent utilization are among some of the other challenges on WFGD plants than can lead to unplanned plant downtime (URS Corporation, 2008).

In line with domestic legislation, the WFGD system is essential in ensuring that the power station operates within its SO_2 license limits, therefore, any critical failure in this plant area will violate the emission license. Critical failures in WFGD plants are those that prevent the flow of flue gas through the scrubber or those that decrease the ability of the scrubber to treat the flue gas either due to corrosion, temperature, or erosion-type failures (Miszczyk & Darowicki, 2002).

To prevent critical failures, license violations and degradation of the air quality in the surrounding area, the power station would need to eventually decrease the specific unit generation output to the grid or must shut down unit operations to remedy the problem. Reducing the generation output or the shutdown of a unit may lead to interrupted electricity supply to the national grid, therefore increasing the probability of load shedding.

Load shedding was first implemented in South Africa in November 2007 to manage the supply to the national grid and prevent a blackout. Load shedding has negatively impacted the economy, where the South African economy has lost an estimated R35 billion from period 2007 to 2019 (Walsh, Theron, & Reeders, 2021).
To alleviate the impact of load shedding, Eskom has implemented a 9-point plan addressing unplanned breakdowns, resolving plant maintenance and addressing the challenges affecting the newly built units which have been documented as not operating reliably and optimally. (RSA DPE, 2019).

The newly built power stations have only been operated for approximately six years. During this early operational phase failures due to design flaws, material defects, and commissioning changes are expected. The failures attributed to WFGD that have been incurred thus far are Mist eliminator blockages, spray bank nozzle breakages, recycle pump erosion damages, glass fibre piping cracking, and absorber rubber lining delamination. However, as stipulated in the 9-point plan, it is therefore imperative that all preventable breakdowns of the WFGD plant are managed effectively. Plant breakdowns can be prevented through modelling optimal plant operations to ensure increased system availability (Davidson, Goffredi, & Wedig, 1985)

There are generally three types of FGD system models namely, mass transfer-related models, reaction kinetic models, and recently data-driven models which implement machine learning software (Yishan Guo, 2019). The WFGD system, particularly the absorber is described by a series of complex, 3 phase non-ideal reactions in the WFGD scrubber/absorber. ***Therefore, a model based on reaction kinetics is more suitable for describing simultaneous reactions. The WFGD absorber will be simulated using ASPEN software V12.*** ASPEN steady-state simulation would be able to simulate and assist in predicting efficient operation and control of the WFGD absorber (Aspen, 1998).

The project aim is to simulate a wet flue gas desulfurization (WFGD) plant to ensure a continuous supply of electricity to the grid and conform to SO_2 emission limits as set out by the South department of environmental affairs. A further objective of this project is to simulate the design and current operations of the WFGD plant to provide efficient operation regimes and facilitate online diagnostics.
The simulation design and optimization will take into consideration suboptimal conditions that may affect the absorption process such as;

- Variable limestone feed and quality
- High volumetric airflows into the absorber
- Variable inlet sulphur

By successfully carrying out the optimization and simulation operations outlined earlier, we anticipate determining the final SO_2 emissions that meet the licensing requirements of 500 mg/Nm^3.

1.1PROBLEM STATEMENT

Eskom has invested in technology to reduce emissions of sulphates at the newly built power stations, where Eskom power station A has already been constructed with flue gas desulphurisation (FGD) (RSA DPE, 2019). The newly built power stations are in the early stages of operation, with the plants under six years old. During this phase of operation, early failures occur due to, among other things, design faults, material defects, and operational defects.

Additionally, the WFGD is more prone to erosion and corrosion damage, due to the corrosive nature of flue gas and the limestone slurry used for desulphurisation. Common failures of WFGD system rubber lining delamination, piping fractures, and corrosion on absorption equipment. (Gong & Yang, 2018). These failures can cause contravention of SO_2 emission limits or eventual shutdown of an operational unit leading to insufficient electricity supply to the grid.

The main condition that causes abnormal operation of the absorber are;

- Low limestone quality (CaCO3 less than 89%) or low limestone reactivity
- Liquid-gas ratio imbalance where the flue gas being treated is substantially more than the alkali available for reaction
- Variable inlet sulphur due to multiple sources of coal

To prevent power outages caused by the collapse of the WFGD plant, it is essential to conduct research to reduce the likelihood of predictable plant failures. In this regard, simulations aid in online defect diagnostics and are essential for providing optimal operating conditions and early problem detection.

The following research questions emerge from the study;

- Can a simulation tool be created for an FGD plant that can mimic real-case scenarios?
- Can the performance of the plant be improved with the simulation tool?
- Can predictive analysis be accomplished with the simulation tool?

1.2RESEARCH OBJECTIVE(S)

The objectives of the study are therefore as follows;

a) To simulate abnormal operational conditions of the WFGD absorber in Aspen to determine the final SO_2 removed, which should align with the domestic legislation of emission less than 500mg/Nm^3.

b) To simulate conditions of the WFGD absorber that will predict limiting operations that will lead to decrease in the output power generation to the grid

1.3 BENEFITS OF THE STUDY

The main benefits of the study would be to achieve the following.

a) To improve plant availability of the WFGD plant

b) To reduce load losses (MW) due to the WFGD system

c) To reduce the number of reoccurring plant failures due to suboptimal operational conditions

1.4METHODOLOGY

The outline of the research is given in Figure 1.4.1.

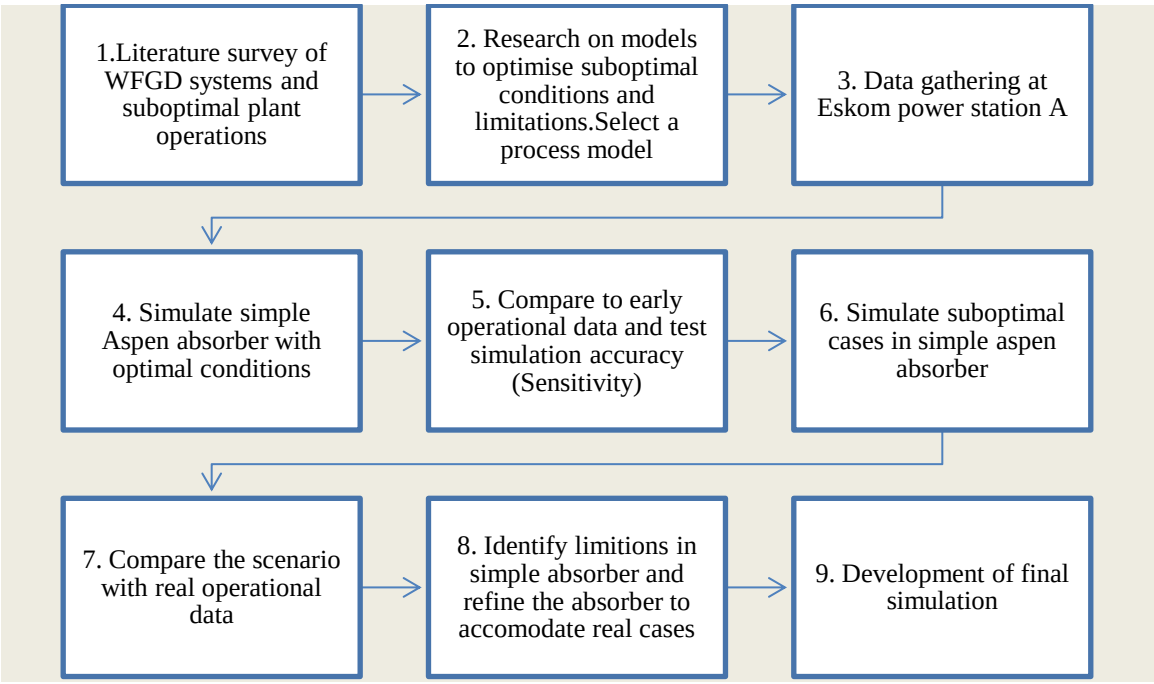

Figure 1.4-1 Research methodology

The scope of the research includes a literature survey of WFGD plans to establish normal operating principles and abnormal operations. Research on available process models for the prediction of

expected plant performance will be covered. The research is mainly focused on current operational trends observed rather than observation on a design basis.

The main condition that causes abnormal operation of the absorber are;

- Low limestone quality or low limestone reactivity
- Liquid-gas ratio imbalance where the flue gas being treated is substantially more than the alkali available for reaction.
- Variable inlet sulphur due to multiple sources of coal

1.5DISSERTATION STRUCTURE

Chapter 1

This chapter focuses on the purpose and motivation for this research. The aims, objectives and scope of the research are also outlined.

Chapter 2

This chapter provides an overview of the WFGD system at an Eskom power station. The Chapter discusses the challenges associated with the technology, which served as the main impetus for the master's research.

Chapter 3

This chapter focuses on the power station overview, and the FGD system as a whole where different technologies are discussed, as well as the processes associated with the different FGD systems.

Chapter 4

This chapter focuses on the process simulator and model development.

Chapter 5

This chapter focuses on the results of the simulation.

Chapter 6

This chapter focuses on the conclusions that are derived from the work. Recommendations and opportunities for further improvements and future studies.

CHAPTER 2: CASE STUDY BACKGROUND

This section explains the current plant configuration and the process issues incurred that motivated the master's studies.

2.1 Process Overview

Eskom power station A has six absorbers that treat 100% flue gas, and each absorber is connected to an 800 MW boiler. The WFGD is post-combustion technology and is located after the fabric filter plant. The system is a limestone-forced oxidation Wet Flue Gas desulphurisation (LSFO-WFGD) system. The plant consists of three sections which is the reagent preparation, the absorber area, and the dewatering system.

The **reagent system** is where the limestone is prepared for the reaction. The limestone which is 19 mm in size will be stored in a silo before being conveyed into the ball mill for crushing. The ball mill is a wet mill where the limestone is mixed with water (reclaim water) in the mill to form a slurry while crushing is also taking place. The slurry is transferred into a hydrocyclone cluster where gravitational and centrifugal forces separate the slurry. Only a slurry product less than -44µm will exit the hydrocyclone cluster as product and the remainder of the product will be recycle back to the mill for recrushing as given in Figure 2.2-1. The outlet density of the mill is controlled (~1230-1250kg/m^3) to achieve the required separation or 30% solid content.

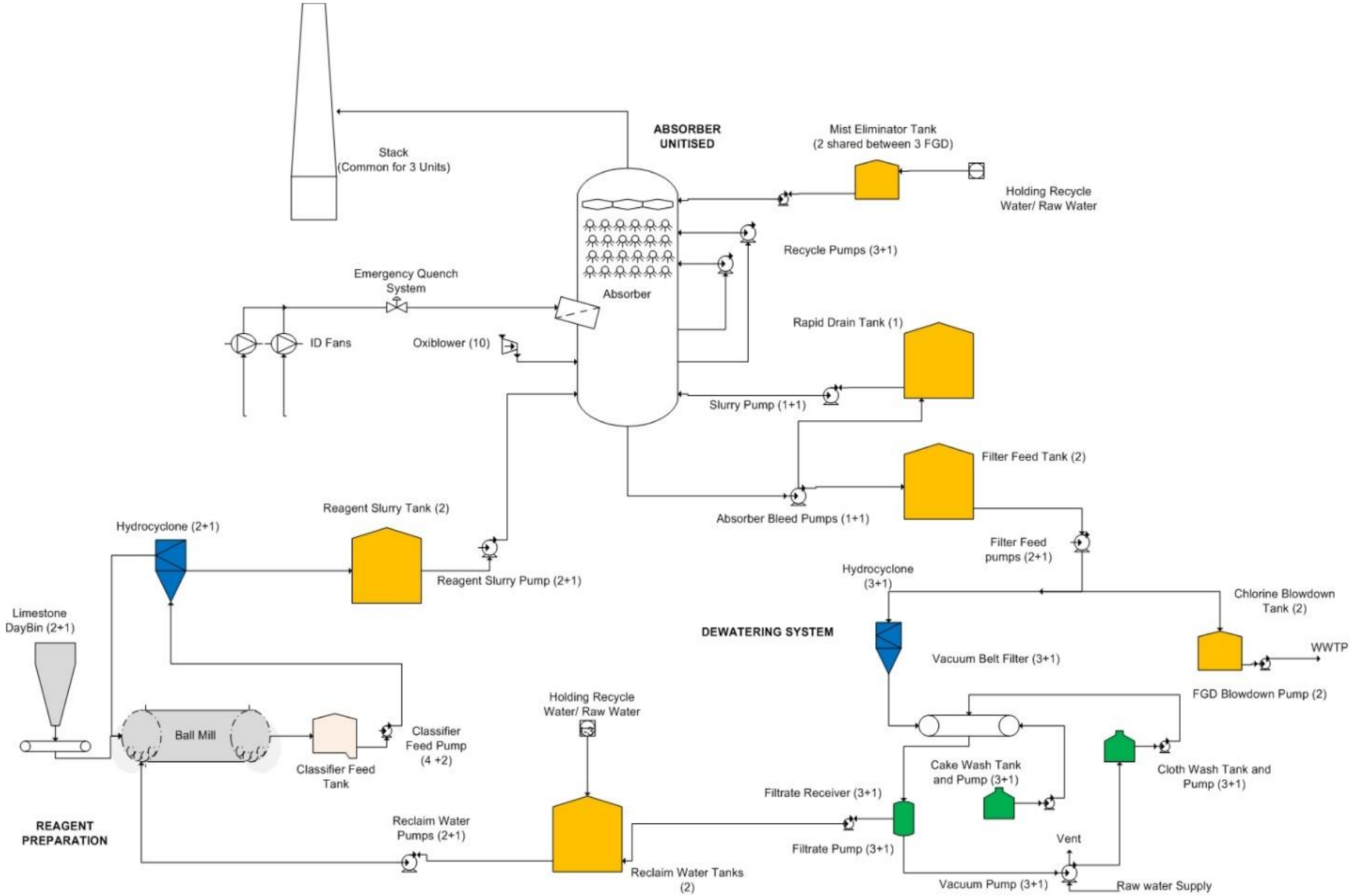

Figure 2.1-1: WFGD Plant Process Flow

The reagent once prepared is pumped into the **absorber system**. The absorber is described by two areas or sections; where the bottom section is the reaction tank, and the top of the absorber is the absorption section where the spray headers are located.
The absorber is a spray tower where the flue gas enters at the middle of the tower at ~130 ℃ and moves upwards into the tower and is sprayed with the limestone slurry through various nozzles located at the spray header. The spraying of limestone slurry takes places in a countercurrent manner where the flue gas is moving upwards into the tower and the limestone slurry is moving downwards through the tower.
The flue gas must be sprayed with copious amounts of limestone slurry to ensure that the SO_2 is absorbed. Several pump arounds indicated as recycle pumps in Figure 2.2-1, to ensure that sufficient limestone slurry is sprayed on the flue gas within the absorber tower. The ratio of limestone slurry in relation to flue gas flow (L/G) is essential in achieving the desired SO_2 removal. For limestone scrubber, the L/G ratio ranges from 2-13 L/m^3 is acceptable depending on the final SO_2 removal that is required (EPA, 2013)

During this interaction, the SO_2 in the flue gas reacts with the $CaCO_3$ in the limestone slurry to form an intermediate product $CaSO_3$. The solid formed ($CaSO_3$) by gravity will move down the tower to the continuously stirred reaction tank where air is pumped via an air compressor into the reaction tank to convert the $CaSO_3$ to $CaSO_4$. The overall reaction is given by reaction 1.

$$\mathbf{CaCO_3 + SO_2 + \tfrac{1}{2}O_2 + 2H_2O \rightarrow CaSO_4 \bullet 2H_2O + CO_2} \qquad \mathbf{(1)}$$

The remainder of the flue gas that did not react moves up the tower to modules called demisters/dehumidifiers/mist eliminators, which solely serve the purpose of disturbing the flue gas path to capture slurry droplets back into the absorber column. This is to ensure that excessive water and large limestone particles do not exit the absorber column. The demystified flue gas exits the absorber at ~45℃.

The absorber reaction tank as discussed above is a holding tank for further reaction. The pH and the density in the reaction tank is monitored continuously to ensure efficient absorption of SO_2. This monitoring is facilitated by an absorber bleed pump which circulates slurry to and from the reaction tank.
In the absorber, the two main variables that control the reactions in the reaction tank are pH and density. The set points for pH and density are targeted to achieve maximum SO_2 removal while minimizing limestone consumption (EPRI, 1979)
The reaction tank pH is used to indicate the amount of unreacted alkaline $CaCO_3$ present in the absorber. The relationship between pH and reagent feed is not linear but in general, when the pH is low, the limestone slurry is added to the absorber, and conversely the opposite is true, that when the pH is high, the limestone slurry into the absorber is reduced (EPRI, 2007).

To prevent the absorber from becoming supersaturated, the level of solids can be minimized by bleeding a controlled amount of volume from the absorber into a storage tank prior to dewatering. The amount is controlled by the density and pH that is being monitored. When the density is between 1140-1200 kg/m^3 and a pH above 5, a controlled amount of absorber slurry can be bled from the reaction tank and transferred to the gypsum dewatering plant.

The **dewatering plant** functions to separate the gypsum ($CaSO_4$) from everything else that was withdrawn from the absorber. The absorber slurry will contain the majority of $CaSO_4$, minor amounts of $CaSO_3$ that did not fully convert, some unreacted $CaCO_3$ and water which is our solvent. The slurry from the absorber is transferred to a hydrocyclone cluster where the gypsum crystal which is slightly heavier than other components is separated. The $CaSO_3$ and water will be collected as overflow from the separation and stored as reclaim water for use in the milling plant. The gypsum is further dewatered on a vacuum belt to remove excess moisture and reduce the final moisture to 10%. The water from the vacuum process is also collected for use as reclaim water in the milling plant. Reclaimed water is a fundamental link between the dewatering and reagent process.

2.2 Process Challenges

The WFGD system requires all systems to function well since each process from reagent, absorber to dewatering all tie into each other. The absorber is the heart of the operation, and it is vital that all processes and reactions function optimally to ensure expected product formation.

The two main process challenges (root cause) that have been encountered in the operation of the WFGD absorber are as given below;

- Liquid-to-gas ratio imbalance
- High ash ingress into the absorber

2.2.1 Liquid-to-gas ratio imbalance

As was discussed in section 2.1, the liquid-to-gas (L/G) ratio is a fundamental concept in the design of the WFGD systems. In the power plant operation, the flue gas volume can be increased or decreased depending on the boiler plant operations. Low flue gas volume is not a problem since the recycle pumps will over-supply liquid slurry. High flue gas rate flow is a concern since the recycle pumps may not be able to supply the required amount of slurry to efficiently desulphurise and meet the emissions limits.

High flue gas flow rate can be caused by (not limited to) inefficient combustion leading to increase in excess air requirement at the boiler or it can be caused by air leakage on unit operations or air attemperation for gas cooling into unit operations that have strict temperature setpoints. The unavailability of a recycle pump due to mechanical failure or maintenance will also result in an imbalance to the L/G ratio.

The liquid to gas ratio imbalance where the liquid is insufficient to treat the flue gas will lead to low pH conditions in the absorber and consequently high sulphur emissions. It is worthy to note that the reaction as described by reaction 1 will not go to completion and therefore the absorber reaction tank holds a solution with *abnormal chemistry* which leads to equipment damage. In this case pumps failures will be due to corrosion and under certain conditions scaling or deposit build up within the absorber module will be evident as shown in Figure 2.2.1-1.



Figure 2.2.1-1: Deposits on spray headers

In general, a high flue gas flow rate will also lead to increased velocities within the absorber module lowering the efficiency of the mist eliminator system, increasing the system pressure drop and ultimately disturbing the chemistry of the absorber.

2.2.2 High Ash Ingress

The WFGD absorber is located after the fabric filter plant and the efficiency of this plant is important as it ensures that dust/ash content into the absorber is below 50mg/Nm^3. Depending on the coal used for combustion and the conditions thereof, the resulting ash can be either alkaline or acidic.

In the Eskom plant case, the ash is alkaline and when the ash content entering the absorber is above the required limit, the ash starts to participate in the absorber reactions. The ash in turn raises the pH in reaction tank rendering the $CaCO_3$ useless. The phenomenon that occurs is that pH in the absorber tank is above 5 but the sulphur content exiting the absorber is higher than the license limit. In this situation more $CaCO_3$ is added to the reaction tank to mitigate the sulphur emission. This operation leads to various failures of plant equipment where in this case, abrasion is the failure mode that evident since the addition of excess limestone increased the overall density in the reaction tank.



Figure 2.2.2-1: Limestone slurry buildup

High ash content into the absorber has led to the following;

- Cementitious deposits in the absorber

- Blockage of piping system
- Increased absorber densities
- Increased solids content in the reclaim water
- Excessive bleeding of the absorber leading to changes in material balances

2.2.3 Consequences of failure in WFGD system

The consequences of failure of the WFGD unit operation are given with an expected load loss. When the boiler plant is in operation, the expected load losses that will be incurred per unit in operation, if the failures given in Table 2.2.2-1 occur.

Table 2.2.2-1Consequence of equipment failure

Failed Component	**Consequence**	**Expected Load loss per unit in operation (MW)**
Fabric filter bag failure	Increase dust to FGD	80-400 MW
O_2 measurement deviation	Increase in volumetric flowrate to FGD	80-400 MW
pH meter	Low pH condition, high emissions, corrosion damage	800 MW
Recycle pump failure	Increase in SO_2 emissions	250 MW per pump
Mist eliminator system	Scaling and high carryover	800 MW

2.2.4 Ultimate Challenge

A process engineer is required to monitor, analyse plant operations, and implement sound engineering principles to optimize plant performance. In the two cases that are discussed in section 2.2.1 and 2.2.2, the fundamental parameters for control of the absorber are flue gas flow rate, limestone concentration or reactivity, pH (which is linked to sulphur content) and density.
The dissertation will show that the WFGD has a series of complex reactions and in order diagnose problem earlier, process simulation is required. Process simulators enable easier calculation of equipment design, and operations; various scenarios can be simulated to ensure safe plant operations and further enable economic assessments of unit operations. The challenges discussed have led to numerous plant failures which ultimately contributed to the inability to supply power to the grid due to the unavailability of the WFGD absorber. To prevent further power outages caused by the collapse of the WFGD plant unit operations, it is essential to conduct research to reduce the likelihood of predictable plant failures. In this regard, simulations aid in online defect diagnostics and are essential for providing optimal operating conditions and early problem detection.

CHAPTER 3: LITERATURE REVIEW

The literature review presented in this chapter focuses on aspects of the WFGD plant to provide a background of the basis of the plant design. Since WFGD plants are post-combustion technology, an overview of a typical coal-fired power plant is discussed at the beginning of this chapter.

3.1 Coal-fired power station

When coal is combusted, it releases several airborne components including sulphur dioxide, nitrogen oxides, carbon dioxide, volatile organic compounds, ash, and a range of heavy metals. These components lead to air pollution when released into the atmosphere in large quantities. The air pollution resulting from these emissions is known to lead to numerous health impacts and environmental problem; therefore, these emissions require reduction or elimination where possible (Munawer, 2018)

In many countries globally, coal is still the largest source of energy available for various industries and other alternatives such as nuclear, diesel, renewable energy sources, and electricity generated from pump sources are currently not sustainable. Coal is still the major source of electricity in South Africa, generating approximately 86.1% of the country's power in 2021 (StatsSA, 2021).

Coal-fired power station involve the pulverization of coal in a mill to provide the required heat energy to convert water to steam in the boiler as given in Figure 3.1-1 (Eskom Holdings SOC Ltd, 2021). The steam generated is fed into a turbine where the steam turns turbine blades to generate mechanical energy. The turbine in turn provides the rotational energy required to drive the generator which convert the rotational energy to electrical energy (Eskom Holdings SOC Ltd, 2021).

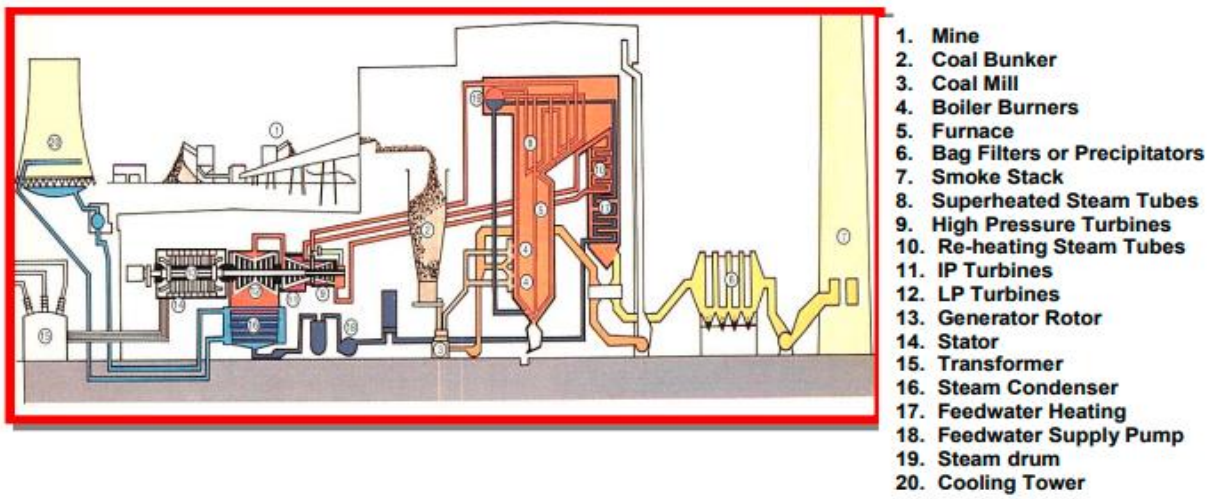

Figure 3.1-1: Typical coal-fired power station (Eskom Holdings SOC Ltd, 2021)

The power station consists of the following system;

3.1.1 Coal handling and milling

The coal handling and milling plants involve the storage, transport, handling and pulverizing of coal. The coal is obtained from a local mine where possible (1) and transported to the station. The coal is stored in stockpiles and conveyed to bins prior to entering the mills. The coal is pulverized in the mills (3) and fed into the boiler through burners (4). The coal is combusted in the boiler or furnace (5) and ash is formed in the process. The combustion of coal involves the reaction of carbon, sulphur, and nitrogen with oxygen and production of their respective oxides (Eskom Holdings SOC Ltd, 2008)

3.1.2 Ash system

The coarse ash in the boiler is discharged at the bottom of the boiler (5). The fine ash escapes the boiler with the flue gas stream which will be discussed in section 3.1.4

3.1.3 Water & Steam system

Feed water (18) enters the boiler through tubes where it is superheated (8) by virtue of being contact with the hot flue gas. The boiler tubes carrying the water are designed in such a way that they achieve multiple passes of contact due to their tube bundle design so that superheated steam is ultimately the result. Once the steam enters the turbine (9,11,12), some steam will condense (6) in the process. The condensate formed goes through feed water heating (17) and thereafter reused back into the system (Eskom Holdings SOC Ltd, 2008).

3.1.4 Air & Flue gas system

The air in the boiler is used to dry, transport, and provide the coal combustion air required. An induced draught (ID) fan is used to provide negative suction through the boiler. During the combustion process the flue gas is pulled through the boiler to an air heater. The air heater is a heat exchanger that power stations employ to ensure that the ambient air used in the operation is heated sufficiently well before entering the boiler. At the exit of the air heater, fine ash particles will be entrained in the flue gas because of the combustion process. The flue gas stream is treated in either an electrostatic precipitator (ESP) or a bag filter (6) to remove the fine ash particles contained in the flue gas stream (Eskom Holdings SOC Ltd, 2008).

As was discussed in section 3.1.1, various oxides are formed in the combustion process such as sulphur dioxide, nitrogen oxides, carbon dioxide, volatile organic compounds, and a range of heavy metals. Sulphur dioxide has been linked to many health impacts and environmental problems and therefore flue gas desulphurisation technologies are employed to remove SO_2 to acceptable levels prior to the flue gas being emitted to the atmosphere.

3.2 SO_2 Emissions

When SO_2 gas is released into the atmosphere, it can be oxidized to form sulphate aerosols that contribute to acid deposition (Skinder, Sheikh, Pandit, & Ganai, 2014). These SO_2 particles fall to the earth in a wet or dry state depending on which medium the gas may encounter such as dust, rain, or snow; and may deposit in water, soil, plants, and surrounding infrastructure (EPA, 2023).

According to NASA OMI data capture regions with high capacity for coal combustion for power generation contributed 31% across the world in 2018 which is 15217 kt/year. The largest SO_2 emission hotspots in 2018 were found in Russia, South Africa, Iran, and Saudi Arabia to mention a few countries (Green Peace, August 2019).

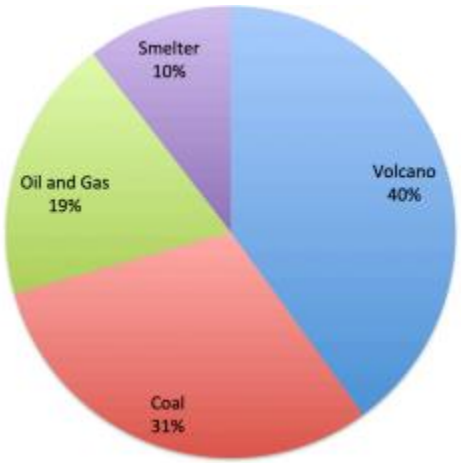

Figure 3.2-1: SO_2 emissions (kt/year) across the world

In South Africa, Mpumalanga province holds a cluster of power stations where approximately 12 power stations are located within 200 km of densely populated areas (Green Peace, August 2019).

The main concern with emissions from coal-fired power stations is the release of large quantities of SO_2 gas near residential areas affecting the ambient air quality and the immediate environment (Morosele & Langerman, 2020). Inhalation of SO_2 gas can lead to strenuous breathing, respiratory illness, and exacerbation of cardiovascular comorbidities (Srivastava & Jozewicz, 2001).

South Africa has shown great commitment in responding to the global climate crisis by aligning itself with targets set out by the United Nations Convention to Combat Climate Change, its Kyoto Protocol, and the Paris Agreement (RSA DPE, 2019).

In 2010 the South African Department of Environmental Affairs (DEA) announced a set of Minimum Emission Standards (MES) for criteria pollutants that that came to effect in 2015 where limits for SO_2 for new and old solid fuel combustion installation is 500 mg/Nm^3 and 3500 mg/Nm^3 respectively (Department of Environmental affairs, 2010).

The new limits as given in Table 3.2-1, entail that any new build project that would use coal as a solid fuel, would need to ensure that all emissions from point sources are within the set restrictions. In terms of the power generation industry, these new limits required a new approach in dealing with SO_2 emissions and opened exploration into FGD technologies.

Table 3.2-1: Subcategory 1.1: Solid fuel installations (Minimum Emission Standards)

Description	Solid fuels (excluding biomass) combustion installations used primarily for steam raising or electricity generation

Application	All installations with design capacity equal to greater than 50MW heat input per unit, based on the lower calorific value of the fuel used		
Substance or mixture of substance		**Plant Status**	**mg/Nm^3 under normal conditions of 10% O_2, 273 Kelvin and 101.3 kPa**
Common name	**Chemical Symbol**		
Particulate matter	N/A	New	50
		Existing	100
Sulphur dioxide	SO_2	New	500
		Existing	3500
Oxides of nitrogen	NOx expressed as NO_2	New	750
		Existing	1100

As the largest power producer in South Africa, Eskom has committed to progressively reduce its environmental footprint and carbon emissions as detailed in "Roadmap for Eskom in a reformed electricity supply industry" (RSA DPE, 2019). Eskom has invested in technology to reduce emissions of sulphates, nitrates and particulate matter in some of the coal-fired power stations. Kusile power station has already been retrofitted with a Wet Flue Gas Desulphurisation (FGD) system and a similar project is currently being implemented at Medupi Power Station (RSA DPE, 2019).

3.3 Flue Gas Desulphurisation Technology

FGD systems are conventionally classified as either once-through or regeneration technology. Once-through process is where the sorbent is used up and disposed as waste. The regenerative process generates no waste in the desulphurisation process (Srivastava & Jozewicz, 2001). FGD systems can further be categorized as dry or wet (EPA, 2023). The classification of different FGD systems is given in Figure 3.3.1.

The typical equipment in a FGD system is an absorber/scrubber where the absorption of the acidic gas occurs, a reaction tank where most of the reactions take place and finally all associated pumping, agitation, spraying equipment.

In the once-through FGD technology, in the SO_2 scrubbers/absorbers, the basic principle is that a reagent which is alkaline is injected into a scrubber tower where the alkaline mixture absorbs the acidic SO_2 gas from the flue gas stream. The neutralized compound is formed after the interaction of the SO_2 and the alkaline reagent, and usually a solid is formed. The solid formed from the reaction is removed from the scrubber using various equipment. In most cases, the alkaline is calcium or sodium based. In wet or semi-dry FGD systems, the alkali is a slurry in both systems, but the alkali is present in higher concentration in the semi-dry system. In a dry system, the alkali is in powder form and injected pneumatically into the scrubber.

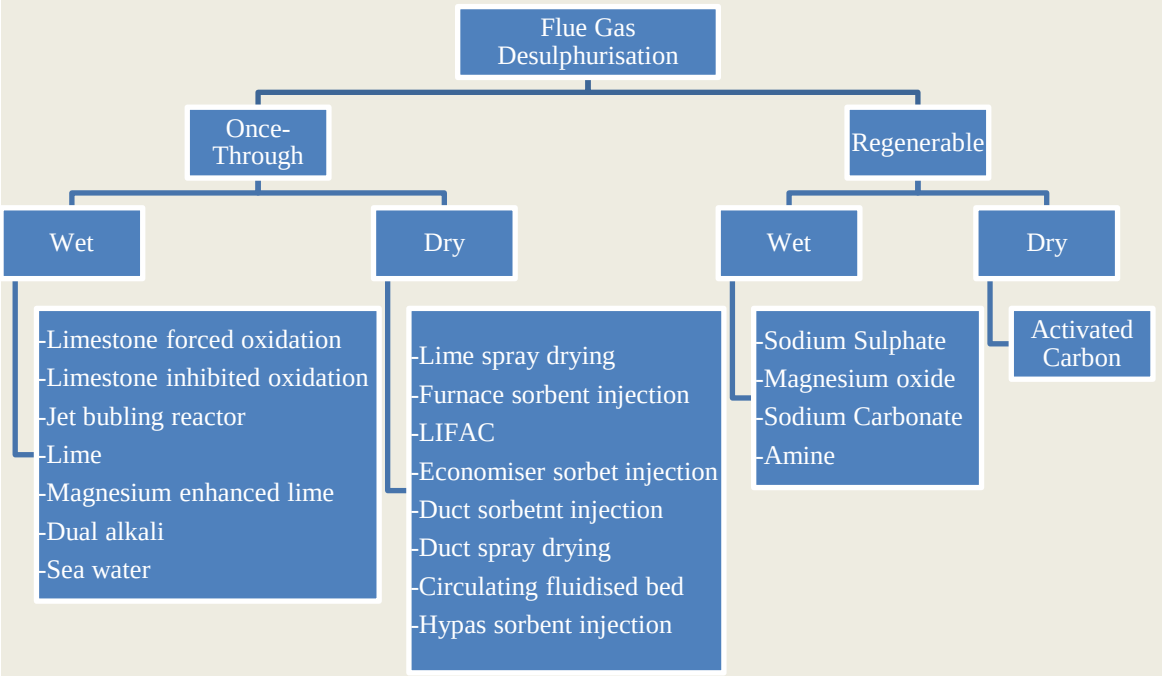

Figure 3.3-1 Classification of FGD technologies *(Srivastava & Jozewicz, 2001)*

In regenerable technologies, no waste is produced since the SO_2 gas is released when the sorbent is regenerated, enabling further processing of SO_2 to either form H_2SO_4, sulphur and liquid SO_2. According to Srivastava et al (Srivastava & Jozewicz, 2001) wet limestone FGD systems, have been predominantly selected over other FGD technologies due to reasonable cost and extensive applications in comparison to regenerable technologies. The research project will focus and expand on a wet FGD systems as shown in Figure 3.3-2.

In wet FGD systems the flue gas enters an absorber/scrubber, and it is sprayed with an alkali slurry. The alkali represented in Figure 3.2.2 can be Lime/limestone. The alkali slurry is circulated by means of withdrawing it from the bottom of the scrubber into various nozzles at the top of the scrubber system. The aqueous alkali slurry is sprayed at different locations using nozzles to ensure good contact for optimal SO_2 removal (EPA, 2023).

In a case where the alkali slurry is limestone; the solid formed during reaction is calcium sulphite ($CaSO_3 \cdot ½H_2O$) or calcium sulphate ($CaSO_4 \cdot 2H_2O$) (EPRI, 2007). The remainder of the flue gas passes through mist eliminator/demister before leaving the scrubber to remove entrained water droplets from the flue gas stream.

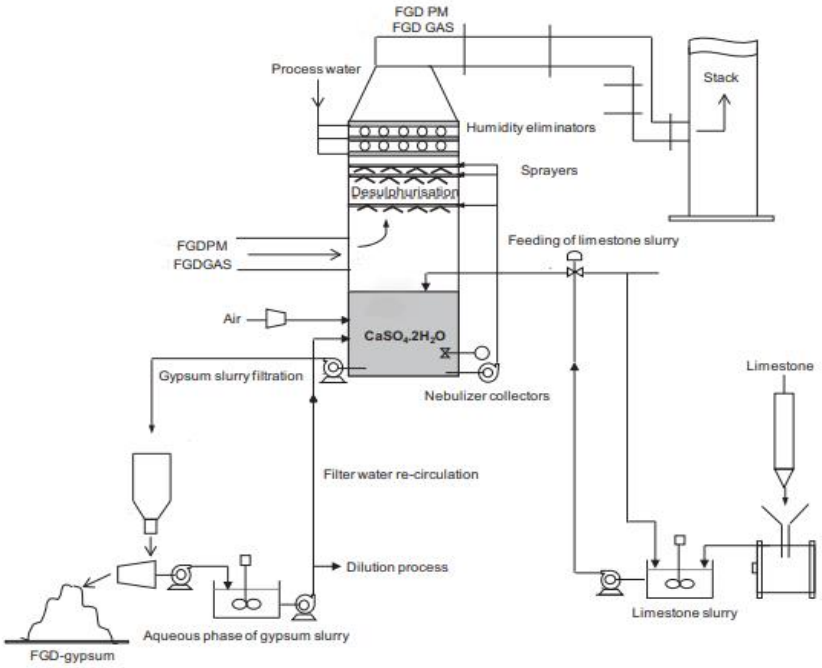

Figure 3.3-2 Typical FGD plant process flow diagram *(Córdoba, 2015)*

At the bottom scrubber if there is the formation of calcium sulphite, oxygen is forced into the scrubber to ensure full conversion to calcium sulphate which is commonly called gypsum. This is limestone forced oxidation (LSFO). This ensures that the byproduct formed is always gypsum and not the intermediate product.

3.3.1 Wet Flue Gas Desulphurisation System Chemistry

There are three types of reactions that occur in alkaline wet scrubbing processes and they are given below (EPRI, 2007) .

- Gas-liquid reactions,
- Liquid-liquid ionic interactions and
- Liquid-solid reactions.

The mass transfer steps and chemical reactions that take place in a WFGD Lime/Limestone system are given in Figure 3.3.1-1.

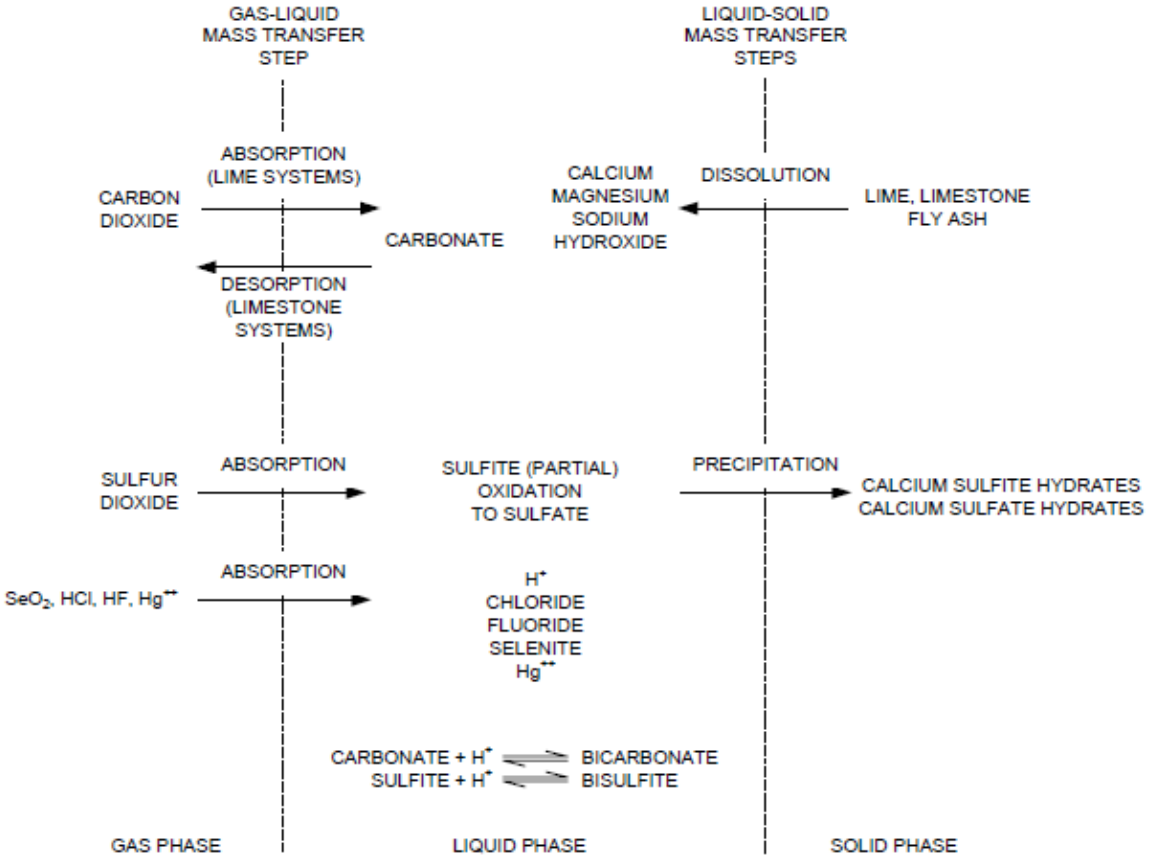

Figure 3.3.1-1: Mass transfer and Chemical reactions for WFGD system

The overall reaction (reaction 1) for wet scrubbing using limestone is given below is given again in this section for easy reference.

$$CaCO_3 + SO_2 + \tfrac{1}{2}O_2 + 2H_2O \rightarrow CaSO_4 \cdot 2H_2O + CO_2 \qquad (1)$$

The limestone forced oxidation WFGD plant consists of 8 subsystems and each section will be described below, with reference to Figure 3.3.1-1 and the associated reactions.

3.3.1.1 Limestone handling and preparation

The limestone will act as an alkaline required in the desulphurisation process. The limestone will need to be milled to the required particle size. The limestone will be mixed with water to form a fine slurry mixture which will be pumped to the absorber or stored if produced in excess. The reaction of limestone dissolution ad dissociation(ionization) is given below. This process describes the solid-liquid mass transfer step.

$$CaCO_3\,(s) \rightarrow Ca^{2+}\,(aq) + CO_3^{\,2-}(aq) \qquad (2)$$

3.3.1.2 Limestone slurry distribution

The limestone slurry is pumped in a controlled manner to the absorber as per stoichiometric ratio that is required for desulphurisation.

3.3.1.3 Flue Gas path

The flue gas from the exit of the ESP or bag filter will enter the absorber tower. As was discussed in section 3.1.4 where various oxides are formed in the combustion process such as sulphur dioxide, nitrogen oxides, carbon dioxide, volatile organic compounds, and a range of heavy metals. The main component that will be removed from the flue gas stream is SO_2. The limestone supply will be equated to the amount of SO_2 entering the absorber.

3.3.1.4 Air supply

The system described is a LSFO, therefore the air supply provides additional oxygen required to convert all the $CaSO_3$ to $CaSO_4$. The reaction describing oxygen dissolution into the absorber is given below by reaction 3.

$$\mathbf{O_2(gas) \rightarrow O_2(aq)} \qquad \mathbf{(3)}$$

3.3.1.5 Absorber/Scrubber

In the absorber, the limestone slurry is firstly pumped to the absorber reaction tank. The slurry in the reaction tank is circulated by withdrawing it from the bottom of the absorber reaction tank to the top of the absorber. The slurry is distributed to various nozzles so that the slurry can spray the flue gas as it travels upwards into the absorber. The carbonate ions reaction with the hydronium ions as shown below. This is the limestone liquid phase to form the bicarbonate and given in reaction 4.

$$\mathbf{CO_3^{2-}(aq) + H^+(aq) \rightarrow HCO_3^-(aq)} \qquad \mathbf{(4)}$$

The SO_2 gas encounters the water in the absorber (gas-liquid mass transfer) and is absorber into the liquid first as per the reaction below. The water in an electrolyte system is represented by reaction 5. Water in the electrolyte system will be represented as either H^+ or H_3O^+

$$\mathbf{H^+(aq) + OH^-(aq) \leftrightarrow H_2O(l)} \qquad \mathbf{(5)}$$

$$\mathbf{SO_2(g) + 2H_2O(aq) \rightarrow HSO_3^-(aq) + H^+(aq)} \qquad \mathbf{(6)}$$

A chemical reaction takes place with the oxygen in the absorber reaction tank as indicated below;

$$\mathbf{HSO_3^-(aq) + 1/2O_2(aq) \rightarrow HSO_4^-(aq)} \qquad \mathbf{(7)}$$

The acid base neutralization reaction takes place as shown by reaction 8 to release CO_2 gas.

$$H^+(aq) + HCO_3^-(aq) \leftrightarrow H_2O(l) + CO_2(g) \quad (8)$$

The absorbed SO_2 reacts with the dissolved limestone to form the intermediate product calcium sulfite ($CaSO_3$) and calcium sulphate ($CaSO_4$), or more commonly known as gypsum. The next series of reactions are called ion pair formations or associations.

$$HSO_3^-(aq) + Ca^{++}(aq) \leftrightarrow CaSO_3(aq) + H^+(aq) \quad (9)$$

$$Ca^{++}(aq) + H_2SO_4(aq) \leftrightarrow CaSO_4(aq) + 2H^+(aq) \quad (10)$$

Further limestone dissolution can take place in the absorber as given below;

$$CaCO_3(s) + H_2O(l) \leftrightarrow Ca^{++}(aq) + HCO_3^-(aq) + OH^-(aq) \quad (11)$$

The calcium sulfite and calcium sulphate remain dissolved in water until the solution in the absorber reaction tank becomes saturated. In this state the solution in the reaction tank forces the calcium sulfite and calcium sulphate to precipitate out of the solution. The precipitation reactions are given below;

$$Ca^{++}(aq) + SO_3^{--}(aq) + {}^1/_2H_2O(l) \rightarrow CaSO_3 \cdot {}^1/_2H_2O\ (s) \quad (12)$$

$$Ca^{++}(aq) + SO_4^{--}(aq) + 2H_2O(l) \rightarrow CaSO_4 \cdot 2H_2O\ (s) \quad (13)$$

3.3.1.6 Demister/Humidity eliminator/Mist eliminator

The absorber in this case, the FGD described is a wet system which is in countercurrent exchange with flue gas. The volumetric flow would naturally carry a large amount of water to the exit of the absorber. The demister acts as a barrier to deter or manipulate the natural path of the flue gas. By doing so the flue gas impacts the mist eliminator plate. As more droplets impact the plate larger droplets combine and fall back into the absorber due to gravity (Kimre, 2020).

3.3.1.7 Absorber slurry discharge stream

In the absorber the liquid will become concentrated with gypsum. Once the liquid is saturated, the gypsum formed will precipitate out of solution. The gypsum formed will need to be pump out of solution to allow further desulphurisation to take place. This frequent purging allows for continuous desulphurisation (EPRI, 2007).

3.3.1.8 Gypsum dewatering and handling

The slurry discharge stream from the absorber contains unreacted $CaCO_3$, $CaSO_3$ and $CaSO_4$ in liquid. The gypsum dewatering plant aims to separate the $CaSO_4$ from all other components. The

slurry can be taken to various separating equipment such as hydrocyclones or vacuum belts. The water collected from the separation process is termed reclaim water and is reused in the limestone preparation and many other waters uses in the WFGD plant.

3.4 Operational conditions that impact WFGD performance

A short overview was given in section 2 of operational challenges that have impacted the Eskom power station A. This section aims to discuss other parameters that will affect the WFGD performance and are given as follows;

- Efficiency of particulate control device
- Inlet SO_2 concentration
- Limestone reactivity
- pH
- Liquid to gas ratio
- Oxidation

3.4.1 Efficiency of the particulate control device

The particulate control device in power stations is either an ESP (electrostatic precipitator) or a fabric filter system. These systems are usually placed upstream before the FGD. The removal efficiency of both ESP and fabric filter is recorded as 99% (Nicol, 2013). Therefore, these control devices should be able to comply with limit of 50 mg/Nm^3 which is current regulatory limit for dust or particulate matter in South Africa (Department of Environmental affairs, 2010).

As with any plant operation, challenges will occur, and an ingress of ash will enter the WFGD absorber. High ash contents can lead to a phenomenon called “limestone blinding” and is caused by aluminium-fluoride which is mainly an aqueous complex in the scrubbing slurry due to coal which has high fluorine content. Aluminium dissolves in the absorber slurry and reacts with the separated HF. Aluminium-fluorine complexes jacket limestone particles and prevent dissolution (Heiting, 2017).
The consequence could be a falling pH value of the scrubbing slurry, and the reagent control system continues to supply limestone in response to the changes. In this case, the SO_2 emissions may also increase above 500 mg/Nm^3. This results in gypsum which contains limestone with carbonate contents above a limit of 1.3% by mass, constituting a contaminant to sellable gypsum.

The formation of aqueous complexes modifies the behaviour of trace elements involved in the FGD process where the measured chemistry is undesirable (Córdoba, 2014). Apart from affecting the absorber chemistry, ash can also increase erosion of absorber internals (EPA, 2013). It therefore important to have an online measurement of the incoming flue gas to measure the incoming particulate into the absorber (EPRI, 2007)

3.4.2 SO_2 Concentration

The inlet sulphur or sulphur dioxide content is an important parameter in the operation of the WFGD system. The sulphur content will vary depending on the coal source that is used in the boiler combustion. The WFGD design removal efficiency is calculated based on the inlet sulphur or sulphur dioxide, and the allowable emissions limit (EPA, 2013).In general, the higher the sulphur content, the more limestone slurry is required to ensure that desulphurisation occurs.

Once the SO_2 is within the absorber, solubility, and displacement of SO_2 become important. (Córdoba, 2014). The SO_2 equilibrium can be represented by equation 14.

$$y^* = \frac{C'10^3[H^+]}{k_1(k_2+[H^+]} \quad (14)$$

where k_1 (mol/L atm) is the equilibrium constant of SO_2 gas to liquid phase reaction, k_2 (mol/L atm) is the equilibrium constant of $CaCO_3$(s) dissociation and bicarbonate formation, C'(mol/L) is the total dissolved concentration of SO_2; $[H^+]$ is the concentration of protons at equilibrium; and y* is the vapour pressure (N m^{-2}) of SO_2 (mg/L).

It can deduced from equation 14, that as the hydronium ions increase (under acidic condition where the system pH is below 4), the pressure of the SO_2 at equilibrium increases, therefore decreasing its capacity to be absorbed into the limestone liquid film (Wilcox and Babcock, 1993).

It has been observed that the reaction of SO_2 to form HSO_3^- as given in reaction 6, increases with increasing of pH from 0 to 4.5 (Dzhonova-Atanasova, Razkazova-Velkova,, & Ljutzkanov, 2011). Therefore, the SO_2 concentration in the electrolyte solution is decreased and the HSO_3^- concentration is increased in solution.

3.4.3 Limestone Reactivity

In the WFGD design phase, the limestone quality and reactivity are used calculate the reaction tank dimensions, the limestone consumption and the final SO_2 removal that can be achieved (Tata Power, 2009). According to Tata Power (2009), limestone reactivity is defined as the "*a direct measure of how readily a limestone will provide alkalinity to neutralize the acid resulting from SO_2 dissolution in water*". The limestone reactivity is considered an important parameter in the operation of the WFGD (Carletti, De Blasio, Makila, Salonen, & Westerlund, 2015).

The limestone dissolution rate is affected by slurry pH, temperature, impurities, surface area, CO_2 stripping, and chlorides concentration (Walsh, et al., 2006).

The slurry pH has an impact on limestone reactivity since the more H+ ions that are present in solution, the more favorable the reaction with carbonate or bicarbonate ions. The limestone dissociation reaction as given by reaction 2 is more favorable as the temperature increases. It has also been seen that the higher the rate of CO_2 stripping the higher the rate of limestone dissolution into solution (Walsh, et al., 2006).

The properties of the limestone such as particle size distribution or structure, porosity and impurities play a vital role in the capacity of the limestone to increase the pH of the absorber reaction mixture so that its able to facilitate the absorption reaction (Córdoba, 2015).

The chlorides in the coal or water used in the WFGD should be monitored since the chlorides concentration decrease the rate of limestone dissolution into solution (Chang, 2005).
Impurities in the limestone such as dolomite will influence the reactivity since the overall percentage of calcium carbonate is decreased. Limestones which contain dolomite are less reactive in general (Chang, 2005). In a study conducted by Lim *et al* (2020) where a WFGD was modeled in ASPEN using low grade limestone and compared to a higher grade limestone, it was found that the SO_2 removal efficiency was satisfactory in both cases but the final quality of gypsum was below standard due to the $MgCO_3$ impurity in the limestone. Therefore, if the intent is to create a sellable gypsum, the limestone should contain minimal impurities.

3.4.4 pH

The pH is a very important process parameter in monitoring the absorption reactions. In conventional FGD system, the reagent supply and oxidation air are controlled by monitoring the pH. The pH should be monitored continuously in the WFGD system and typical limestone WFGD system maintain pH between 5-6 where SO_2 solubility is optimal and scale buildup is minimal (Córdoba, 2014).

The limestone is an alkaline and there increase in the limestone feed into the absorber will result in a higher pH. High pH can achieve greater SO_2 removal in absorber but at the probability of increasing scaling within the absorber module. Therefore, it is important to establish an acceptable operating regime for a specific WFGD system (EPRI, 2007).

Each WFGD system is unique in its operations, but the equilibrium relationships of SO_2 absorption and SO_3 formation hold true for all systems where a typical WFGD is given in Figure 3.4.4-1.

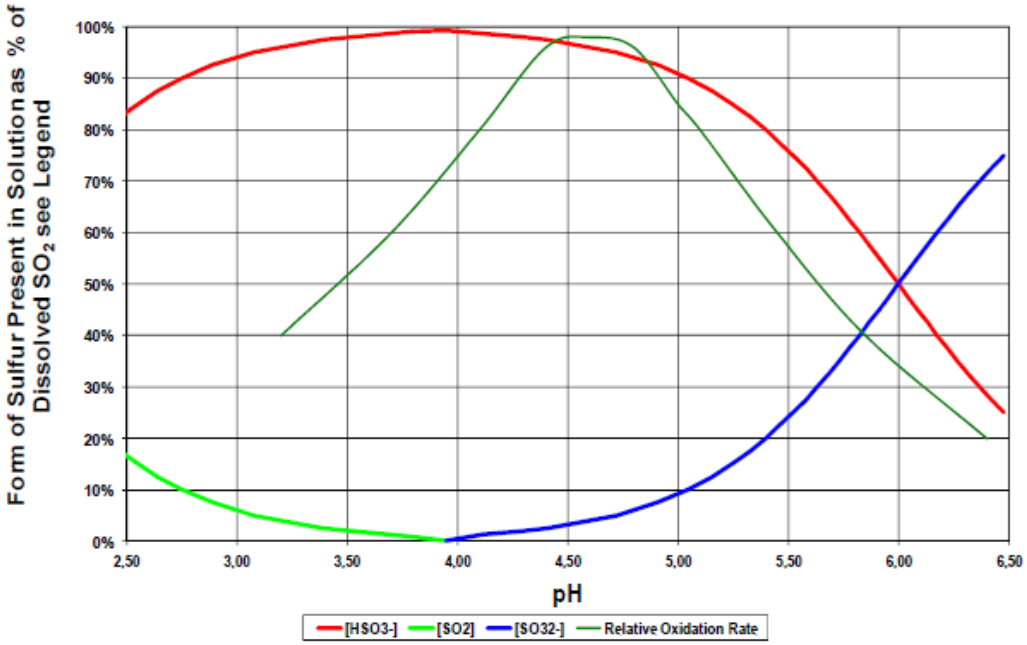

Figure 3.4.4-1: Form of SO_2 present in reaction tank solution (Steinmuller Engineering, 2013)

The pH can be used to indicate which species are dissolved in the electrolyte systems as can be seen in Figure 3.4.4-1 where the sulphur dioxide dissolves and the pH of the system is shifted to low pH regimes. Depending on the particular WFGD in operation, certain pH ranges above pH 6 are avoided due to formation of scale within the absorber module (EPA, 2023). These equilibrium relations assist in determining which reactions are taking place in the absorber, and where fine tuning of operational conditions can be established.

3.4.5 Liquid to gas ration (L/G)

The liquid to gas ratio is defined as the alkaline slurry liquid relative to amount of flue gas that is requiring treatment, where L/G is given in units L/m^3. In practice, the amount of liquid in L/G ratio is indicated by the number of pumps providing the liquid recycle for the flue gas being treated. Operational experience has shown that maintaining the required L/G ration assists in the following;

- enough limestone slurry for sulphur dioxide absorption
- quenching which ensures lower flue gas temperatures within the absorber
- high L/G ratio assist to avoid scaling problems in the absorber since the absorber outlet is more dilute

The liquid to gas ratio is an important principle in mass transfer in the absorber since by decreasing the L/G ratio, the SO_2 removal is effectively decreased. The more liquid available for spraying the flue gas, entails, the more surface area and probability for SO_2 absorption. In FGD systems, L/G values tends to the minimum values of 1.1-2.2 (Córdoba, 2014) to reduce the cost and can be as high as 15 (EPA, 2023).

3.4.6 Oxidation

The WFGD system can operate under natural oxidation or forced oxidation. In the forced oxidation system, the air is added to the FGD system through a compressor to force oxidation of the SO_2 from sulphite to sulphate. The stoichiometric amount of O_2 is added to the absorber with an excess of 5% in practice. In limestone forced oxidation WFGD, it is important that oxidation operates continuously to prevent the formation of undesired species such as $CaSO_3$.

3.5 Models to Describe Gas Absorption

A wet limestone scrubbing system, is described by a series of complex kinetic- and equilibrium-controlled reactions which occur in the gas, liquid, and solid phases. Some of the reactions take place simultaneously and therefore a rigorous model is required to compute all these interactions and reactions accurately (Arif Arif, 2015).

There are various studies focusing on modelling and optimization of FGD system and generally three models are used; mass transfer theories, reaction kinetics or data driven models. The next section will briefly discuss each model used for WFGD systems.

3.5.1 Mass Transfer

Mass transfer theories specifically model the interphase mass transfer between gas/liquid and or liquid/liquid interfaces. In the WFGD system there is transfer of material between phases and these relationships are important in separation processes (Green & Perry, 1984)

The main focus of the Masters dissertation is the absorber unit operation. To understand the need for a dynamic tool to model the absorber reactions it is important to understand the basic parameters that govern the absorption. The SO_2 laden flue gas enters the absorber tower. The flue gas encounters the $CaCO_3$ slurry as shown in the Figure 3.5-1-1; where the SO_2 enters the liquid phase and is absorbed into the liquid film.

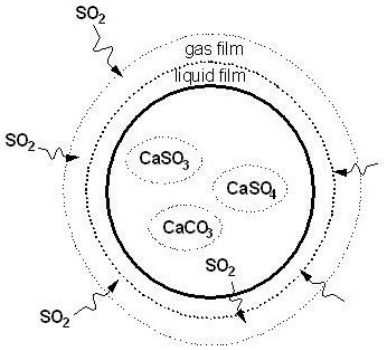

Figure 3.5.1-1Mass transfer across phase boundary (Alstom Thermal Systems, 2014)

Absorption is usually classified as either physical absorption or chemical absorption. In an absorption system where no reaction occurs between the gas-liquid phase are known as physical absorption while the systems where reaction occurs between the phase is referred to as chemical absorption (Green & Perry, 1984).

In the description given of the WFGD absorption process, one must take note that there is mass being transferred between liquid and gas phase. The degree to which a gas is absorbed by a solvent is determined by is its partial pressure (Prakashan, 2015).

Figure 3.5.1-2 shows a gas A being absorbed into a liquid solvent. At the interphase of the two phases, equilibrium exists and there is no resistance to mass transfer. The relationship at the interphase can be describe by Henry's law.

$$P_{ai} = H \cdot C_{ai} \tag{15}$$

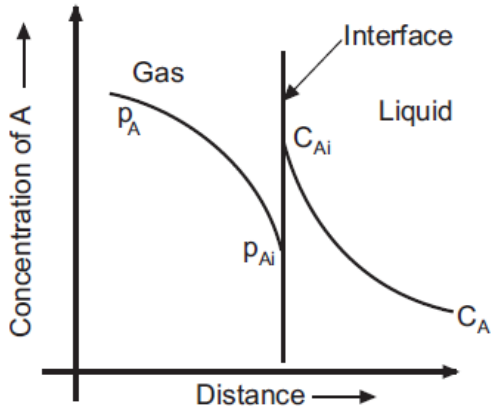

Figure 3.5.1-2 Absorption of a solute gas A in a liquid solvent from a gas mixture

(Prakashan, 2015)

Where, P_{ai} is the partial pressure of the solute gas A at the interphase, C_{ai} is the concentration of the solute gas A in the liquid phase and H is the Henry law constant.

Henry's law is however only applicable in cases where the molecules involved are in equilibrium, the pressure of the system should not be too high, and finally its only applicable in cases where the molecules do not participate in the chemical reactions (Petrucci, Harwood, Herring, & Madura, 2007).

In terms of film theories, known theories to model interphase mass transfer are the penetration theory, surface renewal theory, and film theory. The three theories are all attempted in extending theoretical calculations to suit more complex separation processes such as flue gas desulphurisation system (Green & Perry, 1984)

The film theory which was developed by Nernst in 1904, which states that near the interphase there exist a stagnant film where the bulk liquid is not in motion (Katoh & Yoshida, 2009). Nernst further states that transport at the interphase is only governed by molecular diffusion. Lewis Whitman in 1924 expanded on this concept by proposing a two stagnant layer at the interphase as given by Figure 3.5.1-3. The mass transfer at the interphase is also only by molecular diffusion (Liu, 2023). In Figure 3.5.1-3 δ_g and δ_l represent the thickness of the stagnant film in the gas and liquid phase respectively. C_{gi} and C_{li} represent the concentration of component in either liquid or gas phase at the interphase; which is at equilibrium. Concentration C_g an C_l represent the concentration of the components in the bulk fluid which are not at equilibrium.

When the mass transfer involves droplets, the penetration theory by Higbie which was developed in 1935 is usually used. Penetration theory states that there is a movement of eddies from the bulk of the solution towards the interface. At the point where the eddies are at the interphase, molecular diffusion can take place (Katoh & Yoshida, 2009). Dankwerts in 1951 improved on the penetration theory where a residence time distribution for contact at the interphase was introduced as apposed to fixing a contact time. Ultimately all the discussed theories aim to estimate the mass transfer coefficient (which cannot be measured directly) so that the concentration of the species involved in gas/liquid absorption at equilibrium can be determined.

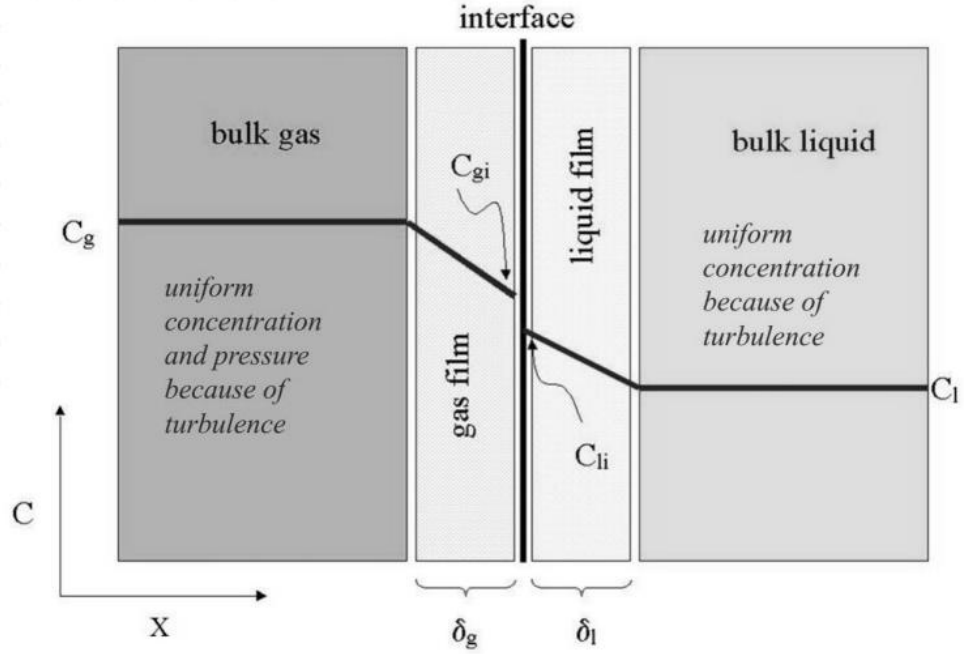

Figure 3.5.1-3: Two film theory (Liu, 2023)

Brogren *et al*. (1997)used the penetration theory to calculate the dynamic absorption rate of sulphur dioxide into a droplet of limestone slurry by estimating high mass transfer coefficients close to the absorber spray nozzles and low mass transfer coefficients below the spray region. The model can be used to quantify the mass transfer within an absorber (Brogren & Karlsson, 1997).

Gerbex *et al.* (1995)developed a non-stationary model to predict the SO_2 removal rate and the chemical composition of the absorber slurry for a 3 MWe coal-fired power plant. Penetration theory was used to estimate the mass transfer coefficients (Gerbec, Stergarsek, & Kocjancic, 1995)

Dou *et al*. (2009)used the two film theory to analyse the SO_2 removal process. The model was able to predict the SO_2 removal efficiency and comparison between calculated and experimental values were in agreement (Dou, Pan, Jin, Wang, & Li, 2009).

Kallinkos *et al* (2010)also used two film theory to simulate a WFGD system for different SO_2 loads and found that the liquid dispersion in the tower affects the SO_2 absorption rate. In this model, the mass transfer coefficients were adopted from available literature sources and were not experimentally determined (Kallinkos, Farsari, Spartinos, & Papyannakos, 2010)

A model using unsteady state theory was developed by Zhong *et al* (Zhong, et al., 2008)which allows for variable coal properties, and unstable boiler operations to provide advice for performance optimization of the WFGD system (Zhong, et al., 2008)

Yao evaluated the SO_2 gas phase mass transfer coefficient of each spray layer, and was able to provide online fault diagnostics and predict performance of the FGD plant (Che Yao, 2022).

3.5.2 Reaction Kinetics

Reaction kinetic model consists of a mathematical model based on the conservation of chemical species and energy during the process.

The model would logically illustrate the chemical absorption process (Neveaux & Moullec, 2011), the gypsum conversion (Tan, Zhang, Li, Li, & Shen, 2017) and finally the limestone dissolution (Carletti, De Blasio, Makila, Salonen, & Westerlund, 2015) in order optimize SO_2 removal. The acid-base equilibrium and associated equilibrium constants are given in Table 3.5.2-1 and are used in generating the kinetic model.

Table 3.5.2-1 Acid-Base Equilibrium constants (Neveaux & Moullec, 2011)

$$\ln K = A + B/T + C \ln T + DT$$

Equilibrium	**A**	**B**	**C**	**D**	**pK_a at 318 K**
$2H_2O = H_3O^+ + OH^-$	140.932	-13445.90	-22.4774		13.40
$SO_2\,(aq) + 2H_2O = HSO_3^- + H_3O^+$	-1.932	-3768.0	-20		2.07
$HSO_3^- + H_2O = SO_3^{2-} + H_3O^+$	-21.274	1333.40			7.42
$2H_2O + SO_3(aq) = HSO_4^- + H_3O^+$	6.908				-3.00
$H_2O + HSO_4^- = SO4^{2-} + H_3O^+$	-4.490				1.95
$CO_2\,(aq) + 2H_2O = HCO_3^- + H_3O^+$	235.482	-12092.10	-36.7816		6.29
$HCO_3^- + H_2O = CO_3^{2-} + H_3O^+$	12.450	-6.286.89		-0.0506280	10.19

3.5.3 Data Driven Models

Data driven models are based on large amounts of operating data and used to forecast optimal plant performance. These models do not consider any reactions, mass transfer or any relations considered in above discussions; they directly analyse the relationships between the process data that is available (Yin, et al., 2023).

There are various models developed to design and evaluate FGD systems such as a model by Guo *et al* (2019)using artificial neural network (ANN) which uses 9 input process parameters to forecast SO_2 emissions (Yishan Guo, 2019).

Qiao *et al* (2019) used a comprehensive evaluation criterion and introduced an algorithm thereby improving the accuracy of the mining target data. The final model was able to establish the plant operating base, and by using the minimum cost as an objective function was able to successful determine optimal operating conditions (Qiao, et al., 2019).

A process control and optimization of a WFGD plant was built using a framework of mixed logical dynamical system in which a predicative control problem was solved in MIQP solver. Therefore, the system used the number of slurry pumps in service and the pH set point online to predict the optimal operation (Shi, et al., 2007)

3.5.4 Limitations of the models

The models used to describe gas absorption in section 3.5.1 and 3.5.3 are developed based on the assumption of typical plant operation and design base conditions. Nevertheless, like any operational facility, a running plant will inevitably encounter diverse circumstances that necessitate immediate troubleshooting and online diagnostics. Hence, the predictive accuracy of the mathematical models is constrained (Yishan Guo, 2018).

The mass transfer models estimate the mass transfer coefficients to determine the equilibrium concentration. The laminar film thickness is unknown in the film theory, the contact time in the penetration theory is unknown and the fractional surface renewal rate is unknown in the surface renewal theory (Katoh & Yoshida, 2009). Therefore, these models are more reliant on experimental data for the feasibility of implementation, are prone to errors when operating outside of the experimental ranges or study range that are discussed.

The data driven model present an attractive solution to a very complex WFGD system, however due to the early life operation of the plant, and numerous systems changes due to commissioning, and design modification, the data mining would not have sufficient data to predict long term plant operation. This model can be used in future works when the plant operations are more stable and the numerous equipment modifications are resolved.

The mass transfer and the data driven models fail to account for the factors mentioned below:

-Variable water quality (aqueous medium) which will affect limestone dissolution. The absorber reaction tank is an electrolyte system with various species involved in reactions. Therefore, all these interactions need to be considered instead of only evaluating only one aspect such as mass transfer and neglecting the dynamic of real cases.

-Changes in limestone quality where the concentration of the limestone slurry may become contaminated, or the quality of limestone may deteriorate due to some species ($MgCO_3$) in the

liquid phase. These interactions can only be considered when the real electrolyte system is analysed.

-Changes in flue gas conditions can arise due to the nature of post combustion operations. The boiler load does not remain constant and therefore the interface conditions may change over time. A model would need to take these parameters into considerations.

-The final neglected concept is equipment failure or ageing where the reaction chemistry does not yield simulate results and therefore the simulation must be adjusted to specifically suite the system.

The reaction kinetic model accurately describes the chemical interaction within the absorber system without any major assumptions and is by far the best model to use in establishing the operating base since water chemistry, limestone purity, flue gas conditions, and equipment efficiency can be taken into consideration.

CHAPTER 4: PROCESS MODEL DESCRIPTION AND METHODS

4.1 Process model/simulation review

The WFGD absorber will be simulated using Aspen Plus software V12. The review covers which property method was used and its suitability for the application of the flue gas process. The review also discusses which unit operations were selected to describe the flue gas desulphurisation process better.

4.1.1 Simulation Tool: Aspen Plus

In chemical engineering, a process engineer is required to analyse plant operations, and implement sound engineering principles to optimize plant performance. Process simulators enable easier calculation of equipment design, and operations; various scenarios can be simulated to ensure safe plant operations and further enable economic assessments of unit operations.

There are various process simulators in the market, ranging from expensive to open-source simulators for academic students and educators. Process simulators such as Aspen Plus, Aspen Hysys, CADsim Plus, Chemcad, ChomWorks, COCO, Design II for Windows, DWSim, DynoChem, EMSO, Eq-comp, HydroFlo to name a few, which assist in steady to dynamic state analysis, process optimization, and advanced process control (Simulate Live, 2023). The list is endless, and the choice of process simulator is based on the application and the ease of access of the software.

The WFGD system, particularly the absorber is described by a series of complex reactions and various three-phase non-ideal reactions in the WFGD scrubber/absorber. Therefore, a rigorous model is required to simulate these reactions. The absorber holding/reaction tank is a “batch” operation where reactions in electrolyte solution take place while the gas-liquid reaction continue to take place in the absorption section at the top of the tower. The absorber reaction tank can be

classified as complex electrolyte systems since molecular species dissociate partially or completely into ions in a liquid solvent, and some of the molecular species precipitate as salts. The process simulator chosen for the WFGD absorber analysis is Aspen Plus. Aspen Plus is one of the commonly known simulator tools in the chemical industry and readily available in the academic sphere.

Aspen Plus is a chemical process simulator that allows the construction of a process model; which can be an existing design. The user inputs the required information through a flowsheet. To model the operations within Aspen, sound process engineering is required to simulate conditions that apply to actual industrial applications. Aspen Plus can compute calculations for complex industrial process such as distillations, electrolyte reactions, chemical reactors and recycle or bypass streams (Aspen, 1998).

4.1.2 Property Method

The unit operations in Aspen Plus require property calculations to generate results; these will include thermodynamic and transport properties. The choice of the property method will determine the accuracy of the results obtained since physical and transport properties are calculated for all process streams. Aspen Plus has mainly an ideal, Equation of State, Activity Coefficient, and Special Systems property method available (Aspen Technology, 2001).

In the WFGD absorber the reaction tank is extremely non-ideal because of the presence of charged species within the reaction tank. The Electrolyte NRTL property method is recommended for flue gas-cleaning for fossil power plants since the model is more suited to run electrolyte solutions of all strength and can also compute electrolyte systems with dissolved gases (Aspen Technology, 2001).
The ELECNRTL property method was used in modelling flue gas desulphurisation system to utilize low grade limestone (Lim, Choi, Kim, & Kim, 2020). This property method was also used to model WFGD wastewater treatment plant (Noah Yakah, 2022) & (Idaho National Engineering and Environmental Laboratory , 2002)

4.1.3 Absorber Unit operation

RADFRAC in Aspen Plus is a unit operation that can be used to simulate vapour-liquid operations. RADFRAC can be used for distillation, absorption, and stripping. The RADFRAC unit operation can handle chemical reactions and also adapts in the simulation environment when pump arounds or recycle streams are present. RADFRAC is recommended by Aspen for simulating absorption operations by indicating that the tower does not contain a reboiler or a condenser (Aspen, 1998).

Aspen software was used in a simulation on the demercuration performance of WFGD system, where the effect on WFGD on mercury transformation and its influence on SO_2 removal efficiency was investigated (Kunkun, Guozhen, & Jianjun, 2016).

The RADFRAC unit operation in Aspen was also used to model an absorber for a wet cement kiln exhaust gas stream and Aspen was able to resolve convergence issues associated with the absorption process (Carlos Duque, 2010).

Yahak *et al* (2022) used the RADFRAC to simulate a WFGD wastewater treatment using membrane distillation (Noah Yakah, 2022).

4.1.4 Stream Class

Aspen Plus has 7 stream classes as given in Table 4.1.4-1. Stream classes are used to integrate solids and fluids into one simulation.

Table 4.1.4-1: Stream Classes *(WR Training Pro, 2023)*

	Stream Class	**Definition**
1	CONVEN	Simulation does not involve solids
2	MIXNC	Non-conventional solids with no PSD
3	MIXCISLD	conventional inert solids with no PSD
4	MIXNCPSD	Non-conventional solids with PSD
5	MIXCIPSD	conventional inert solids with PSD
6	MIXCINC	Both conventional and Non-conventional solids with no PSD
7	MIXCINCPSD	Both conventional and Non-conventional solids with PSD

Substream classes are building blocks for stream classes and are given in Table 4..1.4-1.

Table 4.1.4-2: Substream Class in Aspen *(WR Training Pro, 2023)*

	Stream Class	**Definition**
1	MIXED	Fluids only
2	CISOLID	Conventional inert solids that participate in reactions
3	NC	Non-conventional solids
4	NCPSD	Non-conventional solids with PSD
5	CIPSD	Conventional solids with PSD

In the WFGD absorber, the calcium sulphite and calcium sulphate that form in the reaction precipitate out of solution in the reaction tank and thus do not participate in the electrolyte reactions. Furthermore, there is currently no PSD available for the absorber slurry either from design phase or current operations; therefore, there will be no comparison possible. The stream class chosen in Aspen Plus is MIXCISLD (Arvidsson, 2021).

4.2 Methodology

4.2.1 Data Selection for Model (Operational conditions)

The operational data from an existing WFGD plant treating a 800MW boiler unit was sampled. The data is used to simulate operational parameters rather than design data.

4.2.1.1 Flue Gas flowrate

The flue gas flow rate was evaluated from April 2023 to August 2023. The actual flue gas flow fluctuates between 4,0 x 10^6 Am^3/h to 5,1 x 10^6 m^3/h.

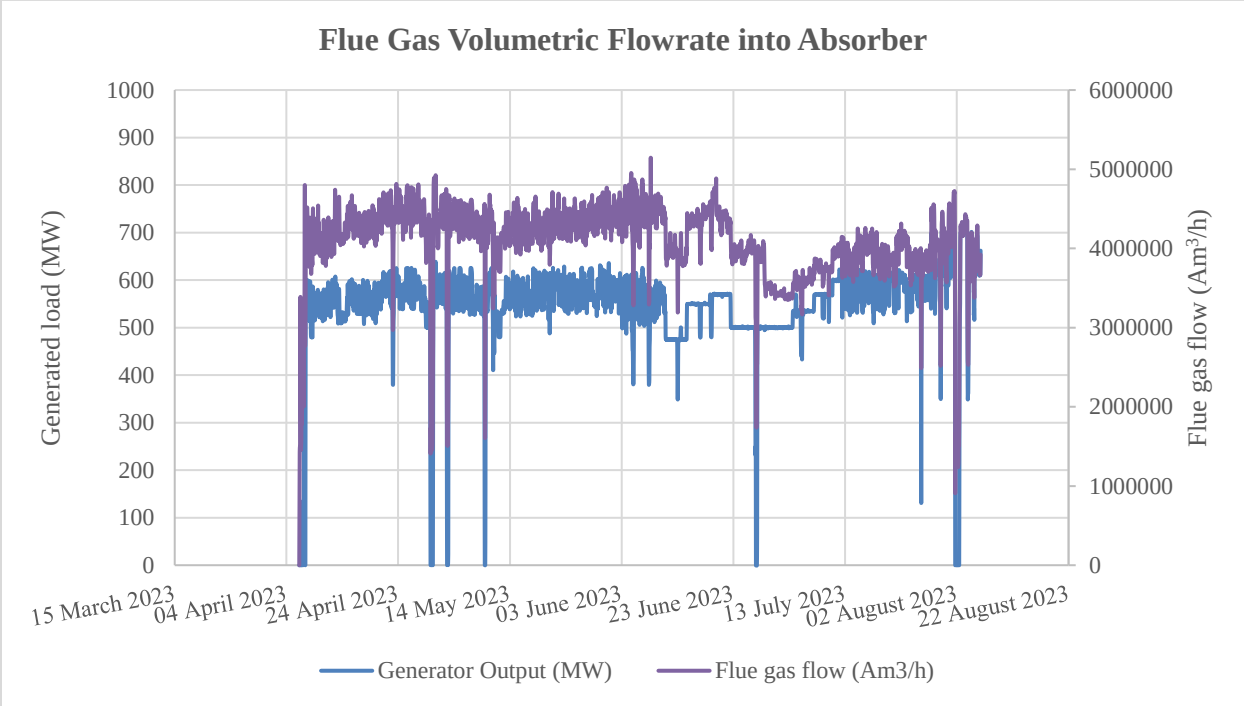

Figure 4.2.1.1-1: Actual Volumetric Flue Gas Flowrates

4.2.1.2 Absorber Inlet Outlet temperature

The absorber outlet temperature was evaluated from April 2023 to August 2023. The inlet temperature is on average 122 ℃with a maximum of 132℃ observed, and outlet temperature is on average 45℃, where a maximum of 47℃ is observed at times.

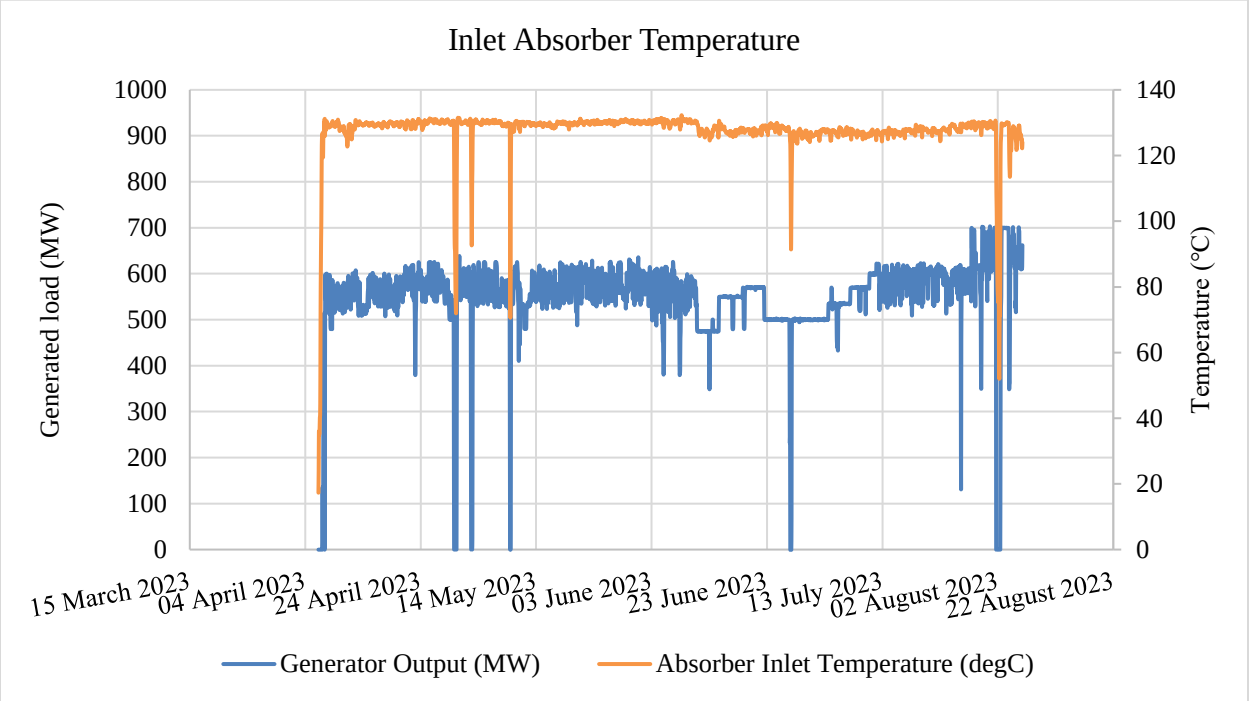

Figure 4.2.1.2-1: Actual Inlet absorber temperature

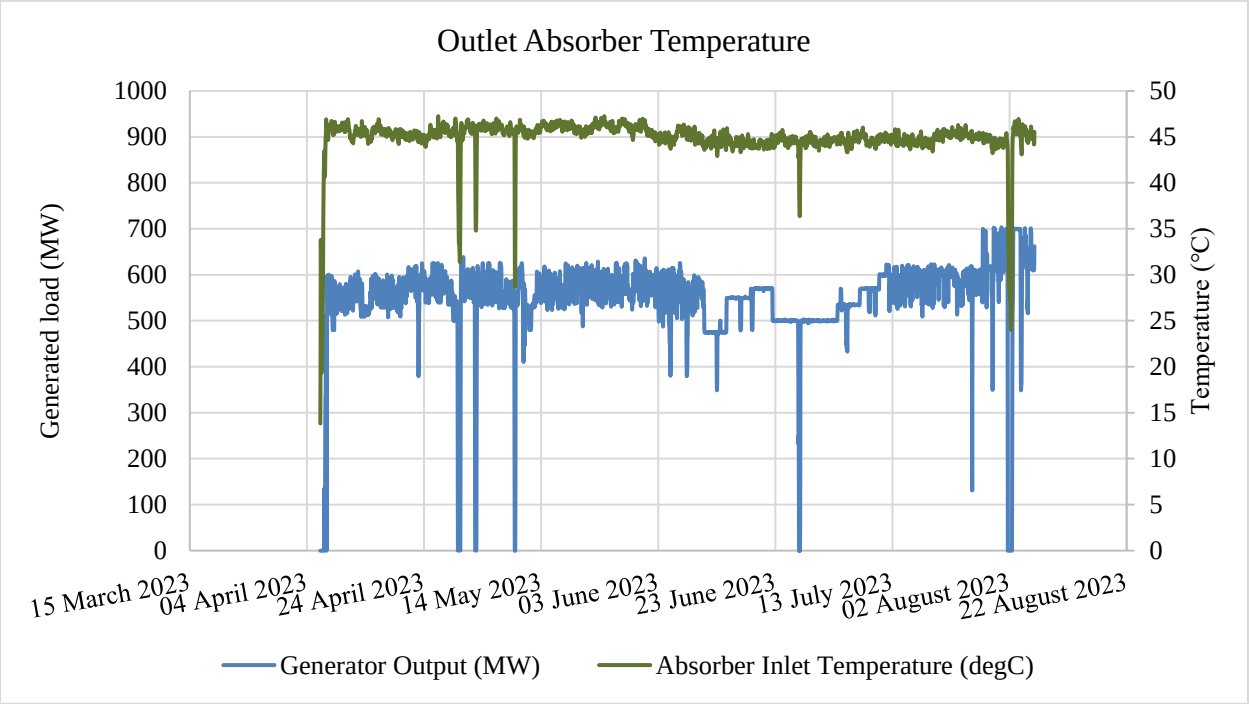

Figure 4.2.1.2-2: Actual Inlet and Outlet absorber temperature

4.2.1.3 Absorber pH and density

The absorber pH and density were evaluated from April 2023 to August 2023. The pH fluctuates around 5, where the density is on average 1144 kg/m^3 and at maximum 1230 kg/m^3 as given in Figure 4.2.1.3 1and 4.2.1.3 2.

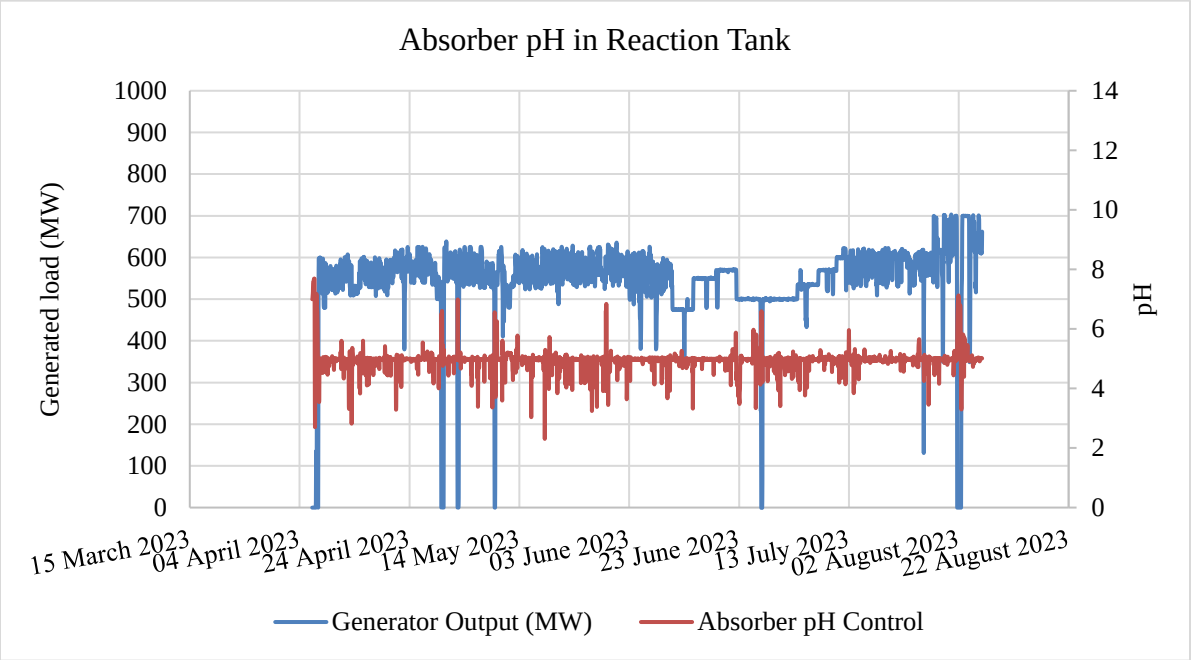

Figure 4.2.1.3-1: Actual absorber pH

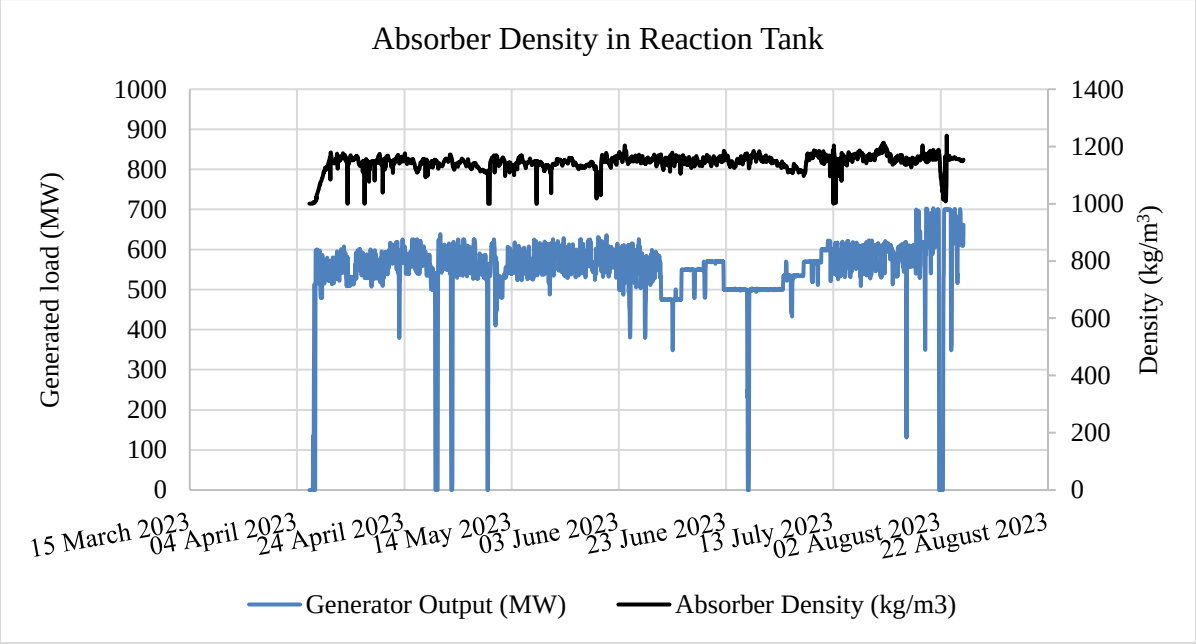

Figure 4.2.1.3-2: Actual absorber density

4.2.1.4 Oxidation air

The oxidation air is on average 2.45 m^3/s. There is however no flow measurement on the piping and the value is calculated based on inlet temperatures and pressures.

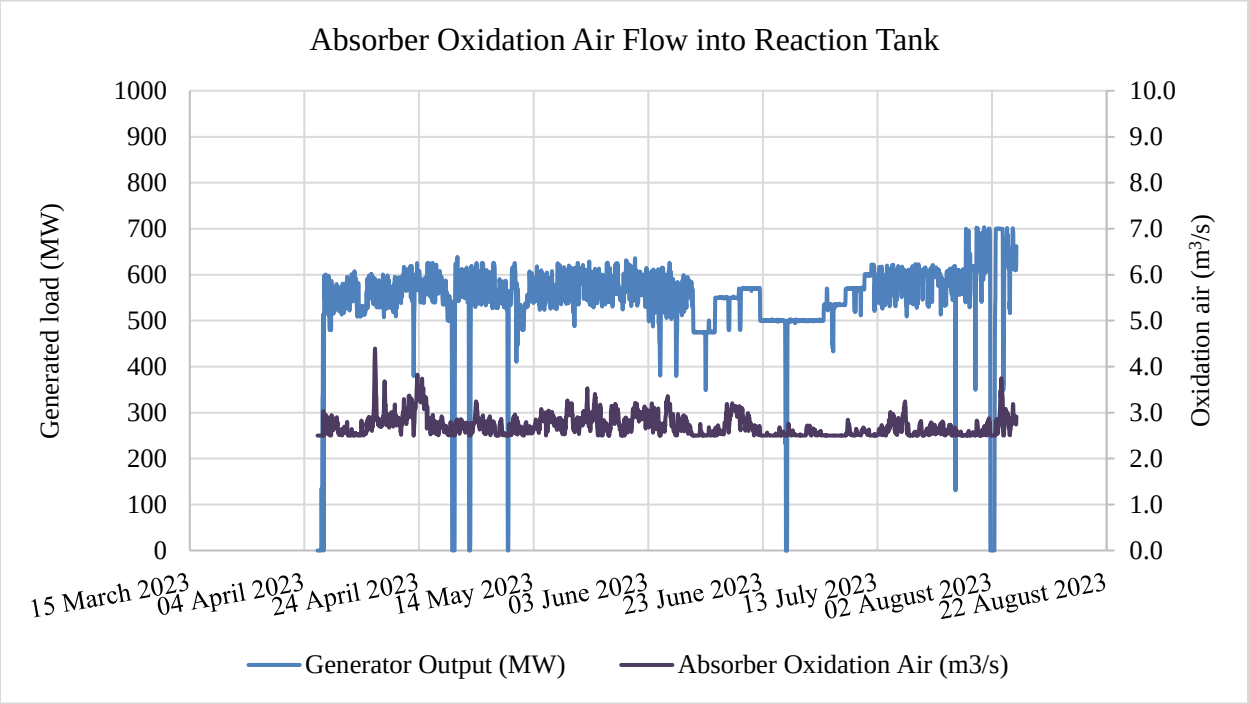

Figure 4.2.1.4-1: Actual oxidation air

4.2.1.5 Limestone consumption

The limestone consumption as given in Figure 4.2.1.5 1 is 8.92 l/s on average and 19.95 l/s at maximum. The limestone slurry contains approximately 75% water, therefore the limestone only consumption on mass basis is given as 9.87 tons/h on average and 22.08 tons/h at maximum.

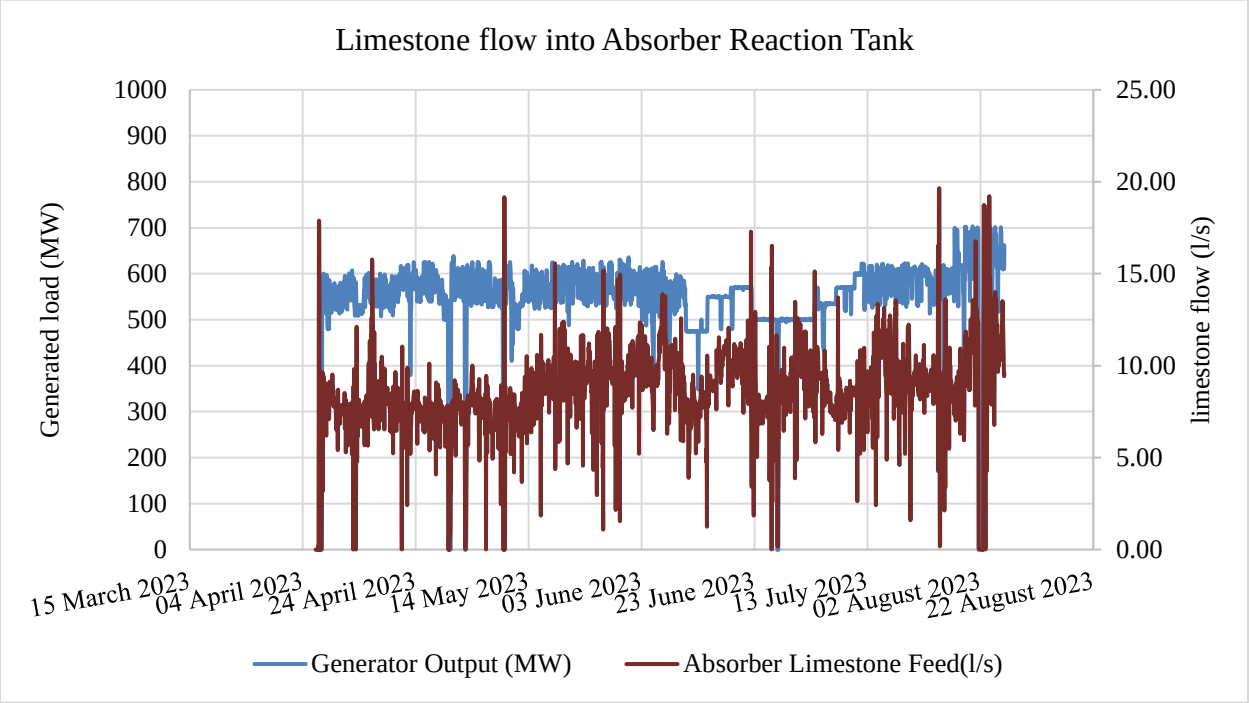

Figure 4.2.1.5-1: Actual Limestone feed to absorber

4.2.1.6 SO_2 emissions

The period analysed was from April 2023 to August 2023. The SO_2 emissions were below the limit of 500 mg/Nm^3. The inlet $SO_{2\ \text{on average}}$ 767 ppm and 1169 ppm at maximum.

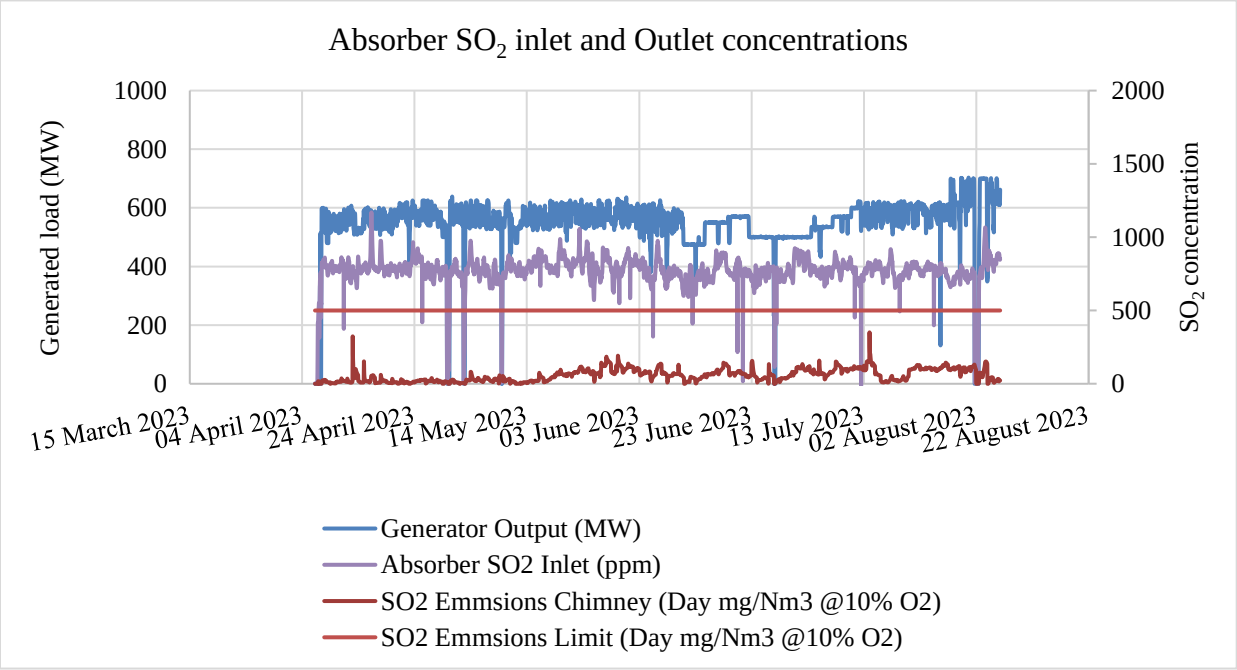

Figure 4.2.1.6-1: Actual SO_2 emissions

4.2.1.7 Absorber Carbonate and sulphite analysis

The absorber reaction tank filtrate and solid samples were analysed from April to August 2023. The data indicates that the sulphite is mostly in the liquid whereas the carbonates are usually evident in the solid stream analysis.

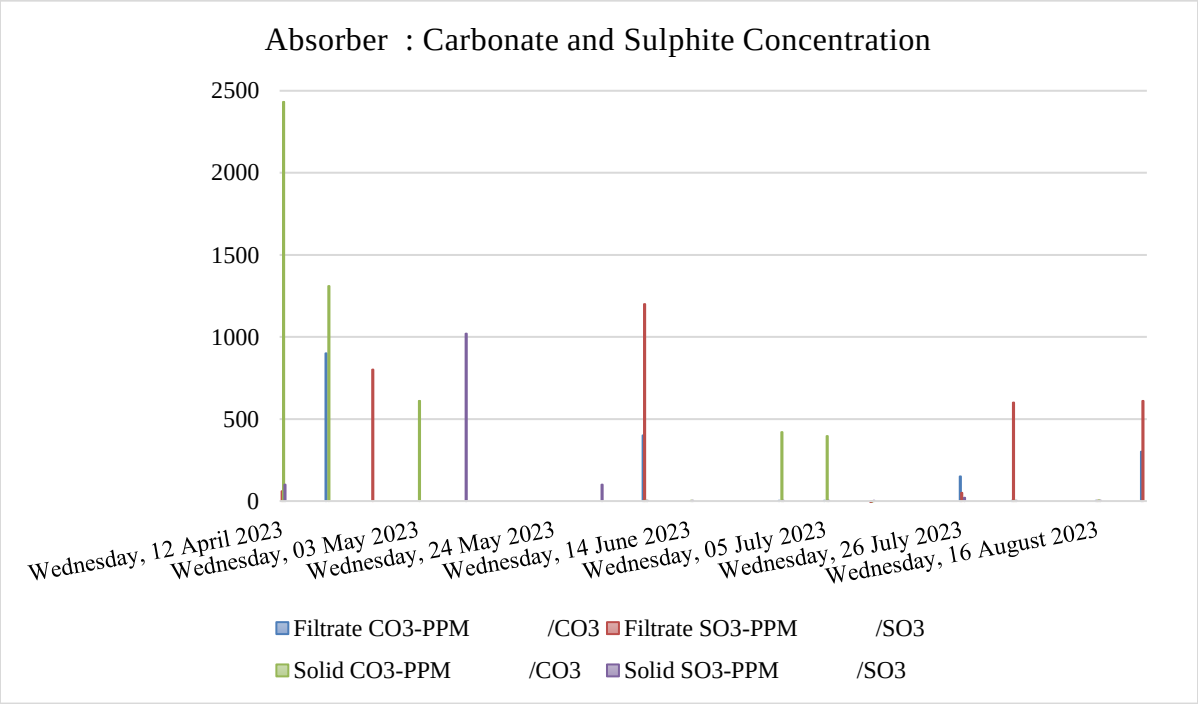

Figure 4.2.1.7-1: Actual absorber carbonate and sulphite concentrations in the reaction

4.2.1.8 Coal specifications and Emissions for Case study 3

The Eskom Power Station A sulphur content in the coal is minimum 0.46 to maximum 1.3% S (air dried mass basis) at a 4% moisture content. The design base is 0.9 % S. Normal operation is 1.1% Sulphur (Base case)

Table 4.2.1.8-4.2.1.8-1: Fuel specifications (Coal) & Projected Emissions

Parameters	Units	Design coal	Best Coal	Normal Operation coal	High Sulphur test coal
Coal fuel input	kg/s	108.7	90.6	108.7	115.3
Sulphur (as received)	g/kg coal	8.6	7.7	11.31	16
Sulphur (as received)	kg/kg coal	0.0086	0.0077	0.01131	0.016
Sulphur (as received)	%	0.86%	0.77%	1.13%	1.60%
Emissions					
SO_2	kg/h	6730.704	5022.864	See base case results. 4.2.8.3	See Table 5.3.3
N_2	kg/h	2191066	2148467		
CO_2	kg/h	644679	623711		
H_2O	kg/h	153477	140713		
O_2	kg/h	145.566	142.767		
Total	kg/h	2996098.27	2918056.631		
Emissions fractions					
SO_2	Frac	0.22%	0.17%	0.2897%	0.44%
N_2	Frac	73.1%	73.6%	71.0%	71.05%
CO_2	Frac	21.5%	21.4%	18.0%	17.95%
H_2O	Frac	5.1%	4.8%	4.3%	4.25%
O_2	Frac	4.63%	4.66%	6.1%	6.05%

4.2.2 Model

The purpose of model development is to find the best suited unit operations in Aspen that could model the industrial WFGD absorber. The model will be used to simulate the three cases;

- **Case1:** Low limestone quality or reactivity. This will be simulated by lowering the $CaCO_3$ sequentially and establishing the lowest limit to achieve SO_2 emissions of 500mg/$Nm^{3.}$
- **Case 2:** Liquid-gas ratio imbalance where the flue gas being treated is substantially more than the alkali available for the reaction. This will be simulated by increasing the flue gas volumetric flow to 6 x10^6 Am^3/h
- **Case 3:** Variable inlet sulphur due to multiple sources of coal. This will be simulated by increasing the sulphur content to 1.6% as per Table 4.2.1.8 1 and studying the effects and establishing the lowest limit to achieve SO_2 emissions of 500mg/$Nm^{3.}$

4.2.3 Model Assumptions

1. The process is at steady state conditions.
2. The influence of dust into the absorber is neglected and no HF, HCl is considered in the simulation
3. Equilibrium reactions were assumed for all reactions, and no reaction kinetics would be forced.
4. The oxidation reaction does occur in the absorption section of the absorber tower. However, it is rather limited to the reaction tank.
5. The mist eliminator system was not simulated or modelled in the model development. It does not participate in the reactions, but the water used for washing is accounted for in the reaction tank hold up volume calculation.
6. Mass transfer in relation to slurry spraying through the column is not considered in the model.
7. It is assumed that the water used is clean and only assist as a solvent for electrolyte reactions.

4.2.4 Property Method

It is important to choose the correct property method since the method chosen specifies a collection of property data that enables calculation to be done as an entity (Aspen Technology, 2001).

It is recommended that for acid gas treatment that an electrolyte coefficient activity property method be used (Aspen Technology, 2001) . The Electrolyte NRTL model was used to model the absorber.

4.2.5 Chemical Reactions

The chemical reactions were obtained from using the Aspen Plus electrolyte wizard. The reactions were defined as equilibrium reactions and labelled as Aspen Reactions (AR).

The reactions that addressed the dissociation of limestone and water is given below;

$$\mathbf{CaCO_3(s) \leftrightarrow Ca^{2+}(aq) + CO_3^{2-}(aq)} \qquad \mathbf{(AR1)}$$

$$\mathbf{H_3O^+(aq) + OH^-(aq) \leftrightarrow 2H_2O(l)} \qquad \mathbf{(AR2)}$$

The absorption reactions are given below.

$$\mathbf{SO_2(g) + 2H_2O(l) \leftrightarrow HSO_3^-(aq) + H_3O^+(aq)} \qquad \mathbf{(AR3)}$$

$$2H_2O(l) + HSO_3^-(aq) \leftrightarrow + H_3O^+(aq) + SO_3^{2}(aq) \quad \textbf{(AR4)}$$

The carbonate reactions are given below;

$$H_3O^{+\,-}(aq) + HCO_3^-(aq) \leftrightarrow 2H_2O(l) + CO_2(g) \quad \textbf{(AR5)}$$

$$H_3O^{+\,-}(aq) + CO_3^{2-}(aq) \leftrightarrow H_2O(l) + HCO_3^{\,-}(aq) \quad \textbf{(AR6)}$$

The following chemical reaction describes the oxidation process

$$2SO_3^{2-} + O_2 \leftrightarrow + 2SO_4^{2-} \quad \textbf{(AR7)}$$

$$HSO_3^-(aq) + {}^1/_2O_2(g) \leftrightarrow HSO_4^-(aq) \quad \textbf{(AR8)}$$

The following chemical reactions describe the precipitation reactions where calcium sulphate or calcium sulphite precipitates out of the absorber liquor.

$$Ca^{2+} + SO_3^{--} + {}^1/_2H_2O(l) \rightarrow CaSO_3 \cdot {}^1/_2H_2O\ (s) \quad \textbf{(AR9)}$$

$$Ca^{2+} + SO_4^{--} + 2H_2O(l) \rightarrow CaSO_4 \cdot 2H_2O\ (s) \quad \textbf{(AR10)}$$

4.2.6 Unit Operations Selection

The absorber reactions that took place in RADFRAC unit operation are represented by reactions AR1-10. RADFRAC is a rigorous model and requires sensible information in order for convergence of the model to be achieved. This was the only feasible model in Aspen which could model the absorber; and Aspen V12 further recommends how to model RADFRAC as an absorber. The number of stages were six, further stages yielded no difference in results.

The precipitation reactions were modelled with a CSTR. This reactor was best suited since the bottom of the absorber is a continuously stirred tank where oxygen is injected at the bottom of each agitator or stirrer. The CSTR unit operation also enables the user to input the tank dimensions or to input a residence time if available.

In the CSTR, there is some formation of gaseous streams and these needed to be circulated back to the absorber; and therefore, a flash unit was required to enable the separation. The vapour stream was mixed with the clean air exit and not cycled back to the absorber to prevent convergence issues on the RADFRAC unit operation.

The liquid product from the CSTR is pump back to the absorber RADFRAC since it is reactive and contains some unreacted limestone. The return of slurry back to the absorber is modelled through three recycle pumps which operate at different pressures.

4.2.7 Convergence

The unit operation selected for the absorption is RADFRAC. The entire integrity of the simulation is dependent upon convergence of the RADFRAC unit block. The RADFRAC block does not converge when salt or precipitations reactions are selected as part of the electric wizard model (Arvidsson, 2021). These reactions were added separately in the CSTR unit block. The RADFRAC unit operation is highly sensitive to operating ranges, where the feed streams should not be over specified and therefore preventing convergence of the simulations.

However standard convergence did not converge in the maximum number of iterations of 200. Various methods were applied as advised through consulting Aspen help files (Aspen Technology, 2002). Therefore, the absorber algorithm was selected as opposed to STANDARD, initial estimates were provided for the model, solid and precipitation reactions were not included in the RADFRAC model, the damping level was marked as severe to prevent high oscillations that prevent convergence (Carlos Duque, 2010).

Further to the above, convergence is obtained by deactivating other unit operations and adding them sequentially in the model, so that the model converges faster since initial estimates of feed streams into the next unit operation are available.

4.2.8 Base Model: Normal Operation

This section describes the simulation of the base case and the inputs thereof.

4.2.8.1 Process Flow

The base model is given in Figure 4.2.8.1-1where the flue gas and limestone (LSTONE) enter the RADFRAC absorber. The absorber has 6 stages where a clean air stream exits the absorber (AIROUT1) and an absorber slurry (ABSLURRY) exits from the absorber as a bottom's product. As was discussed earlier (refer to section 4.2.7) the RAFRAC unit operation does not converge when solid streams are present in feed streams and therefore solids reactions needed to be removed for convergence to established. Therefore, the RADFRAC unit operation only represents the absorption section of the absorber and not the formation of the gypsum and calcium sulphite salt.

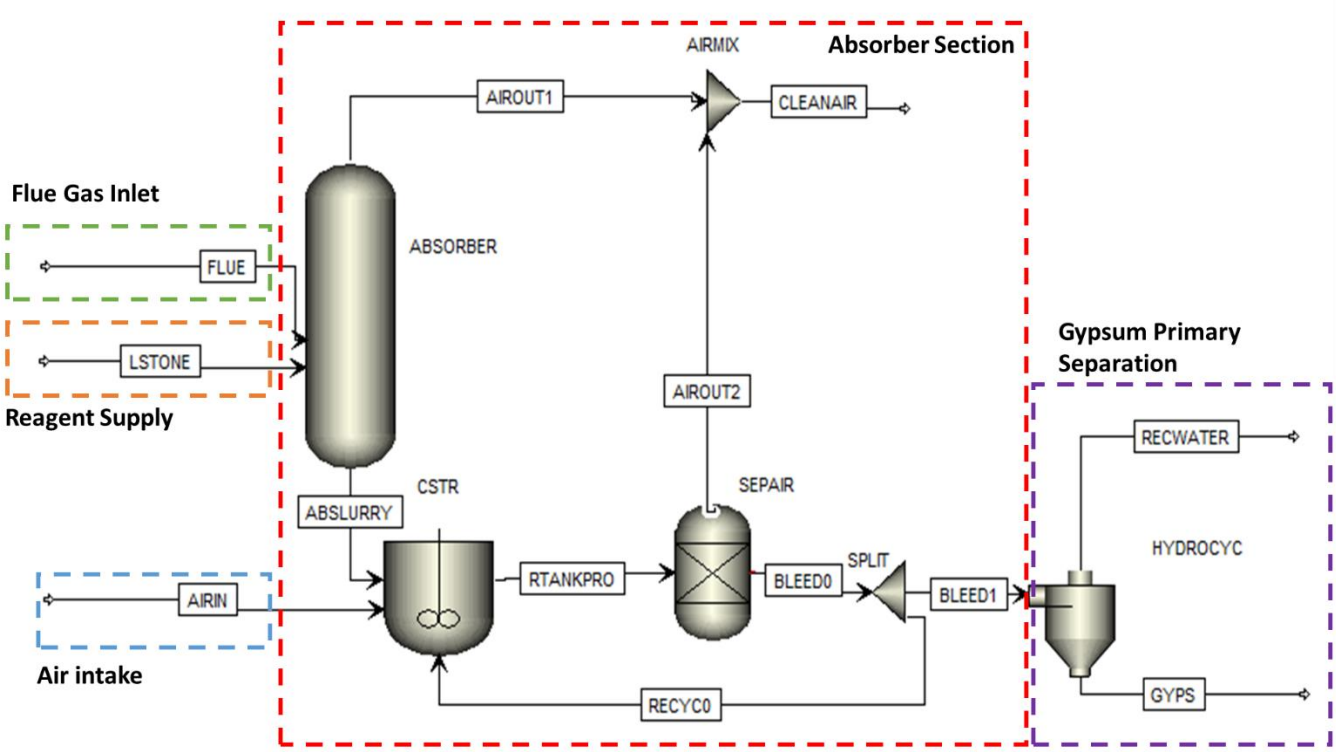

Figure 4.2.8.1-1: WFGD Absorber Base Model

A CSTR unit operation was used to simulate the reaction component of the absorber . In practice the absorber has a reaction tank that forms part of the absorber column. The absorption column usually houses the spray banks with the demister, while the reaction tank holds the reacting liquid in agitation. In the Eskom Power Station A operations, the reactor tank has five agitators in continuous operation where air is bubble at the bottom of the agitators to assist with gypsum conversion. Therefore, the CSTR is a perfect choice to mimic the industrial case.
The air (Airin) enters the CSTR where a reaction product is created (RTANKPRO). Some gaseous products are formed in the CSTR and are removed with a flash unit operation (SEPAIR) and combined as an outlet stream with the clean air. It was assumed that since these gases do not contribute to the absorption reaction, nor do they participate in the gypsum formation that they will not be returned to the RADFRAC unit operation so that convergence challenges are avoided but rather be combined with an already existing AIROUT1 stream. The slurry product from the flash unit operator has some slurry that contains unreacted limestone, and therefore 30% of the mixture is circulated back to the CSTR. The 70% portion of the split enters a primary separation of gypsum which has a 12 hydrocyclone cluster. This was done to determine the final reclaim water (RECWATER) quality that will be used for limestone milling in future simulation work and expected gypsum (GYPS) quality.

4.2.8.2 Simulation Inputs

There are 7 inputs were used to compute the simulation which are the flue gas conditions, limestone required, air required, CSTR reaction conditions, flash separator conditions, recycle split and the hydrocyclone operational parameters.

4.2.8.2.1 Flue Gas

Since RADFRAC is a rigorous unit operation with only certain conditions that will reach convergence, it was found after numerous tedious simulations, design specification tests, and sensitivity analysis that at flue gas inlet pressure 86kPa, only an absorber temperature of 30℃ reaches convergence. Therefore, the volumetric flue gas flow was corrected using the ideal gas law where at STP (Arvidsson, 2021), the flue gas volume was 2 668 8201 Nm^3/h (wet), therefore at 30℃, the flue gas volume used was 2 961 410 m^3/h in the simulation as calculated in Appendix A. The mass fraction was as specified by Eskom Power Station A and given in Table 4.2.8.2.1 1 .

Table 4.2.8.2.1-1:Flue Gas Conditions

Component	**Mass Fraction**
H_2O	0.043
SO_2	0.0029
O_2	0.0061
N_2	0.71
NO_2	0.0031
Temperature (℃)	30
Volumetric flow rate (m^3/h)	2 961 410

4.2.8.2.2 Limestone

The limestone flow at 30 ℃ was 148 kmol of $CaCO_3$ and 1806 kmol of water fed into the absorber as per Eskom Power Station A mass balance.

4.2.8.2.3 Oxygen into CSTR

The oxygen added was 50kmol/h which is 17 kmol/h less than Eskom Power Station A mass balance due to a RECYC0 that was incorporated as a recycle back to the CSTR. However, there is excess air in RECYC0 which assisted with conversion of reactants.

4.2.8.2.4 CSTR conditions

The CSTR is operated at 0.8bar and 30°C, where the valid phases for reaction are both vapour and liquid. The reaction tank is 2827 m^3 as per Eskom Power Station A absorber dimensions; where the operating level of the reaction tank is 9m, the diameter is 20m. The three reactions that are used in the reaction are given by reactions AR7,10 and 11. All the reactions were modelled as equilibrium reactions.

$$2\ SO_3^{2-} + O_2 \ \text{<--> } 2\ SO_4^{2-} \qquad \textbf{(AR7)}$$

$$Ca^{2+} + SO_4^{2-} + 2\ H_2O \ \text{<--> } CaSO_4{*}2H_2O \qquad \textbf{(AR10)}$$

$$Ca^{2+} + SO_3^{2-} \ \text{<--> } CaSO_3 \qquad \textbf{(AR11)}$$

AR 11 is an aqueous phase reaction in the electrolyte and does not precipitate out of solution as does AR10. This is based on operational experience where minimal $CaSO_3$ is found in absorber slurry due to LSFO process.

4.2.8.2.5 Flash separator and Recycle split

The flash separator is operating at 1 bar. Therefore, an intermediate pump to raise the pressure is required but this was not added to the base case.
The recycle split was specified at 30% of the total stream. This was obtained on a trial-and-error basis by checking the stoichiometric requirement of air into CSTR.

4.2.8.2.6 Hydrocyclone

The hydrocyclone was modelled according to Eskom Power Station A dimensions where 12 hydrocyclone with a diameter of 0.15m. The Bradley efficiency correlation was used and provided expected classification results.

4.2.8.3 Mass balance

The mass balance for the base scenario is provided in Table 4.2.8.3-1. The mass balance aligns with the Eskom Power Station A case where the Sulphur content is normally between 0.46- 1.1% (mass basis). In the case presented in Table 4.2.8.3-1, the 1.13% maximum for normal operation was simulated at a coal feed rate of 108.7 kg/s. The pH of the limestone exceeds the anticipated pH of 10. The case studies will address this issue by introducing $CaSO_4$ into the limestone, and HCL in future simulations stream as a feed to decrease the pH (Walsh, et al., 2006).

,

Table 4.2.8.3-1 Base model mass balance

Base Case								
Parameters		**Flue Gas**	**Limestone**	**Clean Air**	**Airin (CSTR)**	**Bleed1**	**Reclaim Water**	**Gypsum**
Temperature	C	30.00	30.00	29.45	30.00	31.08	31.09	31.09
Pressure	bar	0.86	1.00	0.80	0.80	1.00	0.57	0.57
pH at 25°C		2.42	11.52	4.44		7.81	7.81	7.81
Mass Flows	**kg/hr**	**3055269.90**	**47373.30**	**3021914.77**	**1599.94**	**82256.49**	**64038.21**	**18218.28**
H_2O	kg/hr	131370.78	32524.64	101271.61	0.00	58846.80	57941.66	905.14
SO_2	kg/hr	8849.92	0.00	0.00	0.00	0.00	0.00	0.00
$CACO_3$	kg/hr	0.00	0.00	0.00	0.00	0.00	0.00	0.00
O_2	kg/hr	186371.46	0.00	186371.40	1599.94	0.00	0.00	0.00
$CASO_3$	kg/hr	0.00	0.00	0.00	0.00	47.20	46.47	0.73
N_2	kg/hr	2169241.63	0.00	2169241.63	0.00	0.00	0.00	0.00
NO_2	kg/hr	9471.34	0.00	9471.34	0.00	0.00	0.00	0.00
CA++	kg/hr	0.00	5914.87	0.00	0.00	1916.22	1886.75	29.47
CAOH+	kg/hr	0.00	35.50	0.00	0.00	0.01	0.01	0.00
CO_2	kg/hr	549948.58	0.00	555558.77	0.00	8.25	8.12	0.13
HCO_3-	kg/hr	0.00	49.91	0.01	0.00	1216.83	1198.11	18.72
OH-	kg/hr	0.00	3.33	0.00	0.00	0.00	0.00	0.00
CO_3--	kg/hr	0.00	8845.04	0.00	0.00	36.28	35.73	0.56
H_3O+	kg/hr	3.08	0.00	0.00	0.00	0.00	0.00	0.00
HSO_3-	kg/hr	13.12	0.00	0.00	0.00	108.24	106.58	1.66
SO_3--	kg/hr	0.00	0.00	0.00	0.00	2858.77	2814.78	43.97
$CASO_4$*2H_2O	kg/hr	0.00	0.00	0.00	0.00	17217.90	0.00	17217.90

The production of gypsum is lower than expected where at least 23000 kg/h was anticipated. The yield will be further studied in the case studies. The pH of the BLEED 1 stream should be between 5-6, this could be because 2.3% of limestone is still present in the bleed slurry where in practice, the limestone content is minimized to 1.5% to prevent pH above 7 which is known to promote more scaling in the absorber.

4.2.8.4 Model Sensitivity

Sensitivity analysis was conducted to test the viability of the simulation. The RADFRAC conditions were kept constant with 6 stages, with outlet pressure as specified from Eskom Power Station A operations with base models inputs given in Appendix E. It was observed that the number of stages above 4 had no influence on the separation, however a minimum of 2 stages were required for feed inputs.

During the setting up of the simulation in Aspen, it was noted that the RADFRAC unit operations exhibit a high degree of sensitivity to flue gas conditions. Hence, the concentration of SO_2 in the outlet was monitored while adjusting the temperature and pressure of the flue gas. The relationship between the temperature of the flue gas and the concentration of SO_2 in the output can be observed in Figure 4.2.8.4 1. This suggests that the effectiveness of SO_2 removal is influenced by higher temperatures. Nevertheless, the decrease in removal efficiency is negligible due to the concentration being expressed as a significantly small negative exponent. It is evident that the solubility of SO_2 is influenced by a rise in temperature.

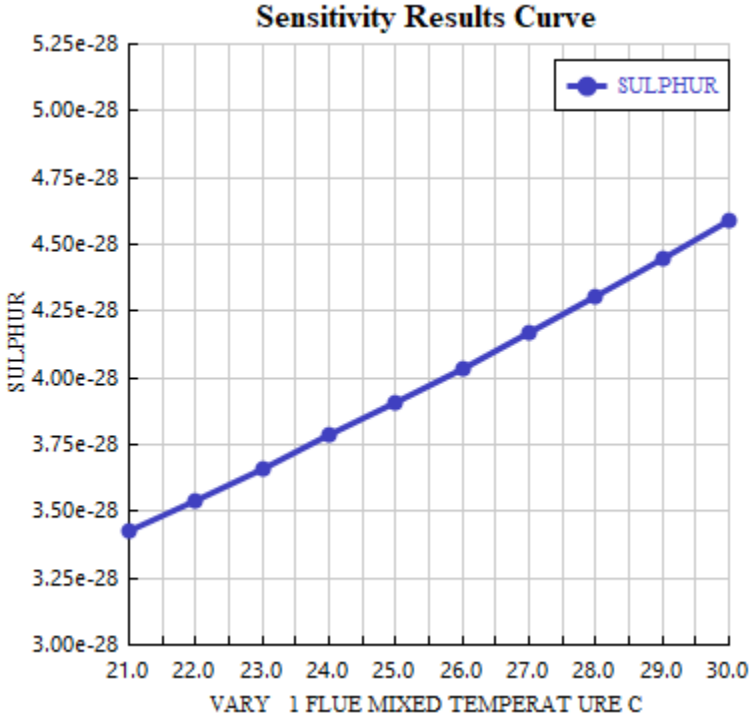

Figure 4.2.8.4-1 RADFRAC Outlet Sulphur vs Flue Gas inlet temperature

The flue gas pressure was increased from 10kPa to 80 kPa and the outlet SO_2 in the clean air stream of the RADFRAC outlet was observed. Figure 4.2.8.4-2at a pressure 0.56 bar, the SO_2 concentration starts to decrease in the clean air stream and starts to increase the absorber slurry as shown in Figure 4.2.8.4-3. This behaviour will be monitored during the case study simulations.

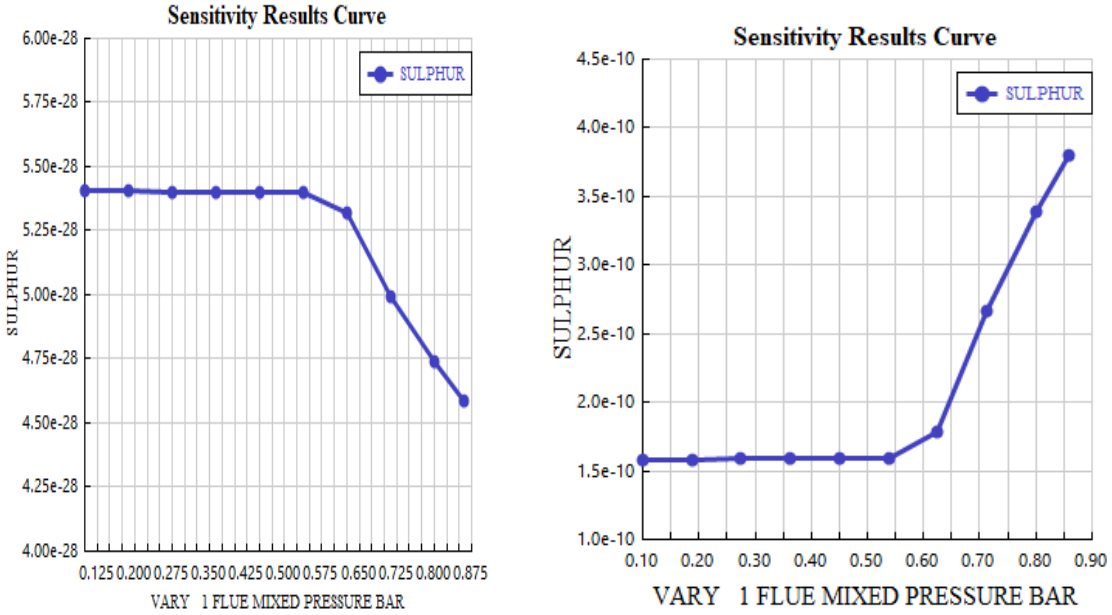

Figure 4.2.8.4-2 RADFRAC Absorber slurry SO_2 concentration (left) vs flue gas pressure & RADFRAC Outlet SO_2 (right) vs Flue Gas Pressure

The simulation also reported on charge imbalance in the CSTR, however the error was very low. The charge balance is an important parameter in electrolyte systems since the pH of the system is computed using the ions in solutions. The error will be monitored in analysis of the case studies.

CHAPTER 5: RESULTS AND DISCUSSIONS

This section aims to juxtapose simulated outcomes with those of the Eskom Power Station A, if feasible. The case studies to be presented and discussed are as follows:

- **Case study 1:** Low limestone quality or reactivity. This will be simulated by lowering the $CaCO_3$ sequentially and establishing the lowest limit to achieve SO_2 emissions of 500mg/Nm^3.
- **Case study 2:** Liquid-gas ratio imbalance where the flue gas being treated is substantially more than the alkali available for reaction. This will be simulated by increasing the flue gas volumetric flow to 6 x10^6 Am^3/h
- **Case study 3:** Variable inlet sulphur due to multiple sources of coal. This will be simulated by increasing the sulphur content to 1.6% on a mass basis and studying the effects and establishing the lowest limit in order to achieve SO_2 emissions of 500mg/Nm^3

5.1 Case study 1: Low Limestone reactivity

The limestone is the base that is required to neutralize the acidic SO_2 in the flue gas stream. In a situation where the limestone feed to the absorber is contaminated or compromised in any way; the slurry is kept in the absorber reaction tank for as long as possible or transferred to a rapid drain tank.

The rapid drain tank functions as an emergency store for absorber slurry that is not satisfactory for gypsum dewatering process. This could be slurry that is contaminated will oil due to boiler light up, or low pH slurry, unoxygenated slurry, slurry that contains high solids content or high $CaCO_3$ content or being stored as seed crystals for startup operations. The rapid drain slurry would thereafter be fed back to the absorber intermittently over days for treatment in a functional absorber reaction tank.

It is important to note that in such a case, the reclaim water or gypsum quality cannot be evaluated since the slurry is not suitable for dewatering. Therefore, only the absorber slurry analysis will be discussed. A scenario to illustrate the industrial case where, the generator is not synced to the national grid during start up however is running on combination of coal and oil, and flue gas flow to the absorber is increasing from 1.7 x$10^6$$m^3$/h to 2.7 x 10^6 m^3/h and the absorber inlet SO_2 ppm is increasing as given in Table 5.1.1.

Table 5.1-1: Low $CaCO_3$ feed to absorber

Timestamp	Generator Output (MW)	Absorber pH Control	Absorber Limestone Feed(l/s)	Absorber SO_2 Inlet (ppm)	Flue gas flow (Am^3/h)
04/06/2023 18:00:00	-0.17	4.87	0.20	189.26	1 779 462.92
04/06/2023 19:00:00	-0.17	2.70	0.00	417.58	1 972 602.92
04/06/2023 20:00:00	-0.17	3.55	9.69	407.62	2 377 834.35
04/06/2023 21:00:00	-0.17	6.27	17.89	467.73	2 675 539.76
04/06/2023 22:00:00	-0.17	6.73	17.81	511.62	2 788 407.06

The pH in the absorber reaction tank started as 4.87 with no limestone slurry feed (0.2 l/s) and dropped to 2.70 as a result. When limestone feed of 9.69 l/s is added which translates to ~13082 kg/h of $CaCO_3$, the pH starts to increase to 3.55 and reaches 6.73 with additional limestone feed to the absorber. The outlet SO_2 emission during the low pH excursion was below 17.72 mg/Nm^3 which is below the emissions limits of 500mg/Nm^3. This is the anticipated outcome when all equipment within the absorber is operating effectively.

The viability of the simulation will depend upon if comparable behaviour is observed within the framework of the simulation. Due to the RADFRAC model's extreme sensitivity to the satisfaction of stoichiometric ratios and the maintenance of charge balance, adopting changes without careful consideration would result in unforeseen convergence issues.
Thus, the feed mass basis remained constant, but the limestone percentage (based on mass) in the slurry feed to the absorber was systematically reduced from 31% as per design to 3%. The difference in percentage was equated to the water. The calculated input figures are given in Appendix B with reults. The process flow is given in Figure 5.1.1.

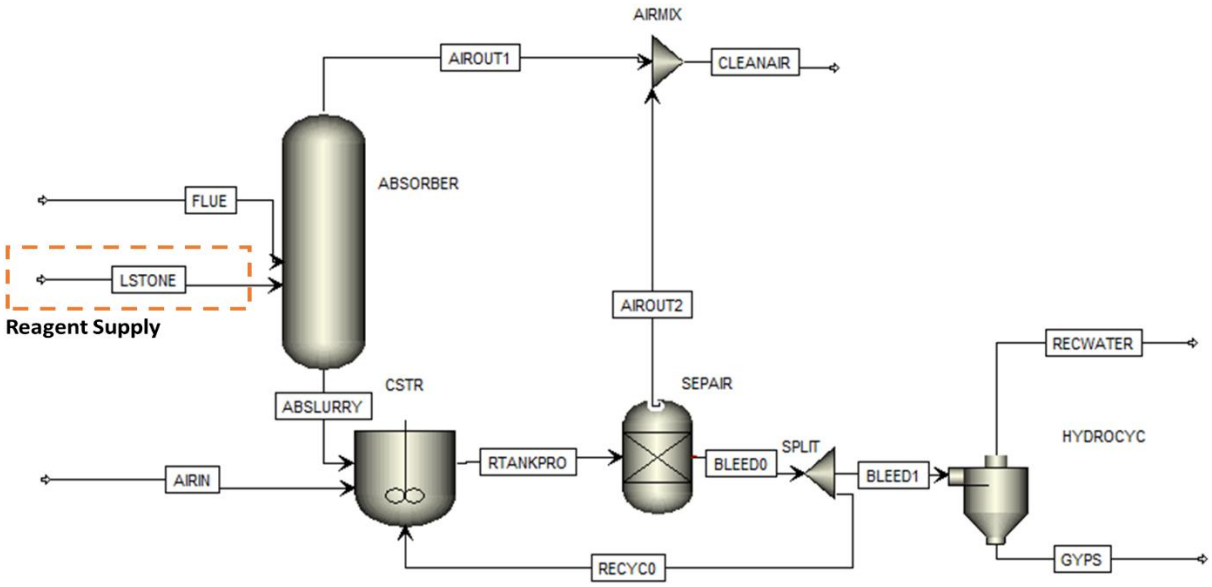

Figure 5.1-1: WFGD Absorber with variable slurry feed

In section 4, it was previously mentioned that when the input feed conditions are modified to the RADFRAC model, there is an observed rise in the SO_2 amount inside the absorber slurry. Hence, the behaviour of SO_2 and SO_3 was observed graphically presented in Figure 5.1.2 as the limestone content decreased from 31% to 3%. The simulation was not able to reach 3% due to convergences challenges, however was able to reach 13% as given in Figure 5.1.2.

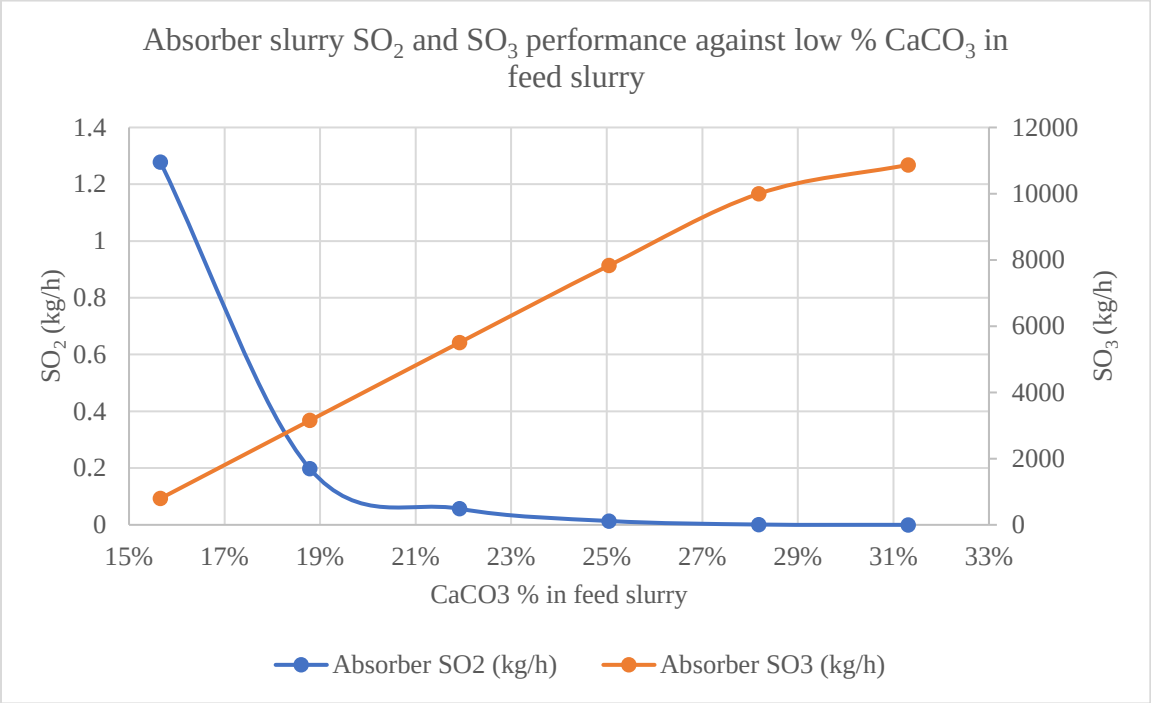

Figure 5.1-2: Absorber slurry SO_2/SO_3 vs $CaCO_3$ feed

As the SO_2 content decreases due to $CaCO_3$ reaction and neutralization in the absorber slurry, the SO_3 content increases. This illustrates the equilibrium relations of SO_2/SO_3 as given by reactions AR3 and 4.

$$\mathbf{SO_2(g) + 2H_2O(l) \leftrightarrow HSO_3^-(aq) + H_3O^+(aq)} \qquad \mathbf{(AR3)}$$

$$\mathbf{2H_2O(l) + HSO_3^-(aq) \leftrightarrow + H_3O^+(aq) + SO_3^{2}(aq)} \qquad \mathbf{(AR4)}$$

At higher concentrations of $CaCO_3$, SO_3 formation is highly favoured, whereas at lower $CaCO_3$, SO_2 is favoured. The observed behaviour aligns with the findings presented in Section 3 where and increase in the limestone feed into the absorber will result in a higher pH and high pH can achieve greater SO2 removal in absorber (EPRI, 2007). A similar relationship is also given in literature which illustrates a sulphite-carbonate equilibrium in Figure 5.1.3. In this equilibrium, the concentration of SO_3 first rises within the pH range of 6 to 7, but then decreases for pH values exceeding 7 (TNO,EnBW, CSIRO, 2011).

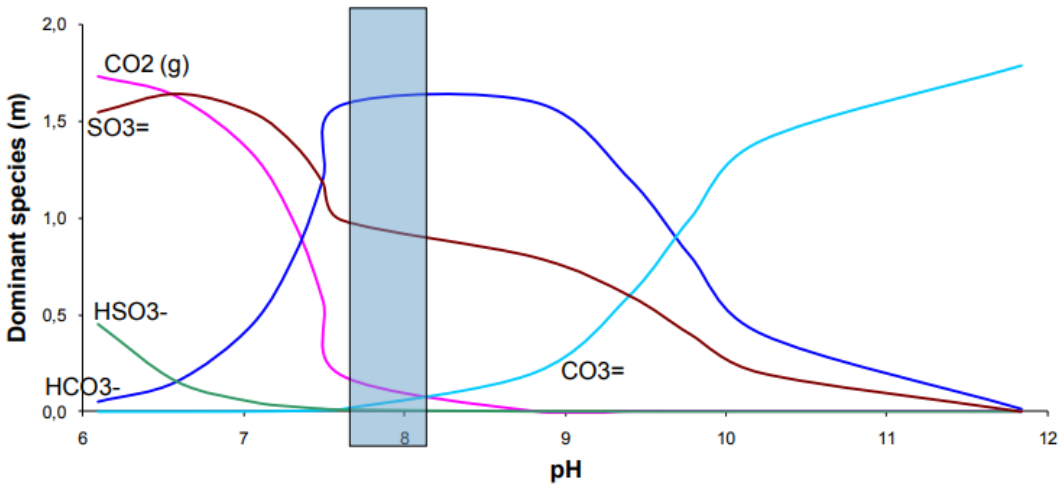

Figure 5.1-3: Sulphite-carbonate equilibrium (TNO,EnBW, CSIRO, 2011)

Upon examining the correlation, it becomes evident that a limestone solid content of 16-18% $CaCO_3$ is the minimum acceptable level, as the pH remains within the range of 5-6, as indicated in Figure 5.1.4. Below this specific region of operation, the pH level dropped to 2.54, as indicated in Figure 5.1.4.

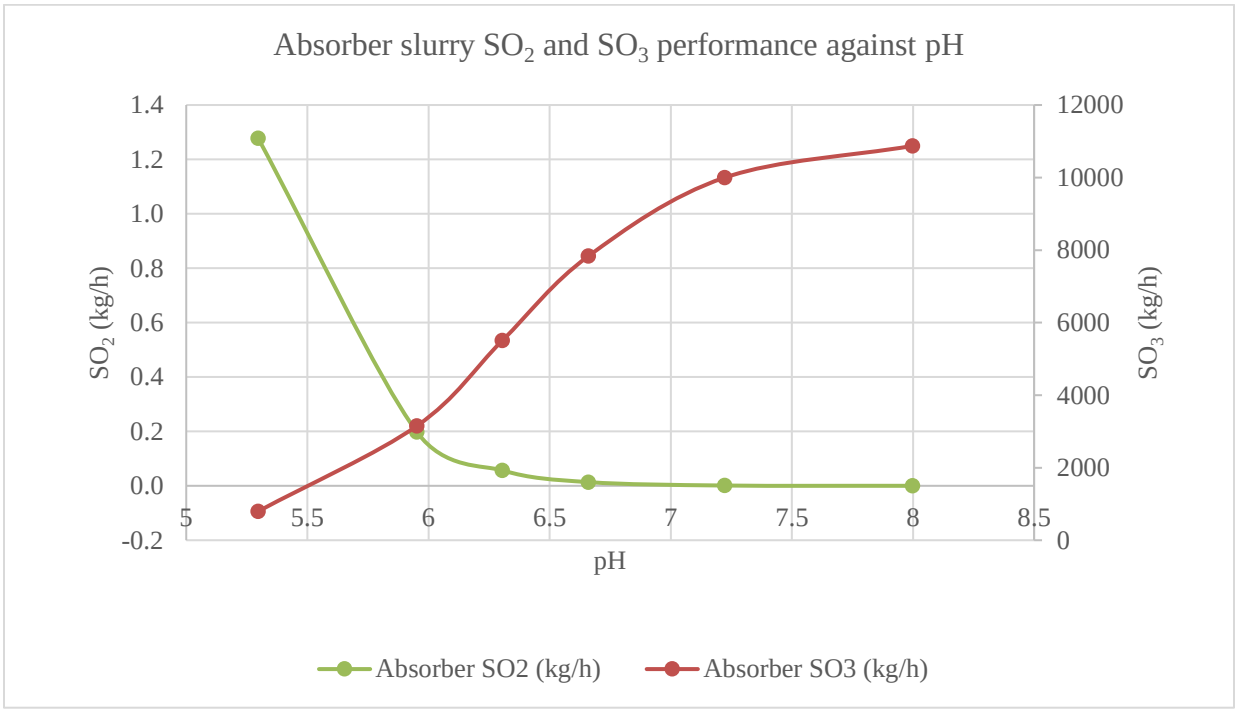

Figure 5.1-4: Absorber SO_2 and SO_3 performance against pH

When the slurry concentration increased above 16%, the pH level of the absorber remains higher than 5. When the concentration is less than 16% ,the pH decreases to 2.54, which aligns with the findings in Table 5.1.1 of the case study.

Table 5.1.1 demonstrates the absence of limestone feed to the absorber, which leads to a low pH. However, the simulation provides additional graphical information indicating that pH instances below 16% $CaCO_3$ would also result in low pH.

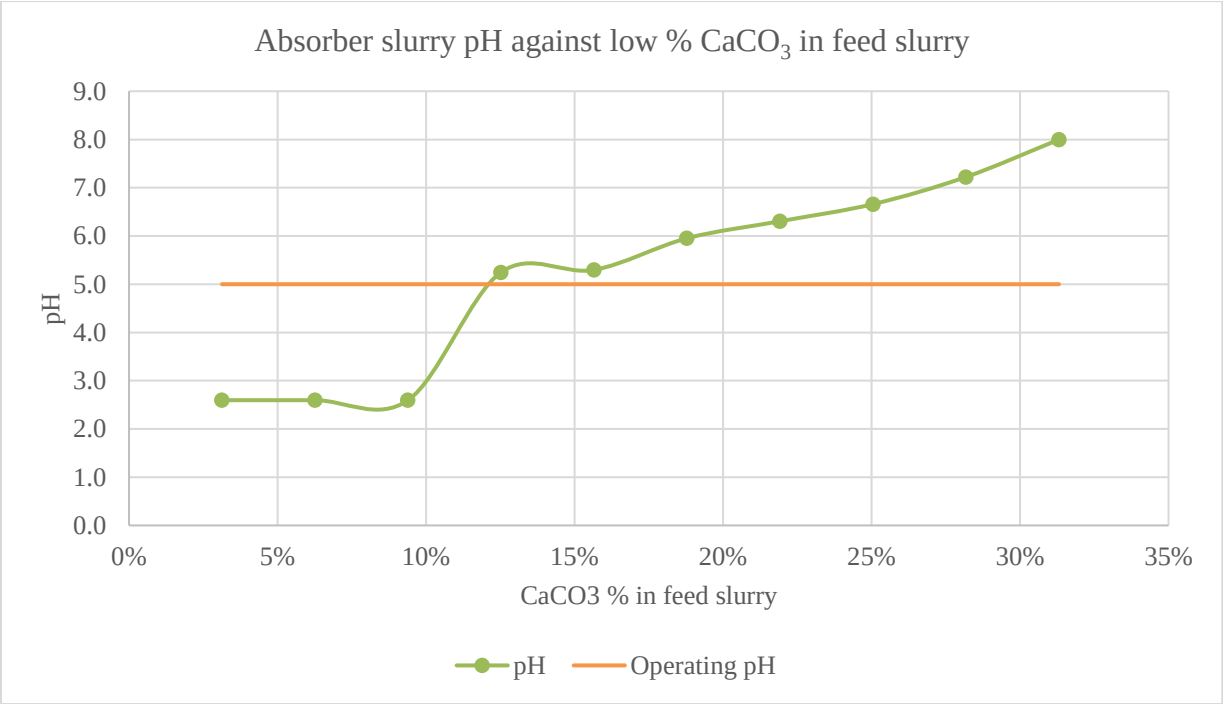

Figure 5.1-5: Absorber slurry pH vs $CaCO_3$ % in feed slurry

5.2 Case study 2: Liquid to gas ratio imbalance

The liquid to gas ratio as discussed in section 3 is the ratio of scrubbing liquid slurry to gas flow (EPA, 2013).
Practically, the absorber L/G ratios determine the number of pumps needed for each boiler's maximum continuous rating. Maintaining the necessary liquid to gas ratio has the following benefits:

- Provide an adequate amount of limestone slurry to absorb sulphur dioxide.
- The process of quenching helps to achieve lower temperatures of the flue gas when it comes into contact with the absorber.

The liquid to gas ratio is given below in Figure 5.2.1 where the minimum is 9.8 and maximum 14.5 l/m^3.

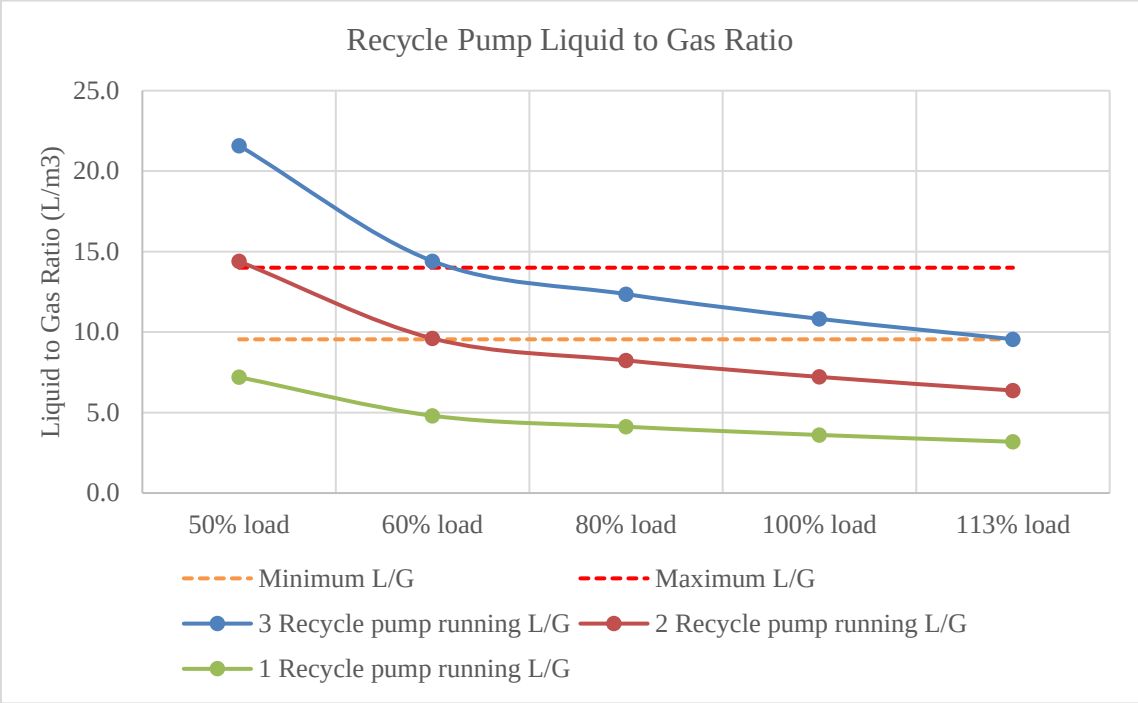

Figure 5.2-1: L/G ratio against Boiler load

The Eskom Power Station A operation has incurred flue gas flowrate of maximum 5.1x 10^6 Am^3/h in the sampled data in section 4. The case study seeks to investigate the highest flow possible within the confines of the design. The normal operating point is 2.916 x10^6 Am^3/h. This will be simulated by increasing the flue gas volumetric flow to 6 x10^6 Am^3/h. It is worth noting that the 113% boiler load in Figure 5.2-1 is equivalent to 4 018 300 Am^3/h. Therefore, the simulation is required to find an optimal value beyond the design base.

The case study 2 scenario is given in Table 5.2-1 where the unit is generating 532MW and the absorber pH is 5.04, with a limestone feed of 10.61 l/s (14323.5 kg/h $CaCO_3$) at a flue gas flow of 5.1 x$10^6$$Am^3/h$. The emissions were low at 43.85 mg/Nm^3. It is observed that even though the absorber was experiencing high flue gas flow, the SO_2 limits were not contravened due to running the highest number of pumps required as given by Figure 5.2.1.

Table 5.2-1: High flue gas flow

Timestamp	**Generator Output (MW)**	**Absorber pH Control**	**Absorber Limestone Feed(l/s)**	**SO_2 Emissions Chimney (Day mg/Nm^3 @10% O_2)**	**Flue gas flow (Am^3/h)**
06/08/2023 05:00:00	532.45	5.04	10.61	43.85	5 145 629.01

In the simulation development it was assumed that the maximum number of pumps are always running, therefore only the flue gas flow rate will be increased as indicated in the process flow given by Figure 5.2.1

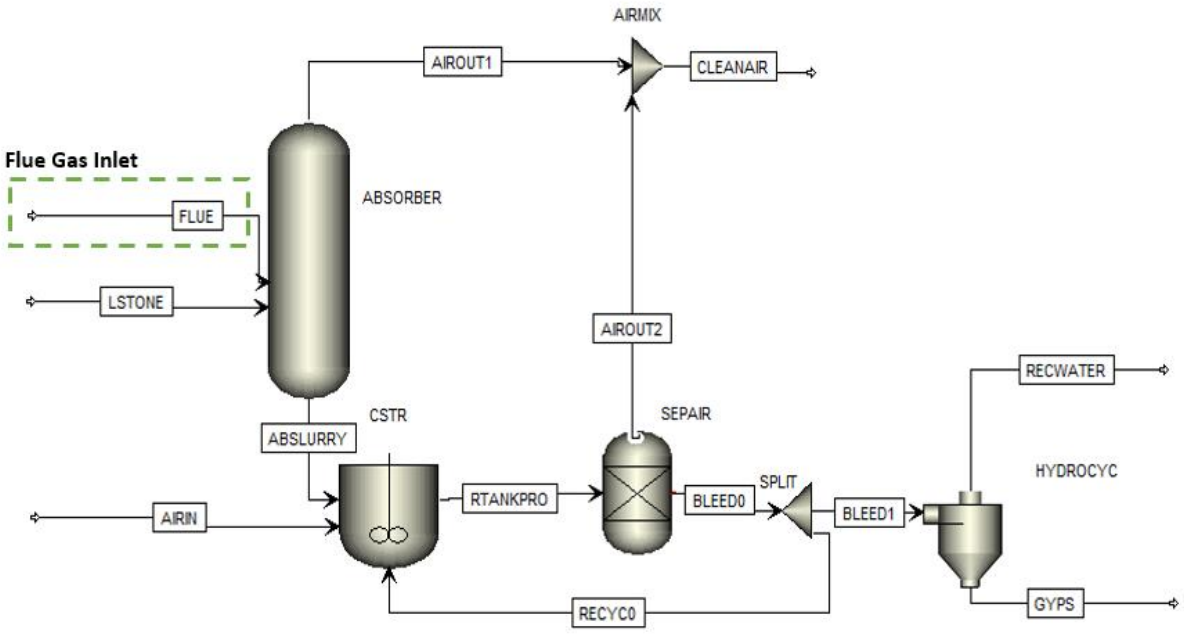

Figure 5.2-2: WFGD Absorber with variable flue gas flow volume

The SO_2/SO_3 equilibrium relation was studied once again so that the limit volumetric flow can be obtained. The calculated input figures are given in Appendix C. The intersection point of the two is approximately at 4.5 $x10^6$ m^3/h in Figure 5.2.3 where above this point high SO_2 emissions will be experienced.

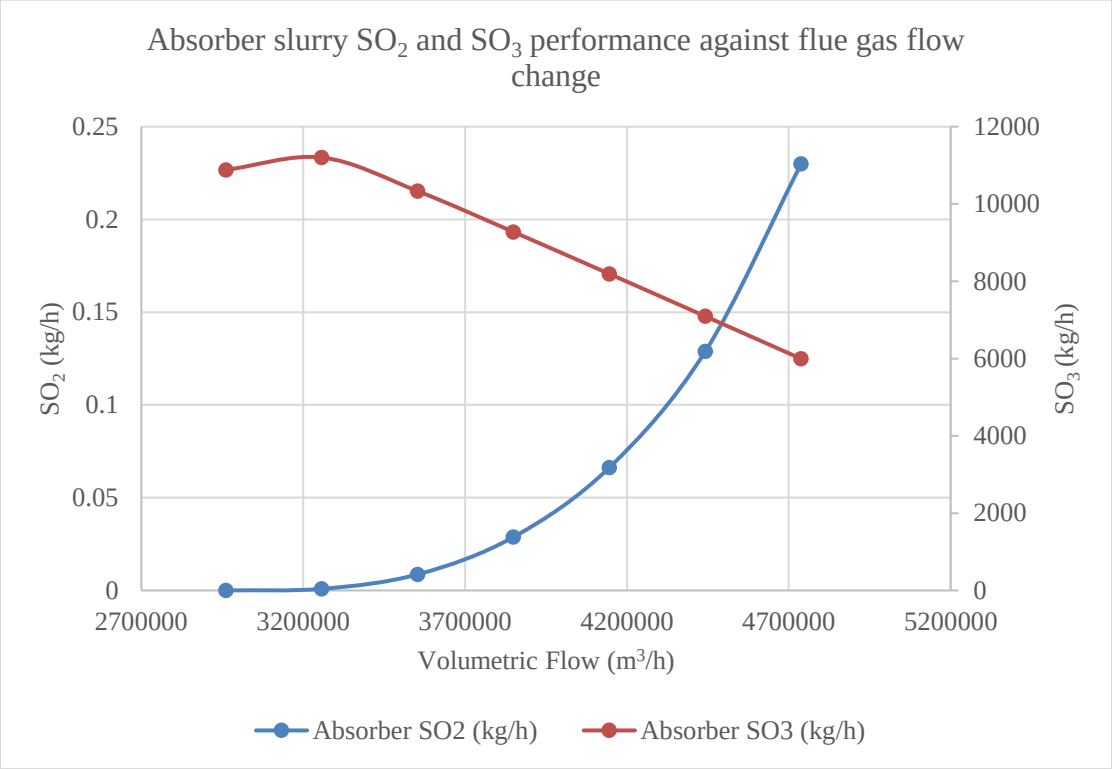

Figure 5.2-3: Absorber SO_2/SO_3 vs flue gas volumetric flowrate

The pH observed in the simulation is given in Figure 5.2.4 where the absorber slurry and reclaim water pH is plotted. The absorber pH decreases from 8 to 6 with increasing volumetric flowrate, however the reclaim water pH drops below the acceptable operation range 5-6 at flow rate 4.5 $x10^6$ m^3/h. The reclaim water would be used in the milling plant for limestone slurry preparation. Therefore, low reclaim water pH would lower the reactivity of the limestone slurry.

The low pH below 4 is not acceptable for absorber internals, pumps, and other auxiliary equipment in the WFGD.

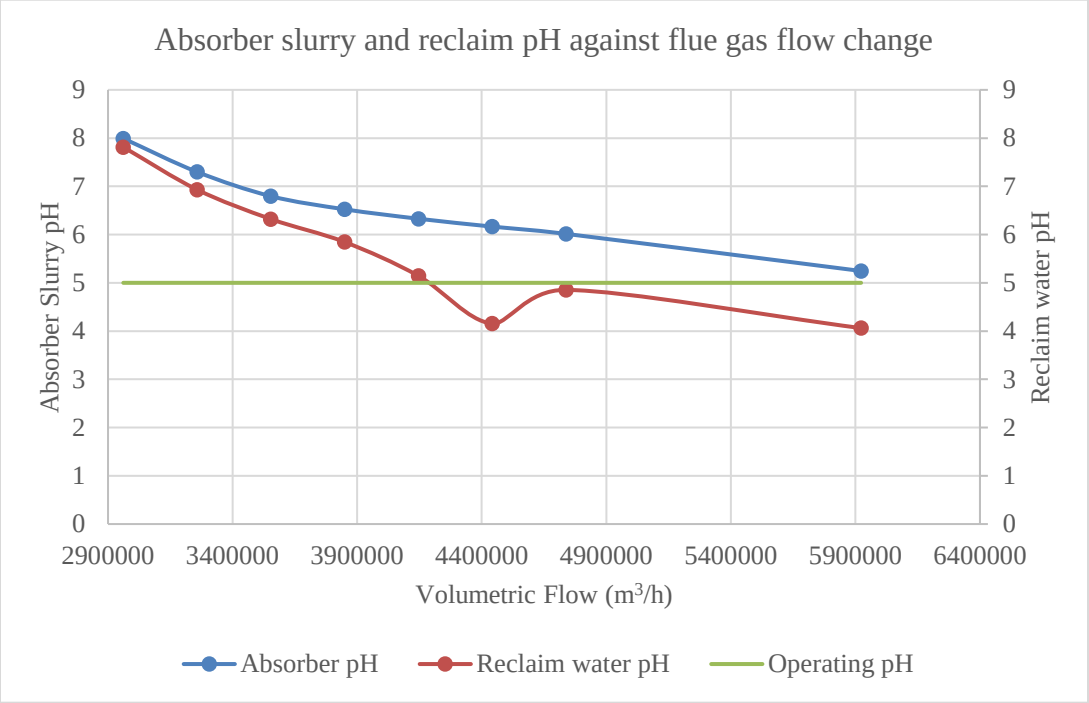

Figure 5.2-4: Absorber and reclaim water pH

The outlet SO_2 from the chimney/Stack indicated an increase to 40mg/Nm^3 at flow rate 4.5 x10^6 m^3/h, which is comparable to Table 5.2.1 where the actual plant emissions were 43 mg/Nm^3.



Figure 5.2-5: Absorber outlet SO_2 emissions

Figure 5.2.6 illustrates the potential impact of an increase in flue gas flow on gypsum production, which is another parameter that will be influenced. The presence of a peak at 4.0 x 10^6 m^3/h indicates the existence of an ideal flue gas volumetric flowrate for achieving maximal gypsum production. The simulation results are not verifiable due to the absence of any way to quantify the gypsum production rate at the Eskom Power Station A site, as the gypsum is currently being co-disposed with ash.

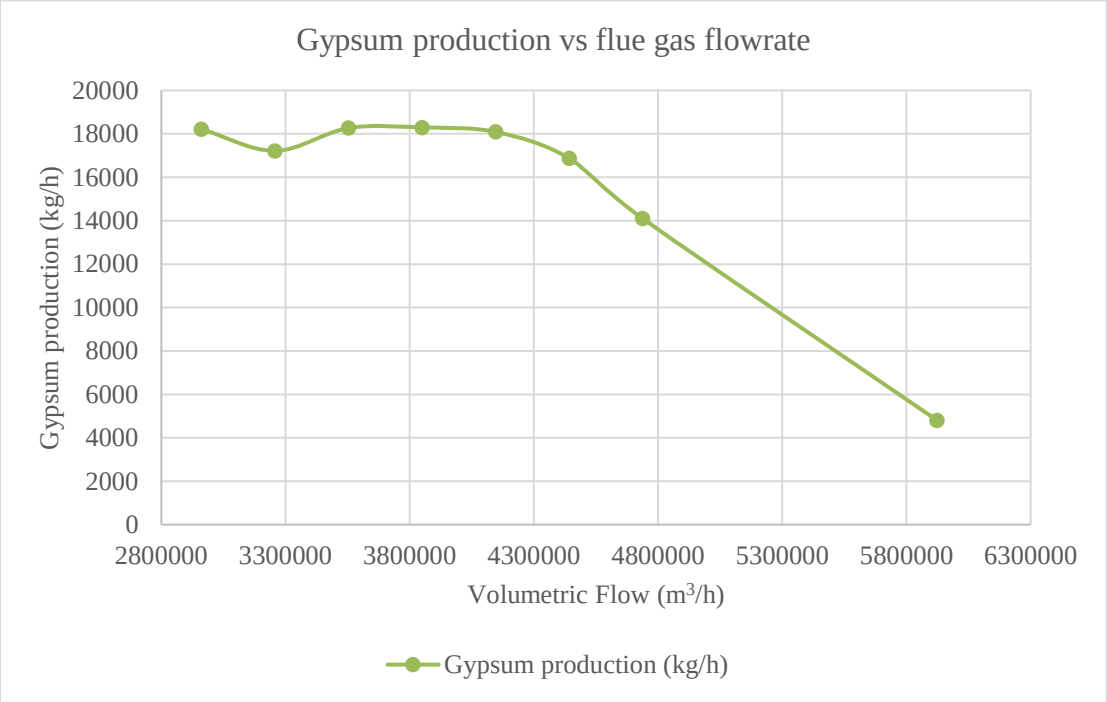

Figure 5.2-6: Gypsum production with increasing flue gas flow

The gypsum dewatering plant is common for all absorbers; therefore, it is also not possible to quantify the production of gypsum per absorber.

However, the design of the WFGD does specify a maximum gypsum production of 26585 kg/h at design flow of 4.7 x 10^6 Am^3/h; where the simulation results only report 18293 kg/h gypsum production. In practice the low gypsum formation is problematic indicating high calcium sulphite in the absorber, which will end up in the dewatering system. The $CaSO_3$ crystals are smaller than the gypsum crystals, and usually remain in the reclaim water and will block the piping systems, hydrocyclones and dewatering cloth over time when operations at high flue gas flow rates occurs over extended periods. There will also be excess water in the dewatering system and ultimately the water balance of the WFGD system will be negatively impacted.

Further simulation on the model would need to be done to investigate the differences as part of future work. The simulation could not be tested above 6 x 10^6 Am^3/h since convergence was not established and model reliability was questionable with numerous variables unable to reach convergence at high volumetric flow rates.

5.3 Case study 3: Variable Sulphur content

The WFGD is a post combustion technology and thus only treats what has already combusted in the boiler. The sulphur content varies mainly due to coal source and boiler combustion. Based on the discussion in section 3, in general the higher the sulphur content, the more limestone slurry is required to ensure that desulphurisation occurs. The design sulphur content is 0.9%, and normal operation ranges from 0.5-1.1% S (mass basis as) given in Table 4.2.1.8 1, however the maximum grab sample measured from a potential coal source is 1.6%. The potential coal source will be named "Test coal"

The Eskom Power Station A system is equipped with online coal analysers for belt scale coal analysis. These analysers allow for the comparison of physical samples of coal quality with the data obtained through online monitoring when the coal enters a given unit. However, the system has been offline because of commissioning processes that are taking place. Currently, coal grab samples are collected at 8am in the morning from the coal mills. However, these samples do not accurately represent the conditions throughout the entire day of operation, nor do they capture any abnormal or test conditions, as described in the case study with a 1.6% sulphur level. The absorber is equipped with a flue gas inlet analyser, which measures the amount of SO_2 entering the absorber and is utilized for controlling the limestone. The maximum sulphur content from the data is 0.7% sulphur as shown in Table 5.3-1; however, our case study requires values higher than the expected range. Therefore, the current simulation analysis will make a comparison of the normal operating coal Table 5.3-2 and the requirement of 1.6% sulphur mass basis as given in Table 5.3-3.

Table 5.3-1:Inlet absorber sulphur content

Timestamp	**Generator Output (MW)**	**Absorber pH Control**	**Absorber limestone Feed(l/s)**	**Absorber SO_2 Inlet (ppm)**	**Absorber SO_2 Inlet (mg/Nm^3 @ 10% O_2)**	**SO_2 Emissions Chimney (Day mg/Nm^3 @10% O_2]**	**Flue gas flow (Am^3/h)**
04/16/2023 08:00:00	567.05	5.03	14.69	1169.10	3719.31	54.49	4360351.97

To simulate the high sulphur test coal in Aspen, new feed ratios for limestone had to be calculated based on stoichiometry. RADFRAC could only converge when the stoichiometric ratios were perfectly balanced. The limestone solids percentage in the slurry feed to the absorber was still kept at 31% even though the mass required had to be changed. The results for the high sulphur test case is summarized in Table 5.3.2 and full results are given in Appendix D.

A 1.6% sulphur content is almost double the design base sulphur where the SO_2 in the flue gas is 13429 kg/h in Table 5.3.1, in comparison to 6669 kg/h (design) and 8849 kg/h (normal coal). The limestone feed requirement is at a value of 94316 kg/h for the high sulphur test coal.

The amount of gypsum in the high sulphur test coal has almost doubled compared to the normal operating coal, as gypsum is considered a waste product. There if the gypsum is not sold, running

with the high sulphur test coal would generate more waste, and require extended life for disposal beyond what the station has made provision for.
The moisture content of gypsum remains constant at 4.3% under all situations. Under conditions that promote gypsum production, the formation of $CaSO_3$ is negligible in the absorber.

The amount of oxidation air has increased from 1599 kg/h in the normal coal to 2656 kg/h in the high sulphur test coal. As the amount of oxidation air is raised in proportion to the sulphur concentration, the simulation shows no emissions of SO_2.

Practically, the management of limestone is automated through a control valve, meaning that if the sulphur levels rise within the predetermined range, the control system can effectively reduce and prevent the release of pollutants by increasing the limestone control valve % opening.

However, the maximum limestone supply feed rate that is possible on plant is 20 l/s which is 90000 kg/h of total limestone feed. Therefore, it is not feasible to utilize coal with a sulphur concentration of 1.6% as it will lead to emissions above 500 mg/Nm^3. The equipment limitation in this case is helpful to determine if a simulation finding is feasible. Therefore 1.6% sulphur content will not be treatable and will result in high emissions.

To address the limestone supply limitation, an Aspen simulation was further generated for the limestone supply maximum of 90 000kg.

The results are given in Table 5.3.4. where the closest value obtained in Aspen for limestone maximum is 90086.50 kg/h**.** The sulphur content is 11739.02 kg/h which is maximum sulphur content of 1.4% corresponding to 115.5 kg/s of coal fed to the boiler.
The gypsum production is 27544.66 kg/s which is inline with the current plant design. All parameters in Table 5.3.4 are feasible and acceptable.

In section 4 where the gypsum quality was discussed, and represented by the analysis from April 2023 to August 2023 in Figure 4.2.1.7-1(5.3-4) .
The $CaSO_3$ is captured in the filtrate which represents the reclaim water as given in Table 5.3.4. The simulation results and the actual gypsum analysis of the plant corroborate.

It can also be seen in Figure 4.2.2.7.1(5.3.4) that there was a performance issue with the absorber since carbonates CO_3 were picked up in the solid phase analysis of the gypsum. However, the simulation results have no carbonates in excess in the gypsum analysis. In practice the carbonates are limited to 1.5% total in the gypsum stream. This could be adapted in the model for future work.

Table 5.3-2: Normal operating coal (Base Case 1.1 % S content) analysis Aspen simulation output.

Normal Operating coal								
Parameters		**Flue Gas**	**Limestone**	**Clean Air**	**Airin (CSTR)**	**Bleed1**	**Reclaim Water**	**Gypsum**
Temperature	C	30.00	30.00	29.45	30.00	31.08	31.09	31.09
Pressure	bar	0.86	1.00	0.80	0.80	1.00	0.57	0.57
pH at 25 ℃		2.42	11.52	4.44		7.81	7.81	7.81
Mass Flows	**kg/hr**	**3055269.90**	**47373.30**	**3021914.77**	**1599.94**	**82256.49**	**64038.21**	**18218.28**
H_2O	kg/hr	131370.78	32524.64	101271.61	0.00	58846.80	57941.66	905.14
SO_2	kg/hr	8849.92	0.00	0.00	0.00	0.00	0.00	0.00
$CACO_3$	kg/hr	0.00	0.00	0.00	0.00	0.00	0.00	0.00
O_2	kg/hr	186371.46	0.00	186371.40	1599.94	0.00	0.00	0.00
$CASO_3$	kg/hr	0.00	0.00	0.00	0.00	47.20	46.47	0.73
N_2	kg/hr	2169241.63	0.00	2169241.63	0.00	0.00	0.00	0.00
NO_2	kg/hr	9471.34	0.00	9471.34	0.00	0.00	0.00	0.00
CA++	kg/hr	0.00	5914.87	0.00	0.00	1916.22	1886.75	29.47
CAOH+	kg/hr	0.00	35.50	0.00	0.00	0.01	0.01	0.00
CO_2	kg/hr	549948.58	0.00	555558.77	0.00	8.25	8.12	0.13
HCO_3-	kg/hr	0.00	49.91	0.01	0.00	1216.83	1198.11	18.72
OH-	kg/hr	0.00	3.33	0.00	0.00	0.00	0.00	0.00
CO_3--	kg/hr	0.00	8845.04	0.00	0.00	36.28	35.73	0.56
H_3O+	kg/hr	3.08	0.00	0.00	0.00	0.00	0.00	0.00
HSO_3-	kg/hr	13.12	0.00	0.00	0.00	108.24	106.58	1.66
SO_3--	kg/hr	0.00	0.00	0.00	0.00	2858.77	2814.78	43.97
$CASO_4$*2H_2O	kg/hr	0.00	0.00	0.00	0.00	17217.90	0.00	17217.90

Table 5.3-3: Test Coal (1.6 % Sulphur content) analysis Aspen simulation output.

High Sulphur test coal								
Parameters		**Flue Gas**	**Limestone**	**Clean Air**	**Airin (CSTR)**	**Bleed1**	**Reclaim Water**	**Gypsum**
Temperature	C	30.00	30.00	29.68	30.00	31.21	31.22	31.21
Pressure	bar	0.86	1.00	0.80	0.80	1.00	0.47	0.47
pH at 25 °C		2.32	11.46	4.44		7.71	7.71	7.71
Mass Flows	**kg/hr**	**3054964.29**	**94315.99**	**3028350.44**	**2655.90**	**123465.24**	**93492.70**	**29972.54**
H_2O	kg/hr	129897.82	71970.99	108160.66	0.00	87488.79	86206.24	1282.55
SO_2	kg/hr	**13429.34**	0.00	0.00	0.00	0.00	0.00	0.00
O_2	kg/hr	184893.74	0.00	184893.64	2655.90	0.00	0.00	0.00
$CASO_3$	kg/hr	0.00	0.00	0.00	0.00	58.67	57.81	0.86
N_2	kg/hr	2170502.17	0.00	2170502.17	0.00	0.00	0.00	0.00
NO_2	kg/hr	8012.64	0.00	8012.64	0.00	0.00	0.00	0.00
H_2SO_4	kg/hr	0.00	0.00	0.00	0.00	0.00	0.00	0.00
CA++	kg/hr	0.00	8897.90	0.00	0.00	2264.56	2231.36	33.20
CAOH+	kg/hr	0.00	55.90	0.00	0.00	0.01	0.01	0.00
CO_2	kg/hr	548209.21	0.00	556781.29	0.00	16.03	15.80	0.24
HCO_3-	kg/hr	0.00	86.58	0.03	0.00	1663.73	1639.33	24.39
OH-	kg/hr	0.00	7.48	0.00	0.00	0.00	0.00	0.00
CO_3--	kg/hr	0.00	13297.15	0.00	0.00	35.61	35.10	0.52
H_3O+	kg/hr	3.68	0.00	0.01	0.00	0.00	0.00	0.00
HSO_3-	kg/hr	15.69	0.00	0.00	0.00	168.77	166.31	2.47
SO_3--	kg/hr	0.00	0.00	0.00	0.00	3187.49	3140.74	46.73
$CASO_4$*2H_2O	kg/hr	0.00	0.00	0.00	0.00	28581.58	0.00	28581.58

Table 5.3-4: Maximum sulphur 1.41% for limestone supply limit

Limestone feed limitation final sulphur								
Parameters		**Flue Gas**	**Limestone**	**Clean Air**	**Airin (CSTR)**	**Bleed1**	**Reclaim Water**	**Gypsum**
Temperature	C	30.00	30.00	29.62	30.00	31.42	31.43	31.42
Pressure	bar	0.86	1.00	0.80	0.80	1.00	0.50	0.50
pH at 25 ℃		2.35	11.46	4.44		8.37	8.37	8.37
Mass Flows	**kg/hr**	**3054575.30**	**90086.50**	**3027277.51**	**2559.90**	**119820.59**	**90908.59**	**28912.00**
H_2O	kg/hr	129882.15	68743.51	107406.33	0.00	85022.15	83762.30	1259.85
SO_2	kg/hr	**11739.02**	0.00	0.00	0.00	0.00	0.00	0.00
O_2	kg/hr	184870.77	0.00	184870.68	2559.90	0.00	0.00	0.00
$CASO_3$	kg/hr	0.00	0.00	0.00	0.00	35.62	35.09	0.53
N_2	kg/hr	2170232.53	0.00	2170232.53	0.00	0.00	0.00	0.00
NO_2	kg/hr	8011.64	0.00	8011.64	0.00	0.00	0.00	0.00
H_2SO_4	kg/hr	0.00	0.00	0.00	0.00	0.00	0.00	0.00
CA++	kg/hr	0.00	8498.90	0.00	0.00	2112.82	2081.51	31.31
CAOH+	kg/hr	0.00	53.39	0.00	0.00	0.03	0.03	0.00
CO_2	kg/hr	549821.12	0.00	556756.29	0.00	7.80	7.69	0.12
HCO_3-	kg/hr	0.00	82.70	0.03	0.00	3113.63	3067.48	46.14
OH-	kg/hr	0.00	7.14	0.00	0.00	0.01	0.01	0.00
CO_3--	kg/hr	0.00	12700.86	0.00	0.00	253.24	249.50	3.75
H_3O+	kg/hr	3.43	0.00	0.01	0.00	0.00	0.00	0.00
HSO_3-	kg/hr	14.63	0.00	0.00	0.00	23.94	23.60	0.35
SO_3--	kg/hr	0.00	0.00	0.00	0.00	1706.68	1681.39	25.29
$CASO_4$*2H_2O	kg/hr	0.00	0.00	0.00	0.00	27544.66	0.00	27544.66

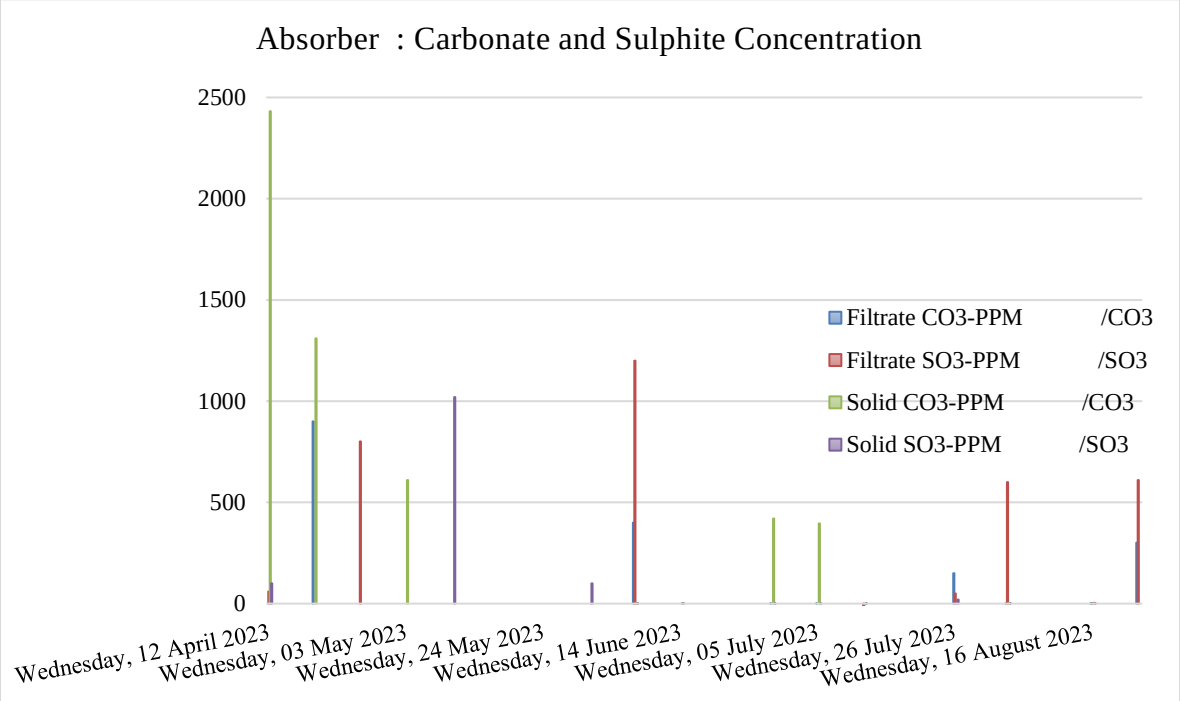

Figure 5.3-1: Actual absorber carbonate and sulphite concentrations in the reaction

CHAPTER 6: CONCLUSIONS AND RECOMMENDATIONS

As of late, the WFGD has emerged as the preferred desulphurization method across most industries due to its exceptionally high removal rate of more than 90%. Nonetheless, several concerns persist, demonstrating the intricacy of the WFGD absorber system and underscoring the need for comprehensive analysis of the WFGD process during actual plant operations.

Hence, the objective of this dissertation was to perform an Aspen Plus simulation of the wet flue gas desulfurization (WFGD) procedure to ensure a steady supply of electricity to the power grid while adhering to the specified SO_2 emission limits.

The Eskom Power Station A design dictates that the solid component of limestone feed to the absorber must contain 31% solids content of $CaCO_3$. However, lower limits were not given as part of the design base. In case study 1, the limestone solids percentage was varied from 31% to a point until a lower limit was determined. There was a transition in the concentration of limestone within the absorber, followed by the establishment of equilibrium among the reactive species, including SO_3 and SO_2. At higher concentrations of $CaCO_3$, SO_3 formation is highly favoured, whereas at lower $CaCO_3$, SO_2 is favoured. It was further observed that an increase in the limestone feed into the absorber will result in a higher pH and high pH can achieve greater SO_2 removal in absorber. The lowest $CaCO_3$ solids percentage that can be fed into the absorber during upset conditions where the pH remains above 4 is 16-18%. The SO_2 emissions remained below 500mg/Nm^3.

The liquid-to-gas ratio is a fundamental concept in the design of the WFGD. However, combustion and attemperation conditions in the boiler operation substantially increase the volumetric flow rate entering the absorber. Therefore, in case study 2, the highest flue gas flow rate was to be determined where the flue gas flow was increased from a design base of 2.916 $x10^6$ to 6 $x10^6$ Am^3/h. The SO_2/SO_3 equilibrium relation was studied again so that the limit volumetric flow can be obtained. Further analysis of the reclaim showed an alarming drop in pH when flue gas flow above 4 $x10^6$ Am^3/h was treated. The gypsum production rate was also stunted by the increase in volumetric flow rate. It has been ascertained through considering plant operations and prevention of damage to auxiliary equipment due to handling low pH slurry that the optimal range for flue gas volume is between 4.0 x 10^6 m^3/h and 4.5 x 10^6 m^3/h. The SO_2 emissions remained below 500mg/Nm^3.

Case study 3 required the determination of the maximum sulphur content that could be practically treated in the WFGD. A potential coal source with a 1.6 % S content was proposed, however there is a plant limitation since the maximum design of the plant is to treat maximum sulphur content of 1.3%. In simulating the 1.6 % S in the flue gas flow, this is the only case that will generate emissions above the license since the limestone feed control valve is the bottleneck of the reagent supply system . As per the conclusive assessment, the maximum allowable concentration of sulphur in the designated WFGD facility was ascertained. The utmost capacity of the limestone

slurry control valve is 90000 kg/h to supply slurry to the absorber Therefore, there exists a little margin of coal with slightly greater sulphur content, but it is restricted to a maximum of 1.41% sulphur for emissions to remain below 500 mg/Nm^3.

The simulation outcomes facilitated the establishment of control limits for both the operational and design bases of the absorber. Further applications of the obtained results to model other WFGD absorption systems are possible, given that they are applicable to any absorption system governed by equilibrium processes.

6.1 Recommendations and current model use

- It is recommended that the above limits be implemented in a best operating practice to govern the conditions of the WFGD at Eskom Power Station A.
- It is also recommended that an exercise of actual plant measurements should be conducted, and the data be used in the simulation so that data-fitting and better real time comparisons can be optimized for simulations.

6.2 Further improvements and studies

- Develop the simulation further to include a reagent and dewatering plant
- Generate a stable reclaim water product that can be recycle back into the absorption process
- Introduce limestone reactivity by mixing the limestone with a reclaim water from the process
- Include $MgCO_3$ and HCl in the limestone feed specifications and water respectively to influence the limestone reactivity
- Simulate a model with absorber internals to account for mass transfer
- Investigate the quality of gypsum in order to build the model for comparison with actual gypsum product, and feasibility for market uptake.

REFERENCES

1. Alstom Thermal Systems. (2014, December 10). WFGD Operation Manual Section 1: 203-43852. South Africa: Eskom Holdings LTD SOC.
2. Arif Arif, C. S. (2015). Modeling of wet flue gas desulphurisation. *Research Gate* (pp. 1-12). North West University. Retrieved May 11, 2023, from https://www.researchgate.net/publication/282672302
3. Arvidsson, S. (2021). *Modelling and Evaluation of a Waste Incineration Flue Gas Treatment Process.* Masters Thesis, Lund University, Department of Chemical Engineering. Retrieved November 2023
4. Aspen. (1998). Unit Operation Models: Reference Manual. In A. T. Inc, *Aspen Plus Steady State Simulation V10* (pp. 1-380). AspenTech.
5. Aspen Technology. (2001, October). Physical properties method and models. Cambridge. Retrieved from http://www.aspentech.com/
6. Aspen Technology. (2001, October). Physical Property Data Aspen. Cambridge.
7. Aspen Technology. (2002, October). Customizing RadFrac Convergence: Advanced Distillation with Aspen Plus. Cambridge.
8. Aspen Technology Inc. (1999). Modeling Processes with Electrolytes. California, USA.
9. Brogren, C., & Karlsson, H. T. (1997, April). Modeling the absorption of SO2 in a spray scrubber using the penetration theory. *Chem. Eng Sci, 52*(18), 3085-3099. Retrieved May 2023, from https://pdf.sciencedirectassets.com/271348/1-s2.0-S0009250900X00632/1-s2.0-S0009250997001267/main.pdf?X-Amz-Security-Token=IQoJb3JpZ2luX2VjEIr%2F%2F%2F%2F%2F%2F%2F%2F%2F%2FwEaCXVzLWVhc3QtMSJHMEUCIQDde0OdoH3GdDVXH8LBEBYcq9IGA2iHDLTc9dXn7hElQQIgVgvzS8juwZSl
10. Carletti, C., De Blasio, C., Makila, E., Salonen, J., & Westerlund, T. (2015). Optimisation of wet flue gas desulphurisation scrubber through mathematical modelling of Limestone dissolution experiments. *Ind. Eng. Chem.*, 9783-9797.
11. Carlos Duque, C. M. (2010). Simulation of two alternatives for SO2 removal from a wet cement kiln exhaust gas . *Rev. Fac. Ing. Univ. Antioquia*, 49-57.
12. Chang, J. C. (2005). *Effects of magnesium and chloride ions on Limestone dual alkali system performance.* New York: EPA.
13. Che Yao, C. H. (2022). Intelligent Online Evaluation Model of WFGD System Performance Based on Gas-liquid Mass Transfer Data Analysis. *IEEE International Conference on Electrical Engineering, Big Data and Algorithms (EEBDA)* (pp. 1-4). Changchun: IEEE.
14. Córdoba, P. (2014). Status of Flue Gas Desulphurisation (FGD) systems from coal-fired power Status of Flue Gas Desulphurisation (FGD) systems from coal-fired power limestone FGDs. *Fuel*, 274–286.
15. Córdoba, P. (2015). Status of Flue Gas Desulphurisation (FGD) systems from coal-fired power plants: Overview of the physic-chemical control processes of wet limestone FGDs. *Fuel, 144*, 274-286. doi:http://dx.doi.org/10.1016/j.fuel.2014.12.065
16. Davidson, L. N., Goffredi, R. A., & Wedig, C. P. (1985). The Importance of Maintenance for Lime Flue Gas Desulphurisation Systems. *Journal of the Air Pollution Control Association, 35*(6), 685-690. doi:https://doi.org/10.1080/00022470.1985.10465946

17. Department of Environmental affairs. (2010). *List of activities resulting in atmospheric emissions which have or may have detrimental effect on environment, including health, social , economic , ecological conditions or cultural heritage, NEMA Act 39 of 2004.* Pretoria: DEA.
18. Dou, B., Pan, W., Jin, Q., Wang, W., & Li, Y. (2009). Prediction of So2 removal efficiency for wet flue gas desulphurisation. *Energy Conversion and Management, 50*, 2547-2553. doi:10.1016/j.enconman.2009.06.012
19. Dzhonova-Atanasova, D. B., Razkazova-Velkova,, N. E., & Ljutzkanov, L. A. (2011). Current problems and developments in flue gas desulphurisation. *Journal of International Scientific Publications:Materials, Methods & Technologies, 5*(1), 74-103. Retrieved May 2023, from http://www.science-journals.eu
20. EPA. (2013). Flue Gas Desulphurisation (Acid Gas Removal) Systems 2.0-7/98. EPA. Retrieved May 2023, from https://www.yumpu.com/en/document/view/29225542/lesson-9-flue-gas-desulfurization-acid-gas-removal-systems
21. EPA. (2023, May 11). *Air Pollution Control Technology Fact Sheet:E:\9010 PRT\9010-241\New Fact Sheets\New English\fs FDG final.wpd*. Retrieved from United States Environmental Protection Agency: https://www3.epa.gov/ttncatc1/dir1/ffdg.pdf
22. EPA. (2023, May 11). *What is Acid Rain?* Retrieved September 2023, from United States Environmental Protection Agency: https://www.epa.gov/acidrain/what-acid-rain
23. EPRI. (1979). *Lime FGD Systems Data Book 2nd Edition, Publication No CS-2781.* Palo Alto, California, USA: EPRI. Retrieved September 2023
24. EPRI. (2007). *FGD Chemistry and Anlaytical Methods Handobook: Volume 1, Revision 2.* Palo Alto, CA: EPRI.
25. Eskom Holdings SOC Ltd. (2008, January). Boiler Training Manual. Eskom Power Station.
26. Eskom Holdings SOC Ltd. (2008). *Process plant principles: Eskom Operator Training.* Emalahleni: Eskom Training Department.
27. Eskom Holdings SOC Ltd. (2021, August). *How-Electricity-is-produced-in-a-Coal-Fired-Power-Station.* Retrieved September 2023, from Eskom: http://www.eskom.co.za/
28. Gerbec, M., Stergarsek, A., & Kocjancic, R. (1995). Simulation model of wet flue Gas desulphurisation plant. *Computers & Chemical Engineering, 19*, 283-286. Retrieved May 2023, from https://pdf.sciencedirectassets.com/271414/1-s2.0-S0098135400X01834/1-s2.0-0098135495870504/main.pdf?X-Amz-Security-Token=IQoJb3JpZ2luX2VjEIr%2F%2F%2F%2F%2F%2F%2F%2F%2F%2FwEaCXVzLWVhc3QtMSJIMEYCIQDwwZdKET%2Fjz5US%2FxXFsYMgKqJ96RHZzVMVecxf1zLC5gIhAOVVCXTod
29. Gingerich, D., Grol, E., & Mauter, M. (2018). Fundamental Challenges and Engineering Opportunities in Flue Gas Desulfurization Wastewater Treatment at Coal Fired Power Stations. *Environmental Science: Water Research & Technology*, 1-55. Retrieved November 2023
30. Girmay, M. E., & Chikobvu, D. (2017, February). Quantifying South Africa's sulphur dioxide emission efficiency in coal-powered electricity generation by fitting the three-parameter log-logistic distribution. *Journal of Energy in Southern Africa, 28*(1), 91-103. doi:http://dx.doi.org/10.17159/2413-3051/2017/v28i1a1530

31. Gong, Y., & Yang, Z.-G. (2018, December 1). Corrosion evaluation of one wet desulfurization equipment – Flue gas desulfurization unit. *Fuel Processing Technology, 181*, 279-298. doi:https://doi.org/10.1016/j.fuproc.2018.10.005
32. Green Peace. (August 2019). *Global SO2 emission hotspot database.* Greenpeace Environment Trust. Retrieved November 2023, from https://www.greenpeace.org/static/planet4-africa-stateless/2019/08/5f139f4c-final-global-hotspot-and-emission-sources-for-so2_19th_august-2019.pdf
33. Green, D. W., & Perry, R. H. (1984). Mass Transfer. In *Perry's Chemical Engineers Handbook, 8th edition* (pp. 5-61).
34. Heiting, B. (2017). *FGD Experience: Absorbers.*
35. Idaho National Engineering and Environmental Laboratory . (2002). *Steady-State Simulation of Steam Reforming of INEEL Tank Farm Waste.* Idaho: U.S. Department of Energy.
36. IEA. (2018, January). World energy balances. (I. E. Agency, Ed.) doi:http://dx.doi.org/10.1787/data-00512-en
37. Kallinkos, L. E., Farsari, E. I., Spartinos, D. N., & Papyannakos, N. G. (2010). Simulation of the operation of an industrial wet flue gas desulphurisation system. *Fuel Processing Technology, 91*, 1794-1802. doi:10.1016/j.fuproc.2010.07.020
38. Katoh, S., & Yoshida, F. (2009). Chapter 6: mass transfer. In *Biochemical Engineering: A textbook for engineers, chemists and Bilogists* (pp. 73-95). Wiley-VCH Verlag GmbH & Co. KGaA. Weinheim.
39. Kimre. (2020, July 7). The Basics of Mist Eliminators. (C. McAniff, Compiler) Homestead, Florida, USA. Retrieved from https://www.kimre.com/the-basics-of-mist-eliminators/
40. Kunkun, H., Guozhen, C., & Jianjun, N. (2016). Simulation study on the demercuration performance of wet flue gas desulphurisation system. *Clean coal technology and sustainable development*, 439-443.
41. Lim, J., Choi, Y., Kim, G., & Kim, J. (2020). Modeling of wet flue gas desulphurisation to utilize low grade limestone. *Korean J. Chem Eng, 37*(12), 2085-2093. doi:10.1007/s11814-020-0639-6
42. Liu, Z. (2023). BAE 820 Physical Principles of Environmental Systems: . *Inter phase mass transfer*. K State Research and Extension: Biological and Agricultural Engineering.
43. Miszczyk, A., & Darowicki, K. (2002, October 29). Reliability of Flue Gas Desulphurisation Installations - the Essential Condition of Efficient Air Pollution Control. *Polish Journal of Environmental Studies, 11*(3), 205-209. Retrieved from https://www.researchgate.net/publication/238683791_Reliability_of_Flue_Gas_Desulphurisation_Installations_-_The_Essential_Condition_of_Efficient_Air_Pollution_Control?enrichId=rgreq-e7c936afe9afef5d1bbdba31ca0e21a3-XXX&enrichSource=Y292ZXJQYWdlOzIzODY4Mzc
44. Moganelwa, A., Schafer, S., & Godana, P. (2018). New water saving FGD technology in south africa: CFB FGDdemonstration. *VGB Powertech: Internation Journal for electricity and heat generation*, 50-56.
45. Morosele, I. P., & Langerman, E. K. (2020, October). The impacts of commissioning coal-fired power stations on air quality in South Africa: insights from ambient monitoring stations. *Clean Air journal, 30*(2), 1-11. doi:https://doi.org/10.17159/caj/2020/30/2.8833

46. Munawer, E. M. (2018). Human health and environmental impacts of coal combustion. *Journal of Sustainable Mining*(17), 87-96. doi:https://doi.org/10.1016/j.jsm.2017.12.007
47. Neveaux, T., & Moullec, Y. L. (2011). Wet Industrial Flue Gas Desulphurisation Unit: Model Development and Validation on Industrial Data. *Ind En Chem*, 7579-7592.
48. Nicol, K. (2013, March). Recent developments in particulate control. Retrieved November 2023, from https://usea.org/sites/default/files/032013_Recent%20developments%20in%20particulate%20control_ccc218.pdf
49. Noah Yakah, I.-e. N. (2022). Wet flue gas desulphurization (FGD)wastewater treatment using membrane distillation. *Energies, 15*(24), 1-12. doi:https://doi.org/10.3390/en15249439
50. Petrucci, R. H., Harwood, W. S., Herring, G. F., & Madura, J. D. (2007). *General Chemistry: Principles and modern applications.* Upper Saddle River: Prentice Hall.
51. Prakashan, N. (2015). Gas Absorption. In *Unit Operations- II.* Pune: Pragati Book House.
52. Qiao, Z., Wang, X., Gu, H., Tang, Y., Si, F., & Romero, C. E. (2019, September). An investigation on data mining and operating optimization for wet flue gas desulphurisation systems. *Fuel, 258*, 1-10. doi:https://doi.org/10.1016/j.fuel.2019.116178
53. RSA DPE. (2019). *Roadmap for Eskom in a Reformed Electricity Supply Industry.* Retrieved from Department of Public Enterprises: www.dpe.gov.za
54. Shi, Y.-T., Sun, D.-H., Li, Z.-J., Chen, N.-S., Qing, W., & Gao, D.-J. (2007). Hybrid Modelling and Control of Nonlinear Wet Flue Gas Desulphurisation Process. *6th International Conference on Machine Learning and Cybernetics*, (pp. 1-5). Hong Kong.
55. Simulate Live. (2023, October). *Complete List of Process Simulators*. Retrieved from Simulate Live: https://simulatelive.com/product-reviews/simulation/complete-list-of-process-simulators-part-1-2
56. Skinder, B. M., Sheikh, A. Q., Pandit, A. K., & Ganai, B. A. (2014, January 11). Brick kiln emissions and its environmental impact: A review. *Journal of Ecology and the Natural Environment, 6*(11), 1-11. doi:10.5897/JENE2013.0423
57. South African Government Gazette. (2010, March 31). National Environmental Management: Air Quality 2004 Act No 39 of 2004. Capetown, Western Cape, South Africa. Retrieved May 10, 2023
58. Srivastava, R. K., & Jozewicz, W. (2001). Flue Gas Desulfurization: The State of the Art. *Journal of the Air & Waste Management Association, 51*(12), 1676-1688. doi:https://www.tandfonline.com/action/showCitFormats?doi=10.1080/10473289.2001.10464387
59. StatsSA. (2021). *Electricity, gas and water supply industry Report 41-02-01.* Pretoria: Statistics South Africa.
60. Steinmuller Engineering. (2013, March). FGD process design.
61. Tan, W., Zhang, Z., Li, H., Li, Y., & Shen, Z. (2017). Carbonation of gyspum from wet flue gas desulphurisation process: experiments and modelling. *Environmental Science and Pollution Research* , 8602-8608.
62. Tata Power. (2009, September 30). News & Technology for the Global Energy Industry. *Techniques for determining Limestone composition and reactivity*, pp. 1-9. Retrieved November 2023, from https://cercind.gov.in/2021/discussion_paper/Comments-Staff-Paper/20Tata-Power-Annexure-2.pdf
63. TNO,EnBW, CSIRO. (2011). *Process concets for combined CO2 and SO2 removal.*

64. URS Corporation. (2008). Wet FGD Chemistry and Performance Factors. In G. Maller (Ed.), *2008 Power Gen Conference*, (pp. 1-68). Retrieved March 24, 2017
65. Walsh, K., Theron, R., & Reeders, C. (2021). Estimating the Economic Cost of Load Shedding in South Africa. *Biennial Conference of the Economic Society of South Africa* (pp. 1-22). Nova Economics – economic and strategy consulting.
66. Walsh, M. A., Mengel, L. M., Evans, A., Gal, E., Cavallari, G., Bienati, M., & Cavezzale, P. (2006). *Parameters impacting limestone dissolution in FGD systems.* Milan, Italy: Termokimik Corporation- Impianti e Procedimenti Industriali SpA.
67. Wilcox and Babcock. (1993). Steam, its generation and Use. In B. a. Wilcox, *Steam, Its generation and Use* (p. 98). New York, USA.
68. WR Training Pro. (2023, October). Steady-State Chemical Engineering Simulation & Process Modeling using Aspen Plus V11. Udemy Online Courses.
69. Yin, X., Sun, K., Li, S., Wang, X., Dong, Y., & Cui, L. (2023). Enhancing deep learning for the comprehensive forecast model in flue gas desulfurization systems. *Control Engineering Practice, 138*. doi:https://doi.org/10.1016/j.conengprac.2023.105587
70. Yishan Guo, Z. X. (2019). Modeling and optimization of wet flue gas desulfurization system based on a hybrid model method. *Journal of the air & waste management association, 69*(5), 565-575. doi:https://doi.org/10.1080/10962247.2018.1551252
71. Zhong, Y., Gao, X., Huo, W., Luo, Z.-Y., Ni, M.-J., & Cen, K.-F. (2008). A model for performance optimisation of wet flue gas desulphurisation system of power plants. *Fuel Processing Technology, 89*, 1025-1032. doi:doi:10.1016/j.fuproc.2008.04.004

8. APPENDIX

8.1 Appendix A:

8.1.1 Flue Gas Volume Calculation

$$\frac{P_1V_1}{T_1} = \frac{P_2V_2}{T_2}$$

$$V_2 = \frac{P_1V_1T_2}{T_1P_2}, were\ P_1\ and\ P\ _2 are\ the\ equal$$

$$V_2 = \frac{(86893)(2668201)(303)}{(273)(86893)}$$

$$V_2 = 2961409.901 m^3/h$$

8.1.2 CSTR Volume Calculation

$$V = \pi r^2\ h$$

$$V = \pi \left(\frac{20}{2}\right)^2 9 = 2727\ m^3$$

8.2Appendix B: Case Study 1 Results

Table 8.2-1Case study 1 Results

No	**$CACO_3$**		**H_2O**		**$CaCO_3$ percentage in Limestone feed mix**	**Absorber SO_2**	**Absorber SO_3**	**Absorber HSO_3**	**pH**	**Operating pH**
Units	kg/h	Kmol/h	kg/h	Kmol/h		kg/h	kg/h	kg/h		
1	14821	148.08132	32513	1804.7457	31%	3.34495E-05	10871.92061	192.449	7.997849225	5
2	13338.9	133.27319	33995.1	1887.0148	28%	0.001159387	9998.413243	1075.208328	7.222841265	5
3	11856.8	118.46505	35477.2	1969.2839	25%	0.013615495	7832.736447	3268.122579	6.660046326	5
4	10374.7	103.65692	36959.3	2051.5529	22%	0.056863196	5504.5762	5625.521688	6.304742699	5
5	8892.6	88.84879	38441.4	2133.822	19%	0.197610017	3152.488211	8007.025891	5.95232349	5
6	7410.5	74.040659	39923.5	2216.091	16%	1.278369003	794.3628084	10393.45378	5.296572654	5
7	5928.4	59.232527	41405.6	2298.3601	13%	78.88376666	21534.36616	880.2032041	5.246680984	5
8	4446.3	44.424395	42887.7	2380.6291	9%			897.6476819	2.595616964	5

8.3 Appendix C: Case study 2 Results

Table 8.3-1 Case Study 2 Results

No	Volume flow (m^3/h)	Absorber SO_2 (kg/h)	Absorber SO_3 (kg/h)	Absorber pH	Clean air SO_2	Gypsum production (kg/h)	Reclaim water pH	SO_2 mg/m3	SO_2 outlet mg/Nm3
1	2961410	3.42792E-05	10882.44766	7.992684683	6.9387E-05	18218.27963	7.813615131	2.34304E-05	6.69712E-05
2	3257551	0.0008773 4	11202.36726	7.299544125	0.0039995 35	17217.95853	6.931657339	0.0012277 74	0.0035093 49
3	3553692	0.0086607 48	10332.02479	6.796337896	0.0513995 45	18269.05417	6.321705674	0.0144637 03	0.0413416 43
4	3849833	0.0288251 91	9275.102149	6.524245143	0.2778533 17	18293.56845	5.845769923	0.0721728 23	0.2062917 86
5	4145974	0.0662838 04	8189.086596	6.328767503	2.1180365 78	18087.73895	5.144810054	0.5108658 61	1.4602093 45
6	4442115	0.1288359 13	7093.843228	6.165479115	53.465678 21	16877.59876	4.155120868	12.036086 01	34.402778 91
7	4738256	0.2299632 25	5994.589484	6.015110786	72.199709 43	14095.71284	4.854203282	15.237612 62	43.553711 53
8	5922820	2.5928237 95	1585.828856	5.24581333	159.70601 49	4806.480558	4.061714885	26.964522 79	77.072772 24

8.4Appendix D: Case Study 3 Results

High sulphur test case

Table 8.4-1 Case Study 3 Results

Material												
Stream Name	Units	ABSLURRY	AIRIN	AIROUT1	AIROUT2	BLEED0	BLEED1	CLEANAIR	FLUE	GYPS	LSTONE	RECWATER
Description												
From		ABSORBER		ABSORBER	SEPAIR	SEPAIR	SPLIT	AIRMIX		HYDROCYC		HYDROCYC
To		CSTR	CSTR	AIRMIX	AIRMIX	SPLIT	HYDROCYC		ABSORBER		ABSORBER	
Stream Class		MIXCIPSD	MIXCIPSD	MIXCIPSD	MIXCIPSD	MIXCIPSD	MIXCIPSD	MIXCIPSD	MIXCIPSD	MIXCIPSD	MIXCIPSD	MIXCIPSD
Maximum Relative Error												
Cost Flow	$/hr											
Total Stream												
Temperature	C	30.12668841	30	31.13506013	31.20513683	31.20513683	31.20513683	29.68343638	30	31.20684541	30	31.2166758
Pressure	bar	0.8	0.8	0.8	1	1	1	0.8	0.86	0.469074128	1	0.469074128
Molar Vapor		0	1	1	0.000373133	0	0	0.993457528	0.978987503	0	0	0

Fraction												
Molar Liquid Fraction		1	0	0	0.999626867	0.967762615	0.967762615	0.006542472	0.021012497	0.305593268	1	1
Molar Solid Fraction		0	0	0	0	0.032237385	0.032237385	0	7.7375E-18	0.694406732	0	0
Mass Vapor Fraction		0	1	1	0.000858641	0	0	0.996020825	0.987173679	0	0	0
Mass Liquid Fraction		1	0	0	0.999141359	0.768505002	0.768505002	0.003979175	0.012826321	0.046407558	1	1
Mass Solid Fraction		0	0	0	0	0.231494998	0.231494998	2.96082E-12	0	0.953592442	0	0
Molar Enthalpy	kcal/mol	-73.42982925	0.033630349	-14.67291306	-67.969895553	-83.444177796	-83.444177796	-15.077058846	-15.697026	-356.7087211	-75.932888903	-70.140443146
Mass Enthalpy	kcal/kg	-3494.47991	1.050987815	-493.170718	-3748.291654	-3480.285831	-3480.285831	-508.2595008	-530.5987808	-2845.11403	-3575.757331	-3683.913697
Molar Entropy	cal/mol-K	-39.200665053	0.582277016	1.701186811	-38.496877303	-43.287226733	-43.287226733	1.396511058	0.721393254	-136.5634225	-39.513344623	-38.745122552

Mass Entropy	cal/gm-K	-1.865534581	0.018196839	0.057178525	-2.122962037	-1.8054233	-1.8054233	0.047077486	0.024395398	-1.089231875	-1.860723848	-2.034970353
Molar Density	kmol/cum	60.82580825	0.031757565	0.031649164	36.29374163	55.43711428	55.43711428	0.032010884	0.034885377	38.13446431	69.05802274	56.68777851
Mass Density	kg/cum	1278.138329	1.016203986	0.941632221	658.1349731	1329.17371	1329.17371	0.949573935	1.03159113	4781.142636	1466.479599	1079.315524
Enthalpy Flow	Gcal/hr	-471.6408276	0.002791319	-1486.570855	-52.61681914	-613.8490201	-429.694314	-1539.187884	-1620.960327	-85.27528546	-337.2511095	-344.4190373
Average MW		21.0130924	31.9988	29.75219842	18.13356638	23.97624276	23.97624276	29.66409567	29.57087508	125.3758961	21.23547042	19.0396511
Mole Flows	kmol/hr	6423.014086	83	101313.9551	774.1194647	7356.403228	5149.482259	102088.0756	103309.9048	239.0613978	4441.436561	4910.420853
H2O	kmol/hr	5958.64609	0	5233.036278	770.7908656	6937.665184	4856.365629	6003.829235	7210.424678	71.19216608	3994.996864	4785.173454
SO2	kmol/hr	9.60867E-07	0	1.78894E-23	2.50836E-08	1.94441E-06	1.36108E-06	2.45304E-06	209.6212139	1.9954E-08	0	1.34163E-06
CACO3	kmol/hr	0	0	0	0	0	0	0	0	0	0	0
O2	kmol/hr	0.00294336	83	5778.143018	5.89241E-08	0	0	5778.143018	5778.145961	0	0	0
CASO4	kmol/hr	0	0	0	0	0	0	0	0	0	0	0
CASO3	kmol/hr	0	0	0	0	0.697601937	0.488321356	0	0	0.007158574	0	0.481162781
N2	kmol/hr	0.020383773	0	77480.6128	0.020383773	0	0	77480.63319	77480.63319	0	0	0
NO2	kmol/hr	2.695941508	0	171.4708531	2.695941508	0	0	174.1667946	174.1667946	0	0	0
H2SO4	kmol/hr	0	0	0	0	9.76602E-35	6.83621E-35	0	0	0	0	6.74643E-35

CA++	kmol/hr	222.9995281	0	0	0	80.72192244	56.50534571	0	0	0.828343304	222.0207882	55.67700227
CAOH+	kmol/hr	0.000471945	0	0	0	0.000188195	0.000131736	0	0	1.93119E-06	0.979211823	0.000129937
H+	kmol/hr	0	0	0	0	0	0	0	0	0	0	0
CO2	kmol/hr	0.103966155	0	12650.69218	0.609283948	0.520487505	0.364341253	12651.3025	12456.52583	0.00534122	1.72733E-06	0.35899131
HCO3-	kmol/hr	27.164044265	0	0	0.001492397	38.9518621	27.266300347	0.00044927	1.32634E-05	0.399711492	1.418904809	26.866401092
OH-	kmol/hr	0.000284828	0	0	1.97608E-09	0.000202197	0.000141538	4.56762E-09	1.30666E-10	2.07501E-06	0.439696442	0.000139601
CO3--	kmol/hr	1.565655978	0	0	7.2004E-10	0.847694598	0.593386218	6.22008E-10	1.81562E-13	0.008699062	221.5810935	0.584876942
H3O+	kmol/hr	2.58725E-06	0	0	0.001494906	4.68865E-06	3.28205E-06	0.000449353	0.193576699	4.81166E-08	6.29217E-10	3.2341E-06
HSO3-	kmol/hr	3.925656621	0	0	2.50349E-06	2.973876508	2.081713556	7.64926E-08	0.193558594	0.030517142	0	2.051395191
SO3--	kmol/hr	205.8891173	0	0	1.05964E-09	56.872995589	39.811097712	9.77724E-11	2.42118E-06	0.58361288	0	39.227285547
HSO4-	kmol/hr	0	0	0	0	5.29477E-18	3.70634E-18	0	0	0	0	3.65314E-18
CALCI(S)	kmol/hr	0	0	0	0	0	0	0	0	0	0	0
CASO3(S)	kmol/hr	0	0	0	0	0	0	0	0	0	0	0
CASO4(S)	kmol/hr	0	0	0	0	0	0	0	0	0	0	0
SALT1	kmol/hr	0	0	0	0	0	0	0	0	0	0	0
SALT2	kmol/hr	0	0	0	0	0	0	0	0	0	0	0

SALT3	kmol/hr	0	0	0	0	237.1512056	166.0058439	0	0	166.0058439	0	0
CACO3(S)	kmol/hr	0	0	0	0	0	0	0	0	0	0	0
SO4--	kmol/hr	0	0	0	0	1.68806E-11	1.18164E-11	0	0	0	0	1.16432E-11
AIR	kmol/hr	0	0	0	0	0	0	0	0	0	0	0
Mole Fractions												
H2O		0.927702479	0	0.051651683	0.995700148	0.943078427	0.943078427	0.058810289	0.069794128	0.297798669	0.899483041	0.974493551
SO2		1.49598E-10	0	1.76574E-28	3.24028E-11	2.64315E-10	2.64315E-10	2.40287E-11	0.002029052	8.34682E-11	0	2.73221E-10
CACO3		0	0	0	0	0	0	0	0	0	0	0
O2		4.58252E-07	1	0.057032055	7.61176E-11	0	0	0.056599588	0.055930222	0	0	0
CASO4		0	0	0	0	0	0	0	0	0	0	0
CASO3		0	0	0	0	9.48292E-05	9.48292E-05	0	0	2.99445E-05	0	9.79881E-05
N2		3.17355E-06	0	0.764757557	2.63316E-05	0	0	0.7589587	0.749982621	0	0	0
NO2		0.000419732	0	0.00169247	0.003482591	0	0	0.001706044	0.001685867	0	0	0
H2SO4		0	0	0	0	1.32755E-38	1.32755E-38	0	0	0	0	1.3739E-38
CA++		0.034718829	0	0	0	0.010973015	0.010973015	0	0	0.003464981	0.049988508	0.01133854
CAOH+		7.34771E-08	0	0	0	2.55825E-08	2.55825E-08	0	0	8.07823E-09	0.000220472	2.64615E-08

H+		0	0	0	0	0	0	0	0	0	0	0
CO2		1.61865E-05	0	0.124866235	0.000787067	7.0753E-05	7.0753E-05	0.12392537	0.120574362	2.23425E-05	3.88912E-10	7.31081E-05
HCO3-		0.004229174	0	0	1.92786E-06	0.00529496	0.00529496	4.40081E-09	1.28384E-10	0.001672003	0.00031947	0.005471305
OH-		4.43449E-08	0	0	2.55269E-12	2.74859E-08	2.74859E-08	4.4742E-14	1.26479E-15	8.67982E-09	9.89987E-05	2.84295E-08
CO3--		0.000243757	0	0	9.30141E-13	0.000115232	0.000115232	6.09286E-15	1.75745E-18	3.63884E-05	0.04988951	0.000119109
H3O+		4.02809E-10	0	0	1.9311E-06	6.37356E-10	6.37356E-10	4.40162E-09	1.87375E-06	2.01273E-10	1.4167E-13	6.5862E-10
HSO3-		0.000611186	0	0	3.23398E-09	0.000404257	0.000404257	7.49281E-13	1.87357E-06	0.000127654	0	0.000417764
SO3--		0.032054907	0	0	1.36883E-12	0.007731087	0.007731087	9.57726E-16	2.34361E-11	0.002441268	0	0.007988579
HSO4-		0	0	0	0	7.1975E-22	7.1975E-22	0	0	0	0	7.43957E-22
CALCI(S)		0	0	0	0	0	0	0	0	0	0	0
CASO3(S)		0	0	0	0	0	0	0	0	0	0	0
CASO4(S)		0	0	0	0	0	0	0	0	0	0	0
SALT1		0	0	0	0	0	0	0	0	0	0	0
SALT2		0	0	0	0	0	0	0	0	0	0	0
SALT3		0	0	0	0	0.032237385	0.032237385	0	0	0.694406732	0	0
CACO3(S)		0	0	0	0	0	0	0	0	0	0	0
SO4--		0	0	0	0	2.29468E-15	2.29468E-15	0	0	0	0	2.37112E-15
AIR		0	0	0	0	0	0	0	0	0	0	0

Mass Flows	kg/hr	134967.3885	2655.9004	3014312.895	14037.5467	176378.9096	123465.2368	3028350.442	3054964.289	29972.53697	94315.99471	93492.69978
H2O	kg/hr	107346.6777	0	94274.6138	13886.01326	124983.9808	87488.78658	108160.6647	129897.8195	1282.546806	71970.98711	86206.23962
SO2	kg/hr	6.15578E-05	0	1.14608E-21	1.60698E-06	0.000124568	8.71975E-05	0.000157154	13429.34114	1.27835E-06	0	8.59513E-05
CACO3	kg/hr	0	0	0	0	0	0	0	0	0	0	0
O2	kg/hr	0.094183994	2655.9004	184893.6428	1.8855E-06	0	0	184893.6428	184893.737	0	0	0
CASO4	kg/hr	0	0	0	0	0	0	0	0	0	0	0
CASO3	kg/hr	0	0	0	0	83.811431 38	58.668001 96	0	0	0.860046885	0	57.807955 08
N2	kg/hr	0.571020418	0	2170501.597	0.571020418	0	0	2170502.168	2170502.168	0	0	0
NO2	kg/hr	124.0282449	0	7888.609191	124.0282449	0	0	8012.637436	8012.637436	0	0	0
H2SO4	kg/hr	0	0	0	0	9.57846E-33	6.70492E-33	0	0	0	0	6.61687E-33
CA++	kg/hr	8937.129786	0	0	0	3235.084413	2264.559089	0	0	33.19743174	8897.904926	2231.361652
CAOH+	kg/hr	0.026940866	0	0	0	0.010743068	0.007520148	0	0	0.000110242	55.898100127	0.007417439
H+	kg/hr	0	0	0	0	0	0	0	0	0	0	0
CO2	kg/hr	4.57552969	0	556754.4325	26.814464 69	22.906550 98	16.034585 68	556781.2929	548209.2104	0.23506604	7.60194E-05	15.799135 76
HCO3-	kg/hr	1657.487134	0	0	0.091062611	2376.752647	1663.726853	0.02741342	0.0008093	24.389471 88	86.578293 8	1639.326333
OH-	kg/hr	0.004844318	0	0	3.3609E-08	0.00343895	0.002407265	7.76857E-08	2.22234E-09	3.52915E-05	7.478308718	0.002374314
CO3--	kg/hr	93.955484 96	0	0	4.32098E-08	50.870407 11	35.609284 97	3.73269E-08	1.08956E-11	0.52203333	13297.147 89	35.098640 73

H3O+	kg/hr	4.92163 E-05	0	0	0.028437102	8.91906 E-05	6.24334 E-05	0.008547885	3.682345672	9.15306 E-07	1.19694 E-08	6.15213 E-05
HSO3-	kg/hr	318.2635423	0	0	0.000202965	241.1001682	168.7701178	6.20146 E-06	15.69231585	2.474106763	0	166.3121263
SO3--	kg/hr	16484.57394	0	0	8.48404 E-08	4553.553478	3187.487434	7.82818 E-09	0.000193852	46.72714034	0	3140.744379
HSO4-	kg/hr	0	0	0	0	5.13974 E-16	3.59782 E-16	0	0	0	0	3.54618 E-16
CALCI (S)	kg/hr	0	0	0	0	0	0	0	0	0	0	0
CASO 3(S)	kg/hr	0	0	0	0	0	0	0	0	0	0	0
CASO 4(S)	kg/hr	0	0	0	0	0	0	0	0	0	0	0
SALT1	kg/hr	0	0	0	0	0	0	0	0	0	0	0
SALT2	kg/hr	0	0	0	0	0	0	0	0	0	0	0
SALT3	kg/hr	0	0	0	0	40830.83532	28581.58472	0	0	28581.58472	0	0
CACO 3(S)	kg/hr	0	0	0	0	0	0	0	0	0	0	0
SO4--	kg/hr	0	0	0	0	1.62163 E-09	1.13514 E-09	0	0	0	0	1.1185E -09
AIR	kg/hr	0	0	0	0	0	0	0	0	0	0	0
Mass Fractio ns												
H2O		0.795352707	0	0.031275656	0.989205134	0.70861069	0.70861069	0.035716033	0.042520242	0.042790732	0.763083582	0.92206386
SO2		4.56094 E-10	0	3.80212 E-28	1.14477 E-10	7.06252 E-10	7.06252 E-10	5.18941 E-11	0.004395908	4.26507 E-11	0	9.19337 E-10
CACO 3		0	0	0	0	0	0	0	0	0	0	0

O2		6.97828E-07	1	0.06133857	1.34318E-10	0	0	0.061054243	0.060522389	0	0	0
CASO4		0	0	0	0	0	0	0	0	0	0	0
CASO3		0	0	0	0	0.000475178	0.000475178	0	0	2.86945E-05	0	0.000618315
N2		4.2308E-06	0	0.720065127	4.06781E-05	0	0	0.716727542	0.710483647	0	0	0
NO2		0.00091895	0	0.002617051	0.008835464	0	0	0.002645875	0.002622825	0	0	0
H2SO4		0	0	0	0	5.43062E-38	5.43062E-38	0	0	0	0	7.07742E-38
CA++		0.066216957	0	0	0	0.018341674	0.018341674	0	0	0.001107595	0.094341421	0.023866694
CAOH+		1.9961E-07	0	0	0	6.0909E-08	6.0909E-08	0	0	3.67809E-09	0.000592668	7.93371E-08
H+		0	0	0	0	0	0	0	0	0	0	0
CO2		3.3901E-05	0	0.184703596	0.001910196	0.000129871	0.000129871	0.183856295	0.179448648	7.84271E-06	8.06007E-10	0.000168988
HCO3-		0.012280649	0	0	6.48707E-06	0.013475266	0.013475266	9.05226E-09	2.64913E-10	0.000813727	0.00091796	0.017534271
OH-		3.58925E-08	0	0	2.39422E-12	1.94975E-08	1.94975E-08	2.56528E-14	7.27454E-16	1.17746E-09	7.92899E-05	2.53957E-08
CO3--		0.000696135	0	0	3.07816E-12	0.000288415	0.000288415	1.23258E-14	3.56652E-18	1.74171E-05	0.140985078	0.000375416
H3O+		3.64654E-10	0	0	2.02579E-06	5.05676E-10	5.05676E-10	2.82262E-09	1.20536E-06	3.05382E-11	1.26907E-13	6.58033E-10
HSO3-		0.002358077	0	0	1.44587E-08	0.001366944	0.001366944	2.0478E-12	5.13666E-06	8.25458E-05	0	0.001778878
SO3--		0.122137459	0	0	6.04382E-12	0.025816882	0.025816882	2.58496E-15	6.34548E-11	0.001558999	0	0.033593472
HSO4-		0	0	0	0	2.91404E-21	2.91404E-21	0	0	0	0	3.793E-21

CALCI (S)		0	0	0	0	0	0	0	0	0	0	0
CASO 3(S)		0	0	0	0	0	0	0	0	0	0	0
CASO 4(S)		0	0	0	0	0	0	0	0	0	0	0
SALT1		0	0	0	0	0	0	0	0	0	0	0
SALT2		0	0	0	0	0	0	0	0	0	0	0
SALT3		0	0	0	0	0.231494998	0.231494998	0	0	0.953592442	0	0
CACO 3(S)		0	0	0	0	0	0	0	0	0	0	0
SO4--		0	0	0	0	9.19402 E-15	9.19402 E-15	0	0	0	0	1.19635 E-14
AIR		0	0	0	0	0	0	0	0	0	0	0

Limestone limit

Table 8.4-2: Limestone Limit Results

Material								
Stream Name	Units	AIRIN	BLEED1	CLEANAIR	FLUE	GYPS	LSTONE	RECWATER
Description								
From			SPLIT	AIRMIX		HYDROCYC		HYDROCYC
To		CSTR	HYDROCYC		ABSORBER		ABSORBER	
Stream Class		MIXCIPSD	MIXCIPSD	MIXCIPSD	MIXCIPSD	MIXCIPSD	MIXCIPSD	MIXCIPSD

Maximum Relative Error								
Cost Flow	$/hr							
Total Stream								
Temperature	C	30	31.41949996	29.62344578	30	31.42118126	30	31.43009137
Pressure	bar	0.8	1	0.8	0.86	0.496301628	1	0.496301628
Molar Vapor Fraction		1	0	0.99366883	0.978996777	0	0	0
Molar Liquid Fraction		0	0.968063919	0.00633117	0.021003223	0.309948491	1	1
Molar Solid Fraction		0	0.031936081	0	4.25567E-17	0.690051509	0	0
Mass Vapor Fraction		1	0	0.99614995	0.987178239	0	0	0
Mass Liquid Fraction		0	0.770117428	0.00385005	0.012821761	0.047292896	1	1
Mass Solid Fraction		0	0.229882572	2.95782E-12	0	0.952707104	0	0
Molar Enthalpy	kcal/mol	0.033630349	-83.5087234	-15.05883271	-15.70503933	-354.9654054	-75.93289682	-70.33586964
Mass Enthalpy	kcal/kg	1.050987815	-3491.349675	-507.5623474	-531.1606223	-2846.433192	-3575.757148	-3696.455228
Molar Entropy	cal/mol-K	0.582277016	-43.26155374	1.404716502	0.719556549	-135.9340247	-39.51334715	-38.76351763
Mass Entropy	cal/gm-K	0.018196839	-1.808687828	0.047346379	0.024336144	-1.090041773	-1.860723605	-2.037191096

Molar Density	kmol/cum	0.031757565	55.318735 03	0.032010414	0.034885033	38.193136 91	69.058039 85	56.547715 28
Mass Density	kg/cum	1.016203986	1323.1550 47	0.949714783	1.031459777	4762.8879 43	1466.4801 88	1075.9856 36
Enthalpy Flow	Gcal/hr	0.002690428	-418.335562 8	-1536.532081	-1622.470117	-82.296066 47	-322.127447 8	-336.039529 7
Average MW		31.9988	23.918750 97	29.668931 88	29.567401 41	124.70533 53	21.235473 68	19.027924 14
Mole Flows	kmol/hr	80	5009.48339	102035.2713	103308.8859	231.842498 5	4242.2647 01	4777.6409 31
H2O	kmol/hr	0	4719.44646 3	5961.95754	7209.555043	69.932115 05	3815.8447 2	4649.5143 86
SO2	kmol/hr	0	5.01228E-08	7.48829E-08	183.2366361	7.4289E-10	0	4.94237E-08
CACO3	kmol/hr	0	0	0	0	0	0	0
O2	kmol/hr	80	0	5777.425273	5777.42816	0	0	0
CASO4	kmol/hr	0	0	0	0	0	0	0
CASO3	kmol/hr	0	0.296450286	0	0	0.00439276	0	0.292057526
N2	kmol/hr	0	0	77471.00801	77471.00801	0	0	0
NO2	kmol/hr	0	0	174.1451584	174.1451584	0	0	0
H2SO4	kmol/hr	0	0	0	0	0	0	0
CA++	kmol/hr	0	52.719201 22	0	0	0.781185942	212.06469 92	51.938014 91
CAOH+	kmol/hr	0	0.000522671	0	0	7.74562E-06	0.9353008 4	0.0005152 85
H+	kmol/hr	0	0	0	0	0	0	0

CO2	kmol/hr	0	0.177279917	12650.73446	12493.15191	0.002627122	1.64987E-06	0.174692261
HCO3-	kmol/hr	0	51.02826324	0.000434815	1.41902E-05	0.756129048	1.355276184	50.27195049
OH-	kmol/hr	0	0.000547688	4.39635E-09	1.39386E-10	8.11669E-06	0.419978644	0.000539927
CO3--	kmol/hr	0	4.219922962	6.01017E-10	2.06373E-13	0.062530838	211.6447222	4.157536368
H3O+	kmol/hr	0	7.82648E-07	0.000434822	0.180505536	1.15986E-08	6.01E-10	7.71287E-07
HSO3-	kmol/hr	0	0.29533691	2.2653E-09	0.180486548	0.004376646	0	0.291065757
SO3--	kmol/hr	0	21.31613603	2.89651E-12	2.39855E-06	0.315859216	0	21.00017132
HSO4-	kmol/hr	0	0	0	0	0	0	0
CALCI(S)	kmol/hr	0	0	0	0	0	0	0
CASO3(S)	kmol/hr	0	0	0	0	0	0	0
CASO4(S)	kmol/hr	0	0	0	0	0	0	0
SALT1	kmol/hr	0	0	0	0	0	0	0
SALT2	kmol/hr	0	0	0	0	0	0	0
SALT3	kmol/hr	0	159.983266	0	0	159.983266	0	0
CACO3(S)	kmol/hr	0	0	0	0	0	0	0
SO4--	kmol/hr	0	0	0	0	0	0	0
AIR	kmol/hr	0	0	0	0	0	0	0
Mole Fractions								
H2O		0	0.942102428	0.058430359	0.069786398	0.301636307	0.899482939	0.973182048
SO2		0	1.00056E-11	7.33892E-13	0.001773677	3.20429E-12	0	1.03448E-11
CACO3		0	0	0	0	0	0	0
O2		1	0	0.056621845	0.055923826	0	0	0

CASO4		0	0	0	0	0	0	0
CASO3		0	5.91778E-05	0	0	1.89472E-05	0	6.11301E-05
N2		0	0	0.759257137	0.749896849	0	0	0
NO2		0	0	0.001706715	0.001685675	0	0	0
H2SO4		0	0	0	0	0	0	0
CA++		0	0.01052388	0	0	0.003369468	0.049988559	0.010871059
CAOH+		0	1.04336E-07	0	0	3.3409E-08	0.000220472	1.07854E-07
H+		0	0	0	0	0	0	0
CO2		0	3.53889E-05	0.123983935	0.120930081	1.13315E-05	3.88912E-10	3.65645E-05
HCO3-		0	0.010186332	4.26141E-09	1.37357E-10	0.003261391	0.00031947	0.010522338
OH-		0	1.0933E-07	4.30866E-14	1.34922E-15	3.50095E-08	9.89987E-05	1.13011E-07
CO3--		0	0.000842387	5.89028E-15	1.99763E-18	0.000269713	0.049889561	0.000870207
H3O+		0	1.56233E-10	4.26149E-09	1.74724E-06	5.0028E-11	1.4167E-13	1.61437E-10
HSO3-		0	5.89556E-05	2.22011E-14	1.74706E-06	1.88777E-05	0	6.09225E-05
SO3--		0	0.004255157	2.83873E-17	2.32172E-11	0.001362387	0	0.004395511
HSO4-		0	0	0	0	0	0	0
CALCI(S)		0	0	0	0	0	0	0
CASO3(S)		0	0	0	0	0	0	0
CASO4(S)		0	0	0	0	0	0	0
SALT1		0	0	0	0	0	0	0

SALT2		0	0	0	0	0	0	0
SALT3		0	0.031936081	0	0	0.690051509	0	0
CACO3(S)		0	0	0	0	0	0	0
SO4--		0	0	0	0	0	0	0
AIR		0	0	0	0	0	0	0
Mass Flows	kg/hr	2559.904	119820.5857	3027277.514	3054575.299	28911.9965	90086.50042	90908.58918
H2O	kg/hr	0	85022.14947	107406.3344	129882.1528	1259.846634	68743.51111	83762.30354
SO2	kg/hr	0	3.2111E-06	4.79736E-06	11739.01844	4.75931E-08	0	3.16632E-06
CACO3	kg/hr	0	0	0	0	0	0	0
O2	kg/hr	2559.904	0	184870.6758	184870.7682	0	0	0
CASO4	kg/hr	0	0	0	0	0	0	0
CASO3	kg/hr	0	35.616189499	0	0	0.527755845	0	35.08843365
N2	kg/hr	0	0	2170232.533	2170232.533	0	0	0
NO2	kg/hr	0	0	8011.642051	8011.642051	0	0	0
H2SO4	kg/hr	0	0	0	0	0	0	0
CA++	kg/hr	0	2112.822155	0	0	31.30751087	8498.895742	2081.514639
CAOH+	kg/hr	0	0.02983655	0	0	0.000442157	53.39145204	0.029414958
H+	kg/hr	0	0	0	0	0	0	0
CO2	kg/hr	0	7.802053674	556756.2932	549821.1179	0.115619099	7.26103E-05	7.688171475
HCO3-	kg/hr	0	3113.626748	0.026531377	0.000865852	46.13724785	82.69582205	3067.478291

OH-	kg/hr	0	0.009315021	7.47727E-08	2.37066E-09	0.000138048	7.142950581	0.009183025
CO3--	kg/hr	0	253.2388429	3.60672E-08	1.23845E-11	3.752494332	12700.86327	249.4950047
H3O+	kg/hr	0	1.48881E-05	0.008271483	3.433697239	2.20637E-07	1.14326E-08	1.46719E-05
HSO3-	kg/hr	0	23.94375778	1.83654E-07	14.63252998	0.354826469	0	23.59748391
SO3--	kg/hr	0	1706.682826	2.3191E-10	0.00019204	25.2893629	0	1681.385017
HSO4-	kg/hr	0	0	0	0	0	0	0
CALCI(S)	kg/hr	0	0	0	0	0	0	0
CASO3(S)	kg/hr	0	0	0	0	0	0	0
CASO4(S)	kg/hr	0	0	0	0	0	0	0
SALT1	kg/hr	0	0	0	0	0	0	0
SALT2	kg/hr	0	0	0	0	0	0	0
SALT3	kg/hr	0	27544.66447	0	0	27544.66447	0	0
CACO3(S)	kg/hr	0	0	0	0	0	0	0
SO4--	kg/hr	0	0	0	0	0	0	0
AIR	kg/hr	0	0	0	0	0	0	0
Mass Fractions								
H2O		0	0.709578817	0.035479514	0.042520527	0.043575221	0.763083379	0.921390424
SO2		0	2.67993E-11	1.58471E-12	0.003843093	1.64614E-12	0	3.48297E-11
CACO3		0	0	0	0	0	0	0
O2		1	0	0.061068295	0.060522577	0	0	0
CASO4		0	0	0	0	0	0	0
CASO3		0	0.000297246	0	0	1.82539E-05	0	0.000385975

N2		0	0	0.716892496	0.710485852	0	0	0
NO2		0	0	0.002646484	0.002622833	0	0	0
H2SO4		0	0	0	0	0	0	0
CA++		0	0.017633215	0	0	0.001082855	0.094341502	0.022896787
CAOH+		0	2.4901E-07	0	0	1.52932E-08	0.000592669	3.23566E-07
H+		0	0	0	0	0	0	0
CO2		0	6.51145E-05	0.183913199	0.179999202	3.999E-06	8.06007E-10	8.45704E-05
HCO3-		0	0.025985741	8.7641E-09	2.83461E-10	0.001595782	0.00091796	0.033742447
OH-		0	7.77414E-08	2.46996E-14	7.76103E-16	4.77476E-09	7.92899E-05	1.01014E-07
CO3--		0	0.002113484	1.19141E-14	4.05441E-18	0.00012979	0.1409852	0.00274446
H3O+		0	1.24253E-10	2.73232E-09	1.12412E-06	7.63133E-12	1.26907E-13	1.61392E-10
HSO3-		0	0.00019983	6.06663E-14	4.79036E-06	1.22726E-05	0	0.000259574
SO3--		0	0.014243653	7.66067E-17	6.28697E-11	0.000874701	0	0.018495337
HSO4-		0	0	0	0	0	0	0
CALCI(S)		0	0	0	0	0	0	0
CASO3(S)		0	0	0	0	0	0	0
CASO4(S)		0	0	0	0	0	0	0
SALT1		0	0	0	0	0	0	0
SALT2		0	0	0	0	0	0	0
SALT3		0	0.229882572	0	0	0.952707104	0	0

CACO3(S)		0	0	0	0	0	0	0
SO4--		0	0	0	0	0	0	0
AIR		0	0	0	0	0	0	0

8.5Appendix E: Aspen Simulation Base Case

The below is the Aspen input text of the Base Case of Eskom Power Station A

```
;
;Input Summary created by Aspen Plus Rel. 38.0 at 12:28:28 Mon Dec 11, 2023
;Directory D:\  Filename C:\Users\LEEUWF~1\AppData\Local\Temp\~ap770d.txt
;


PROP

DYNAMICS
   DYNAMICS RESULTS=ON

IN-UNITS MET VOLUME-FLOW='cum/hr' ENTHALPY-FLO='Gcal/hr'  &
       HEAT-TRANS-C='kcal/hr-sqm-K' PRESSURE=bar TEMPERATURE=C  &
       VOLUME=cum DELTA-T=C HEAD=meter MOLE-DENSITY='kmol/cum'  &
       MASS-DENSITY='kg/cum' MOLE-ENTHALP='kcal/mol'  &
       MASS-ENTHALP='kcal/kg' HEAT=Gcal MOLE-CONC='mol/l'  &
       PDROP=bar SHORT-LENGTH=mm

SIM-OPTIONS MASS-BAL-CHE=YES FLASH-MAXIT=50 MASS-BAL-TOL=0.0001

DESCRIPTION '
   Electrolytes Simulation with Metric Units :
   C, bar, kg/hr, kmol/hr, Gcal/hr, cum/hr.

   Property Method: ELECNRTL

   Flow basis for input: Mass

   Stream report composition: Mass flow
   '

DATABANKS 'APV120 ASPENPCD' / 'APV120 AQUEOUS' / 'APV120 SOLIDS' &
       / 'APV120 INORGANIC' / 'APESV120 ACIDGAS' /  &
       'APV120 PURE38'

PROP-SOURCES 'APV120 ASPENPCD' / 'APV120 AQUEOUS' /  &
       'APV120 SOLIDS' / 'APV120 INORGANIC' / 'APESV120 ACIDGAS' &
       / 'APV120 PURE38'
```

```
COMPONENTS
   H2O H2O /
   SO2 O2S /
   CACO3 CACO3 /
   O2 O2 /
   CASO4 CASO4 /
   CASO3 CASO3 /
   N2 N2 /
   NO2 NO2 /
   H2SO4 H2SO4 /
   CA++ CA+2 /
   CAOH+ CAOH+ /
   H+ H+ /
   CO2 CO2 /
   HCO3- HCO3- /
   OH- OH- /
   CO3-- CO3-2 /
   H3O+ H3O+ /
   HSO3- HSO3- /
   SO3-- SO3-2 /
   HSO4- HSO4- /
   "CALCI(S)" "CA(OH)2" /
   "CASO3(S)" CASO3 /
   "CASO4(S)" CASO4 /
   SALT1 "CASO3*1:2W" /
   SALT2 "CASO4*1:2W:A" /
   SALT3 "CASO4*2H2O" /
   "CACO3(S)" CACO3 /
   SO4-- SO4-2 /
   AIR AIR

CISOLID-COMPS "CALCI(S)" "CASO3(S)" "CASO4(S)" SALT1 SALT2  &
      SALT3 "CACO3(S)"

HENRY-COMPS GLOBAL CO2 SO2 O2 N2

CHEMISTRY GLOBAL
   PARAM GAMMA-BASIS=UNSYMMETRIC
   DISS CACO3 CO3-- 1 / CA++ 1
   STOIC 1 H2O -1 / HSO4- -1 / H3O+ 1 / SO4-- 1
   STOIC 2 H2SO4 -1 / H2O -1 / H3O+ 1 / HSO4- 1
   STOIC 3 CAOH+ -1 / CA++ 1 / OH- 1
   STOIC 4 H2O -1 / HCO3- -1 / CO3-- 1 / H3O+ 1
   STOIC 5 H2O -2 / CO2 -1 / HCO3- 1 / H3O+ 1
   STOIC 6 H2O -1 / HSO3- -1 / H3O+ 1 / SO3-- 1
   STOIC 7 H2O -2 / SO2 -1 / H3O+ 1 / HSO3- 1
```

```
   STOIC 8 H2O -2 / OH- 1 / H3O+ 1
   K-STOIC 4 A=216.050446 B=-12431.700195 C=-35.481899 D=0
   K-STOIC 5 A=231.465424 B=-12092.099609 C=-36.781601 D=0
   K-STOIC 6 A=-25.290564 B=1333.400024 C=0 D=0
   K-STOIC 7 A=-5.978673 B=637.395996 C=0 D=-0.015134
   K-STOIC 8 A=132.89888 B=-13445.900391 C=-22.477301 D=0

PROPERTIES ELECNRTL HENRY-COMPS=GLOBAL CHEMISTRY=GLOBAL  &
      TRUE-COMPS=YES

ESTIMATE ALL

PROP-DATA PCES-1
   IN-UNITS MET VOLUME-FLOW='cum/hr' ENTHALPY-FLO='Gcal/hr'  &
      HEAT-TRANS-C='kcal/hr-sqm-K' PRESSURE=bar TEMPERATURE=C  &
      VOLUME=cum DELTA-T=C HEAD=meter MOLE-DENSITY='kmol/cum'  &
      MASS-DENSITY='kg/cum' MOLE-ENTHALP='kcal/mol'  &
      MASS-ENTHALP='kcal/kg' HEAT=Gcal MOLE-CONC='mol/l'  &
      PDROP=bar SHORT-LENGTH=mm
   PROP-LIST DGAQHG / DHAQHG / S25HG / OMEGHG
   PVAL H2SO4 -177.8279354 / -217.1754084 / 4.800802522 /  &
      26.72966466
   PROP-LIST RKTZRA / VLSTD
   PVAL CACO3 .2918596200 / 298.9063450
   PVAL CASO4 .2918596200 / 298.9063450
   PVAL "CALCI(S)" .2918596200 / 298.9063450
   PVAL "CASO4(S)" .2918596200 / 298.9063450
   PVAL "CACO3(S)" .2918596200 / 298.9063450
   PROP-LIST VLSTD
   PVAL AIR 32.91470000

PROP-DATA PURE-1
   IN-UNITS MET VOLUME-FLOW='cum/hr' ENTHALPY-FLO='Gcal/hr'  &
      HEAT-TRANS-C='kcal/hr-sqm-K' PRESSURE=bar TEMPERATURE=C  &
      VOLUME=cum DELTA-T=C HEAD=meter MOLE-DENSITY='kmol/cum'  &
      MASS-DENSITY='kg/cum' MOLE-ENTHALP='kJ/kmol'  &
      MASS-ENTHALP='kcal/kg' HEAT=Gcal MOLE-CONC='mol/l'  &
      PDROP=bar SHORT-LENGTH=mm
   PROP-LIST DGAQFM
   PVAL CASO4 -1.322

PROP-DATA REVIEW-1
   IN-UNITS MET VOLUME-FLOW='cum/hr' ENTHALPY-FLO='Gcal/hr'  &
      HEAT-TRANS-C='kcal/hr-sqm-K' PRESSURE=bar TEMPERATURE=C  &
      VOLUME=cum DELTA-T=C HEAD=meter MOLE-DENSITY='kmol/cum'  &
      MASS-DENSITY='kg/cum' MOLE-ENTHALP='kcal/mol'  &
```

```
      MASS-ENTHALP='kcal/kg' HEAT=Gcal MOLE-CONC='mol/l'  &
      PDROP=bar SHORT-LENGTH=mm
   PROP-LIST DHVLB / RGYR / VB / VLSTD
   PVAL H2SO4 13.89079966 / 2.5372000E-10 / 65.75890000 /  &
      53.63720000

PROP-DATA MULAND-1
   IN-UNITS MET VOLUME-FLOW='cum/hr' ENTHALPY-FLO='Gcal/hr'  &
      HEAT-TRANS-C='kcal/hr-sqm-K' PRESSURE=bar TEMPERATURE=C  &
      VOLUME=cum DELTA-T=C HEAD=meter MOLE-DENSITY='kmol/cum'  &
      MASS-DENSITY='kg/cum' MOLE-ENTHALP='kcal/mol'  &
      MASS-ENTHALP='kcal/kg' HEAT=Gcal MOLE-CONC='mol/l'  &
      PDROP=bar SHORT-LENGTH=mm
   PROP-LIST MULAND
   PVAL CACO3 81.01616808 -12127.32210 -10.25255770  &
      1126.850000 1706.850000
   PVAL CASO4 81.16998398 -12127.32210 -10.25255770  &
      1126.850000 1706.850000
   PVAL "CALCI(S)" 80.86581028 -12127.32210 -10.25255770  &
      1126.850000 1706.850000
   PVAL "CASO4(S)" 81.16998398 -12127.32210 -10.25255770  &
      1126.850000 1706.850000
   PVAL "CACO3(S)" 81.01616808 -12127.32210 -10.25255770  &
      1126.850000 1706.850000

PROP-DATA SIGDIP-1
   IN-UNITS MET VOLUME-FLOW='cum/hr' ENTHALPY-FLO='Gcal/hr'  &
      HEAT-TRANS-C='kcal/hr-sqm-K' PRESSURE=bar TEMPERATURE=C  &
      VOLUME=cum DELTA-T=C HEAD=meter MOLE-DENSITY='kmol/cum'  &
      MASS-DENSITY='kg/cum' MOLE-ENTHALP='kcal/mol'  &
      MASS-ENTHALP='kcal/kg' HEAT=Gcal MOLE-CONC='mol/l'  &
      PDROP=bar SHORT-LENGTH=mm
   PROP-LIST SIGDIP
   PVAL AIR 26.91910850 1.222222220 4.4891197E-10  &
      -4.938161E-10 1.9962172E-10 -194.4800000 -143.3490000

PROP-DATA HOCETA-1
   IN-UNITS ENG SHORT-LENGTH=in
   PROP-LIST HOCETA
   BPVAL H2O H2O 1.700000000
   BPVAL H2O SO2 1.500000000
   BPVAL H2O CO2 .3000000000
   BPVAL SO2 H2O 1.500000000
   BPVAL CO2 H2O .3000000000
   BPVAL CO2 CO2 .1600000000
```

```
PROP-DATA HENRY-1
   IN-UNITS MET VOLUME-FLOW='cum/hr' ENTHALPY-FLO='Gcal/hr'  &
      HEAT-TRANS-C='kcal/hr-sqm-K' PRESSURE=bar TEMPERATURE=C  &
      VOLUME=cum DELTA-T=C HEAD=meter MOLE-DENSITY='kmol/cum'  &
      MASS-DENSITY='kg/cum' MOLE-ENTHALP='kcal/mol'  &
      MASS-ENTHALP='kcal/kg' HEAT=Gcal MOLE-CONC='mol/l'  &
      PDROP=bar SHORT-LENGTH=mm
   PROP-LIST HENRY
   BPVAL SO2 H2O 72.44767454 -5578.800000 -8.761520000 0.0  &
      -.1500000000 99.85000000 0.0
   BPVAL O2 H2O 144.4080745 -7775.060000 -18.39740000  &
      -9.4435400E-3 .8500000000 74.85000000 0.0
   BPVAL N2 H2O 164.9940745 -8432.770000 -21.55800000  &
      -8.4362400E-3 -.1500000000 72.85000000 0.0
   BPVAL CO2 H2O 159.1996745 -8477.711000 -21.95743000  &
      5.78074800E-3 -.1500000000 226.8500000 0.0

PROP-DATA NRTL-1
   IN-UNITS MET VOLUME-FLOW='cum/hr' ENTHALPY-FLO='Gcal/hr'  &
      HEAT-TRANS-C='kcal/hr-sqm-K' PRESSURE=bar TEMPERATURE=C  &
      VOLUME=cum DELTA-T=C HEAD=meter MOLE-DENSITY='kmol/cum'  &
      MASS-DENSITY='kg/cum' MOLE-ENTHALP='kcal/mol'  &
      MASS-ENTHALP='kcal/kg' HEAT=Gcal MOLE-CONC='mol/l'  &
      PDROP=bar SHORT-LENGTH=mm
   PROP-LIST NRTL
   BPVAL H2O CO2 10.06400000 -3268.135000 .2000000000 0.0 0.0  &
      0.0 0.0 200.0000000
   BPVAL CO2 H2O 10.06400000 -3268.135000 .2000000000 0.0 0.0  &
      0.0 0.0 200.0000000

PROP-DATA VLCLK-1
   IN-UNITS MET VOLUME-FLOW='cum/hr' ENTHALPY-FLO='Gcal/hr'  &
      HEAT-TRANS-C='kcal/hr-sqm-K' PRESSURE=bar TEMPERATURE=C  &
      VOLUME=cum DELTA-T=C HEAD=meter MOLE-DENSITY='kmol/cum'  &
      MASS-DENSITY='kg/cum' MOLE-ENTHALP='kcal/mol'  &
      MASS-ENTHALP='kcal/kg' HEAT=Gcal MOLE-CONC='mol/l'  &
      PDROP=bar SHORT-LENGTH=mm
   PROP-LIST VLCLK
   BPVAL H+ HSO4- 54.80395000 20.24347000
   BPVAL H3O+ HSO4- 54.80395000 20.24347000

PROP-DATA GMELCC-1
   IN-UNITS MET VOLUME-FLOW='cum/hr' ENTHALPY-FLO='Gcal/hr'  &
      HEAT-TRANS-C='kcal/hr-sqm-K' PRESSURE=bar TEMPERATURE=C  &
      VOLUME=cum DELTA-T=C HEAD=meter MOLE-DENSITY='kmol/cum'  &
      MASS-DENSITY='kg/cum' MOLE-ENTHALP='kcal/mol'  &
```

```
      MASS-ENTHALP='kcal/kg' HEAT=Gcal MOLE-CONC='mol/l'  &
      PDROP=bar SHORT-LENGTH=mm
   PROP-LIST GMELCC
   PPVAL H2O ( H+ HCO3- ) 8.045000000
   PPVAL ( H+ HCO3- ) H2O -4.072000000
   PPVAL H2O ( H+ OH- ) 8.045000000
   PPVAL ( H+ OH- ) H2O -4.072000000
   PPVAL H2O ( H+ CO3-- ) 8.045000000
   PPVAL ( H+ CO3-- ) H2O -4.072000000
   PPVAL H2O ( H3O+ HCO3- ) 8.045000000
   PPVAL ( H3O+ HCO3- ) H2O -4.072000000
   PPVAL H2O ( H3O+ OH- ) 8.045000000
   PPVAL ( H3O+ OH- ) H2O -4.072000000
   PPVAL H2O ( H3O+ CO3-- ) 8.045000000
   PPVAL ( H3O+ CO3-- ) H2O -4.072000000
   PPVAL CO2 ( H3O+ HCO3- ) 15.00000000
   PPVAL ( H3O+ HCO3- ) CO2 -8.000000000
   PPVAL CO2 ( H3O+ OH- ) 15.00000000
   PPVAL ( H3O+ OH- ) CO2 -8.000000000
   PPVAL CO2 ( H3O+ CO3-- ) 15.00000000
   PPVAL ( H3O+ CO3-- ) CO2 -8.000000000
   PPVAL H2O ( H+ HSO4- ) 11.01100000
   PPVAL ( H+ HSO4- ) H2O -5.366000000
   PPVAL H2O ( H3O+ HSO4- ) 6.362000000
   PPVAL ( H3O+ HSO4- ) H2O -3.749000000
   PPVAL H2SO4 ( H3O+ HSO4- ) 12.99200000
   PPVAL ( H3O+ HSO4- ) H2SO4 -2.981000000
   PPVAL H2O ( H3O+ SO4-- ) 8.000000000
   PPVAL ( H3O+ SO4-- ) H2O -4.000000000
   PPVAL H2SO4 ( H3O+ SO4-- ) 8.000000000
   PPVAL ( H3O+ SO4-- ) H2SO4 -4.000000000

PROP-DATA GMELCD-1
   IN-UNITS MET VOLUME-FLOW='cum/hr' ENTHALPY-FLO='Gcal/hr'  &
      HEAT-TRANS-C='kcal/hr-sqm-K' PRESSURE=bar TEMPERATURE=C  &
      VOLUME=cum DELTA-T=C HEAD=meter MOLE-DENSITY='kmol/cum'  &
      MASS-DENSITY='kg/cum' MOLE-ENTHALP='kcal/mol'  &
      MASS-ENTHALP='kcal/kg' HEAT=Gcal MOLE-CONC='mol/l'  &
      PDROP=bar SHORT-LENGTH=mm
   PROP-LIST GMELCD
   PPVAL CO2 ( H3O+ HCO3- ) 0.0
   PPVAL ( H3O+ HCO3- ) CO2 0.0
   PPVAL CO2 ( H3O+ OH- ) 0.0
   PPVAL ( H3O+ OH- ) CO2 0.0
   PPVAL CO2 ( H3O+ CO3-- ) 0.0
   PPVAL ( H3O+ CO3-- ) CO2 0.0
```

```
   PPVAL H2O ( H3O+ HSO4- ) 1958.200000
   PPVAL ( H3O+ HSO4- ) H2O -583.2000000
   PPVAL H2SO4 ( H3O+ HSO4- ) -1732.900000
   PPVAL ( H3O+ HSO4- ) H2SO4 -162.3000000
   PPVAL H2O ( H3O+ SO4-- ) 0.0
   PPVAL ( H3O+ SO4-- ) H2O 0.0
   PPVAL H2SO4 ( H3O+ SO4-- ) 0.0
   PPVAL ( H3O+ SO4-- ) H2SO4 0.0

PROP-DATA GMELCE-1
   IN-UNITS MET VOLUME-FLOW='cum/hr' ENTHALPY-FLO='Gcal/hr'  &
      HEAT-TRANS-C='kcal/hr-sqm-K' PRESSURE=bar TEMPERATURE=C  &
      VOLUME=cum DELTA-T=C HEAD=meter MOLE-DENSITY='kmol/cum'  &
      MASS-DENSITY='kg/cum' MOLE-ENTHALP='kcal/mol'  &
      MASS-ENTHALP='kcal/kg' HEAT=Gcal MOLE-CONC='mol/l'  &
      PDROP=bar SHORT-LENGTH=mm
   PROP-LIST GMELCE
   PPVAL CO2 ( H3O+ HCO3- ) 0.0
   PPVAL ( H3O+ HCO3- ) CO2 0.0
   PPVAL CO2 ( H3O+ OH- ) 0.0
   PPVAL ( H3O+ OH- ) CO2 0.0
   PPVAL CO2 ( H3O+ CO3-- ) 0.0
   PPVAL ( H3O+ CO3-- ) CO2 0.0
   PPVAL H2O ( H3O+ HSO4- ) -4.599000000
   PPVAL ( H3O+ HSO4- ) H2O 4.472000000
   PPVAL H2SO4 ( H3O+ HSO4- ) -30.12600000
   PPVAL ( H3O+ HSO4- ) H2SO4 .8060000000

PROP-DATA GMELCN-1
   IN-UNITS MET VOLUME-FLOW='cum/hr' ENTHALPY-FLO='Gcal/hr'  &
      HEAT-TRANS-C='kcal/hr-sqm-K' PRESSURE=bar TEMPERATURE=C  &
      VOLUME=cum DELTA-T=C HEAD=meter MOLE-DENSITY='kmol/cum'  &
      MASS-DENSITY='kg/cum' MOLE-ENTHALP='kcal/mol'  &
      MASS-ENTHALP='kcal/kg' HEAT=Gcal MOLE-CONC='mol/l'  &
      PDROP=bar SHORT-LENGTH=mm
   PROP-LIST GMELCN
   PPVAL CO2 ( H3O+ HCO3- ) .1000000000
   PPVAL CO2 ( H3O+ OH- ) .1000000000
   PPVAL CO2 ( H3O+ CO3-- ) .1000000000
   PPVAL H2O ( H3O+ HSO4- ) .2000000000
   PPVAL H2SO4 ( H3O+ HSO4- ) .2000000000

PROPERTY-REP PCES NOPARAM-PLUS
;
;
;
```

;
;